Technische Universität München
Fakultät für Medizin

Functional analysis of induced pluripotent stem cell-derived cardiomyocytes from patients with hypoplastic left heart syndrome

Zhong Zhang

Vollständiger Abdruck der von der Fakultät für Medizin der Technischen Universität München zur Erlangung eines

Doktors der Medizin

genehmigten Dissertation.

Vorsitz: Prof. Dr. Gabriele Multhoff

Prüfer*innen der Dissertation:

1. apl. Prof. Dr. Markus Krane
2. Prof. Dr. Agnes Görlach

Die Dissertation wurde am 08.11.2022 bei der Technischen Universität München eingereicht und durch die Fakultät für Medizin am 18.04.2023 angenommen.

Abstract

Background:

Hypoplastic left heart syndrome (HLHS) is a severe genetically heterogeneous congenital heart disease that encompasses several pathophysiologies. The genetic mechanism of HLHS is still unclear, and there is a lack of animal models to study the development of hypoplastic left heart structure。

Objective:

The aim of this project is the comprehensive characterization of induced pluripotent stem cell (iPSC) lines derived from patients with HLHS and healthy controls and the production of highly enriched and pure cardiomyocytes (CMs).

Methods:

Before starting this thesis, iPSC lines were established from HLHS patients (n=3) and healthy controls (n=3) by integration-free transduction with Sendai virus. iPSC characterization included Sendai footprinting, the detection of endogenous pluripotency factor gene expression, and the capacity of iPSCs to differentiate were detected in cells of all three germlayers. A direct cardiac differentiation protocol with "small molecules" was applied to obtain high quality CMs. The iPSC-CMs were harvested on day 14 for analysis of gene expression, quality, and purity.

Results:

All iPSC lines were Sendai-virus free after 4 to 12 passages. Endogenous pluripotency factor expression could be detected in all iPSC lines, while expression of the reprogramming factor *c-MYC* was absent in two control lines. Direct cardiac differentiation showed the sensitivity of iPSC lines to CHIR99021 is quite variable. Furthermore, the initial cell seeding density could affect the efficiency of differentiation. The transcription factor *TBX5* and its direct target gene *NPPA* were low expressed in the HLHS group, while expression of *NKX2.5* was retarded until day 8 in the HLHS group but caught up by day 10. The expression of *ISL1* and *TNNT2* was similar in the two groups. iPSC-CMs started spontaneously beating between day 7 and 9. By day 14 more than 60% Trop T^+ CMs could be detected in both the HLHS and control group.

Conclusion:

I have performed a complete characterization of six iPSC lines and determined defined and repeatable conditions for the production of iPSC-CMs of high quality and in large quantities. My results confirm that these iPSC lines are a powerful cellular system to study the molecular dysfunction of HLHS *in vitro* and the results confirm that iPSC-CMs can successfully be used in downstream applications such as the generation of engineered heart tissues.

Abstract

Hintergrund:

Das Hypoplastische Linksherzsyndrom (HLHS) ist eine schwere, genetisch heterogene congenitale Herzerkrankung, die verschiedene Krankheitsbilder umfasst. Die genetischen Ursachen des HLHS sind noch immer unklar und es gibt keine Tiermodelle, um die Entwicklung hypoplastischer Linksherzstrukturen zu untersuchen.

Zielsetzung:

Das Ziel dieser Arbeit ist die umfassende Charakterisierung induzierter pluripotenter Stammzell-Linien (iPS Linien), die von Patienten mit HLHS oder gesunden Probanden etabliert wurden und die Generierung von hoch angereicherten, reinen Kardiomyozyten (KMs).

Methoden:

Vor Beginn dieser Doktorarbeit wurden iPS Linien von HLHS Patienten (n=3) und gesunden Probanden (n=3) durch integrationsfreie Transduktion mit Sendaiviren etabliert. Die Charakterisierung der iPS Linien umfasste ein Sendai footprinting, den Nachweis der endogenen Expression der Pluripotenzfaktoren und die Untersuchung der Fähigkeit der iPS Zellen, sich in Zellen aller drei Keimblätter zu entwickeln. Um KMs von hoher Qualität zu erhalten wurde ein direktes kardiales Differenzierungsprotokoll mit „small molecules“ verwendet. Am Tag 14 der Differenzierung wurde die Genexpression, die Qualität und die Reinheit der aus den iPS Zellen generierten KMs analysiert.

Ergebnisse:

Nach 4 bis 12 Passagen waren alle iPS Linien frei von Sendai-Virus. Die endogene Expression der Pluripotenzfaktoren konnte in allen iPS Linien nachgewiesen werden, während in zwei Kontroll iPS Linien keine Expression des Reprogrammierungsfaktors c-*MYC* gezeigt werden konnte. Bei der direkten kardialen Differenzierung war die Sensitivität der iPS Linien gegenüber CHIR99021 sehr variabel. Darüber hinaus hatte die ursprüngliche Dichte der Zellen beim Aussäen einen Effekt auf die Effizienz für Differenzierung. Während dieser wurden der Transkriptionsfaktor *TBX5* und *NPPA,* ein direktes Zielgen, in der HLHS Gruppe in sehr geringem Ausmass exprimiert. Die Expression von *NKX2.5* war bis Tag 8 in der

HLHS Gruppe verzögert, pendelte sich aber am Tag 10 ein. Die Expression von *ISL1* und *TNNT2* war in beiden Gruppen sehr ähnlich. Aus iPS Zellen generierte KMs begannen spontan zwischen Tag 7 und 9 zu schlagen. An Tag 14 konnten sowohl in der HLHS als auch in der Kontroll-Gruppe über 60% Trop T^+ Zellen detektiert werden.

Schlussfolgerung:

In der vorliegenden Arbeit habe ich bei sechs iPS Linien eine komplette Charakterisierung durchgeführt. Ich habe definierte und reproduzierbare Bedingungen bestimmt unter denen KMs in hoher Qualität und in grossen Mengen aus iPS Zellen generiert werden können. Meine Ergebnisse belegen, dass diese iPS Linien ein leistungsfähiges zelluläres System darstellen, um die molekularen Dysfunktionen des HLHS *in vitro* zu untersuchen. Die Ergebnisse zeigen auch, dass die aus iPS Zellen generierten KMs in Downstream-Anwendungen wie etwa der Generierung von engineered heart tissues verwendet werden können.

Table of Contents

Abbreviations

α-MHC	alpha-**M**myosin **H**heavy **C**chain
AA2P	L-**A**scorbic **A**acid **2**-**P**phosphate
ANF	**A**trial **N**atriuretci **F**acter
Ao	**Ao**rta
APC	**A**denomatosis **P**olyposis **C**oli
AS	**A**ortic valve **S**tenosis
ASD	**A**trial **S**eptal **D**efect
AV	**A**ortic **V**alve
AVSD	**A**trio**v**entricular **S**eptal **D**efect
BMP	**B**one **M**orphogenetic **P**rotein
BPM	**B**eat **P**er **M**inute
BPM4	**B**TB-**P**OZ and **M**ATH domain **4**
BSA	**B**ovine **S**erum **A**lbumin
BTB-POZ	BR-C, Tk and Bab/Pox virus and Zinc finger
CABG	**C**oronary **A**rtery **B**ypass **G**rafting
cDNA	**C**omplementary **DNA**
CF	**C**ardiac **F**ibroblast
CHD	**C**ongenital **H**eart **D**isease
CK1a	**C**asein **K**inase **1a**
CM	**C**ardio**m**yocyte
c-MYC	MYC proto-oncogene
CNV	**C**opy **N**umber **V**ariation
CoA	**C**oarctation of **A**orta
CP	**C**ardiac **P**rogenitor
CPC	**C**ardiac **P**rogenitor **C**ell
cTNT	**C**ardiac muscle **T**roponin **T**
DMSO	**D**i**m**ethyl **S**ulf**o**xide
EBs	**E**mbryoid **B**odies
EC	**E**ndothelial **C**ell
ECT	**E**ngineered **C**ardiac **T**issue
EDTA	**E**thylene**d**iamine**t**etr**a**cetic
EHS	**E**ngelbrecht-**H**olm-**S**warm
EHT	**E**ngineered **H**eart **T**issue
ESC	**E**mbryonic **S**tem **C**ell
FACS	**F**luorescence-**A**ctivated **C**ell **S**orter
FBS	**F**etal **B**ovine **S**erum
FCS	**F**etal **C**alf **S**erum
FGF	**F**ibroblast **G**rowth **F**actor
FHF	**F**irst **H**eart **F**ield
FOX	**F**orkhead box protein
FSC	**F**orward **Sc**attered light
GATA 4	GATA binding protein 4
GATA 6	GATA binding protein 6
GSK3	**G**lycogen **S**ynthase **K**inase 3
HAND 2	**H**eart- **A**nd **N**eural crest **D**erivatives-expressed protein 2

HF	**H**eart **F**ailure
HLHS	**H**ypoplastic **L**eft **H**eart **S**yndrome
HOS	**H**olt-**O**ram **S**yndrome
ICC	**I**mmuno**c**yto**c**hemistry
InDel	**In**sertion or **Del**etion of base
iPSC	**I**nduced **P**luripotent **S**tem **C**ell
Isl1	LIM-homeodomain transcription factor Islet1
Klf4	Kruppel-like factor 4
LA	**L**eft **A**trium
LV	**L**eft **V**entricle
MATH domain 4	**M**eprin **A**nd **T**raf **H**omology domain 4
MI	**M**yocardial **I**nfarction
miRNA	**mi**cro-**RNA**
MSC	**M**esenchymal **S**tem **C**ell
MV	**M**itral **V**alve
NCM	**N**ormal **C**ardiomyocyte **M**edium
NKX 2.5	Homeobox protein Nkx-2.5
Oct4	Octamer binding transcription factor 4
P/S	**P**enicillin/**S**treptomycin
PA	**P**ulmonary **A**rtery
PBMCs	**P**eripheral **B**lood **M**ononuclear **C**ells
PCI	**P**ercutaneous **C**oronary **I**ntervention
PDA	**P**atent **D**uctus **A**rteriosus
PFO	**P**ersistent **F**oramen **O**vale
PGS	**P**oly **G**lycerol **S**ebacate
PH3	**P**hospho-**H**istone **3**
PLB	**P**hospho**l**am**b**an
PP2A	**P**rotein **P**phosphatase **2A**
PSC	**P**luripotent **S**tem **C**ell
qRT-PCR	**q**uantitative **R**eal-**T**ime **P**olymerase **C**hain **R**eaction
RA	**R**ight **A**trium
RPMI	**R**oswell **P**ark **M**emorial **I**nstitute
RT	**R**oom **T**emperature
RV	**R**ight **V**entricle
SAERCA 2	Sarcoplasmic Ca^{2+}-ATPase 2
SC	**S**tem **C**ell
SDS	**S**odium **D**odecyl **S**ulfate
SeV	**Se**ndai **V**irus
SHF	**S**econd **H**eart **F**ield
SMC	**S**mooth **M**uscle **C**ell
SNP	**S**ingle **N**ucleotide **P**olymorphism
Sox2	SRY-related high-mobility-group-box protein-2Sex determining region box 2
SR	**S**arcoplasmic **R**eticulum
ssRNA	**s**ingle-**s**tranded **RNA**
TBX	T-box transcription factor
TCF/LEF	**T**-**C**ell **F**actor/**L**ymphoid **E**nhancer-binding **F**actor
TF	**T**ranscription **F**actor
TKI	**T**yrosine **K**inase **I**nhibitors
TNNT2	Troponin T2

TOF	**T**etralogy **O**f **F**allot
UPR	**U**nfolded **P**rotein **R**esponse
VSD	**V**entricular **S**eptal **D**efect
Wnt	Wingless/INT protein

List of Figures:

List of tables:

Introduction

1.1 Congenital heart disease

Congenital heart disease (CHD), which is also known as congenital heart anomaly or congenital cardiovascular malformation, is a disease of abnormal heart structure that is present at birth. CHD is one of the most common congenital defects in newborns. About 10-12 per thousand neonates are diagnosed with CHD, which is approximately 40,000 babies each year in the United States[1, 2]. In Germany nearly 6,000 babies are born with CHD every year[3].

1.1.1 Hypoplastic left heart syndrome

Hypoplastic left heart syndrome (HLHS) is a very severe CHD with a wide pathophysiological basis. HLHS is manifested by aortic valve and/or mitral valve stenosis or even atresia, with significant hypoplastic left ventricle, and hypoplasia of ascending aorta and aortic arch[4].

The prevalence of HLHS is approximately 0.16-0.36 per 1,000 live births in the United States[5] and around 0.15 per 1,000 newborns in Germany[6], accounting for 2-3% of all CHD[7]. The most common cardiac malformation in HLHS is the single-ventricle defect, due to the hypoplastic or missing left ventricle. Furthermore, there is a significant gender difference in the prevalence for HLHS: approximately 70% of the affected patients are male[8].

In HLHS, due to the severe dysplasia of the left heart structures, the aortic valve (AV) and mitral valve (MV) might be too small or even atretic, resulting in abnormal left ventricular circulation[9]. Whereas the big atrial septal defect (ASD) or small persistent foramen ovale (PFO) assures shunting of returning pulmonary venous blood with oxygen from the left to the right atrium. Meanwhile, the deoxygenated blood coming back from superior and inferior *Vena cava* will mix with the

oxygenated blood in the right atrium. Formerly, the mixed blood could flow through the tricuspid and pulmonary valve to the main pulmonary artery (PA). Part of the mixed blood will flow to the left and right PA for pulmonary perfusion, and another part will support the coronary and systemic perfusion via the maintained patent ductus arteriosus (PDA) (Fig. 1). This circumstance leads to severe cyanosis of the patient, nevertheless it is essential for the survival of the babies. Apart from cyanosis, the newborn HLHS babies suffer from respiratory distress, accompanied by weak peripheral pulse and low blood pressure (less than 40 mmHg).

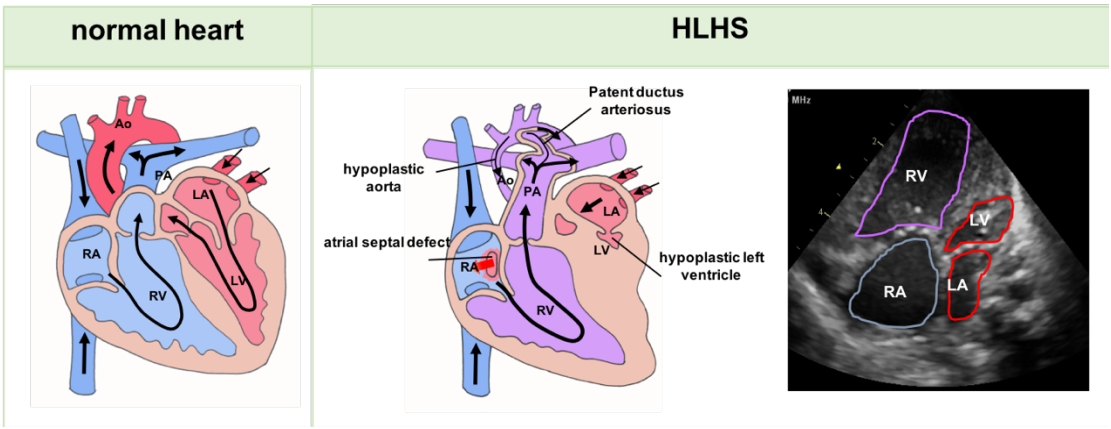

Figure 1 Morphology and blood flow of normal heart and HLHS heart.

Ao: aorta, LA: left atrium, LV: left ventricle, RA: right atrium, RV: right ventricle, PA: pulmonary artery, VSD: ventricular septal defect. The figure is adapted from Lahm et al., 2015[6]. The utilization of the picture has been permitted by the journal.

1.1.2 The causes of HLHS

The provoking pathogenic factors of HLHS are still uncertain. Some environmental factors might favor HLHS, such as intrauterine infection, myocarditis or immunologic injury[10]. A retrospective analysis of a 10-year multi-center database reveals that the incidence of HLHS was seasonally related. This report points out that children with HLHS are mostly born in the summer months[11].

Another hypothesis of the etiology of HLHS is the “flow theory” of cardiogenesis[12]. This theory indicates that the cardiac malformation of HLHS is due to the inappropriate

development of the valves, especially aortic and/or mitral valve stenosis or atresia. Subsequently, the abnormal hemodynamics of the left heart results in the underdevelopment of myocardium and left ventricle hypoplasia. Nevertheless, in a previously published article illustrates that the morphology of LV was not correlated to the degree of valvar stenosis [13].

The prevalence of HLHS is 0.016% - 0.036%[5]. While the risk of recurrence in families with two affected children is 0.5% to 2%, the risk of recurrence of other forms of CHD in families with one child suffering from HLHS will rise up to 2.2% to 13.5%[10]. This phenomenon reflects a strong genetic aspect in this CHD development.

HLHS is generally accepted as multi-gene associated disease. The genetic components include single base-pair variants (single nucleotide polymorphisms (SNPs), point mutations which may occur *de novo*, duplications or deletions of larger sequences (copy number variations (CNVs)) as well as aberrant methylation patterns[5]. At the chromosomal level, the partial or complete absence of an X chromosome causing Turner Syndrome is associated with HLHS. The prevalence of Turner Syndrome in live-born infants with HLHS ranges from 1 to 7%[14].

The mutations in essential cardiac transcription factors (TFs) such as *NKX2.5, HAND1, FOXC2, FOXL1* and combinations thereof have been described in patients with HLHS[6]. The research of Kobayashi and colleagues indicates that the *NKX2.5/HAND1* signal pathway plays an important role in left heart development during cardiogenesis and mutations of *NKX2.5* and *HAND1* could raise the risk of HLHS[15]. Another research has shown that CNVs are associated with HLHS pathogenesis[16]. Using the standard reference genome, CNVs ranges between 1 kb and several megabases and covers approximately 12% of the human genome[17]. Micro RNAs (miRNAs), such as miR-208, miR-30, miR-378 and others may play a critical role in the cardiogenesis of

HLHS[18-21]. Those genes could influence the development of HLHS by modulating the expression of TFs or their pathways.

Our previously published research indicates that *de novo* mutations which drive cardiomyogenesis are strongly associated with the formation of HLHS [22]. Mutations associated with the cell cycle, unfolded protein response (UPR), and autophagy hub affect the cardiac progenitor (CP) specialization at the initial stage of cardiomyogenesis, leading to interruption of CP lineage differentiation, unbalanced distribution of CM subtypes, and CMs immaturation. Immature CMs cause increased apoptosis, abnormal excitation contraction coupling, and ultimately cause ventricular dysplasia.

In general, HLHS is a multifactorial syndrome. Genetic, environmental, and hemodynamic factors alone or together might be the causes of this disease. However, further research is urgently needed.

1.1.3 Therapies for HLHS

Only 35 years ago, HLHS was undoubtedly a fatal CHD. In 1983, the cardiac surgeon William Norwood successfully introduced a surgical procedure to intervene the HLHS. The right heart system was utilized to support the patient's systemic circulation[23].At present, the treatment methods for HLHS patients mainly include the three-staged Norwood palliative surgery, heart transplantation or compassionate care. At the moment, heart transplantation seems to be the best option for its normal cardiac anatomy. However, due to the extreme shortage of donors, heart transplantation is very rarely a possible option. Apart from heart transplantation, Norwood surgery is still the gold standard treatment for these HLHS patients. Since now, great progress has been made in the prenatal diagnostics, pre-, intra-, and postoperative care, surgical techniques, and operation methods. These advances have led to a 90-92 % initial survival rate for standard-risk neonates undergoing surgery[24].

1.2 Pluripotent stem cells

1.2.1 Types of stem cells

Stem cells (SCs) are cells with self-renewal and broad differentiation potential. This kind of cell can proliferate spontaneously while maintaining its undifferentiated state. In addition, it has the ability to differentiate into all cell types of the organism from which it has been derived.

Historically, it was believed that SCs could only be obtained from the differentiated fertilized eggs or the inner cell mass of blastocysts, named embryonic stem cells (ESCs)[25] . Nevertheless, these cells also exist in all adult human tissues, termed adult stem cells like mesenchymal stem cells (MSCs)[26], hematopoietic stem cells[27], endothelial stem cells[28], neural stem cells[29], cancer stem cells[30] and others, which play an important role in tissue renewal and damage repair.

Depending on their regenerative potential, naturally occurring SCs could be divided into totipotent, omni- or pluripotent, multipotent and unipotent SCs. Totipotent SCs can develop into the three primary germ layers of the early embryo (ectoderm-, mesoderm- and endoderm layer) and extra-embryonic tissues such as placenta[31]. Omni- or pluripotent SCs (PSCs) are slightly more committed than totipotent cells and still can differentiate into all kinds of cells of the organism they were derived from[32]. However, without the ability to generate extra-embryonic tissues, PSCs are unable to form a complete organism. Thirdly, multipotency is a feature of adult SCs. These cells have the property to differentiate into all cells of the tissue from which they were derived[33].Finally, the unipotent SCs can only differentiate into one type or two closely related types of cells, such as stem cells in the basal layer of epithelial tissue and myoblasts in muscle.

Because of its vast self-renewal and differentiation potential, PSCs can be used for the research in innovative medicine or as a cell-based therapy to treat a variety of diseases

including heart diseases and diabetes. Nonetheless, decades ago the PSCs could only be isolated from the embryo which is an important ethical issue and therefore limiting the use of PSCs in scientific research and cell therapy. Since the establishment of SC lines and culture is banned for ethical reasons, the generation of induced pluripotent stem cells (iPSCs) has become a milestone in the medical and biological field[34]. iPSCs are a type of pluripotent SCs which are reprogrammed from human somatic cells. In 2007, Japanese scientist Shinya Yamanaka first reprogrammed adult human fibroblasts into pluripotent cells by overexpression of the four TFs (*OCT4, SOX2, KLF4* and *cMYC*)[35]. The Nobel Prize in Medicine 2012 was awarded jointly to Shinya Yamanaka and John B. Gurdon for their research on iPSCs.

As iPSCs are generated from somatic cells by reprogramming, researchers can overcome the ethical restrictions (bypass the need for embryos) and achieve unlimited supply of human pluripotent SCs. Meanwhile, the iPSCs can be derived in a patient-specific manner, which allow to investigate the disease development in specific cases of individual patients.

1.2.2 Reprogramming somatic cells into iPSCs

It has been more than 50 years ago since John Gurdon first proposed the concept of regeneration and cellular reprogramming[36]. At present, numerous somatic cells, including fibroblasts, keratinocytes[37], and peripheral blood mononuclear cells (PBMCs)[38], can be reprogrammed into iPSCs by introduction of the four TFs (*OCT4, SOX2, KLF4* and *cMYC*) with viral infection (non-integrating Sendai virus, lenti- or retroviruses) or non-viral approaches (episomal plasmid, miRNAs, small molecules, or others) (Fig.2).

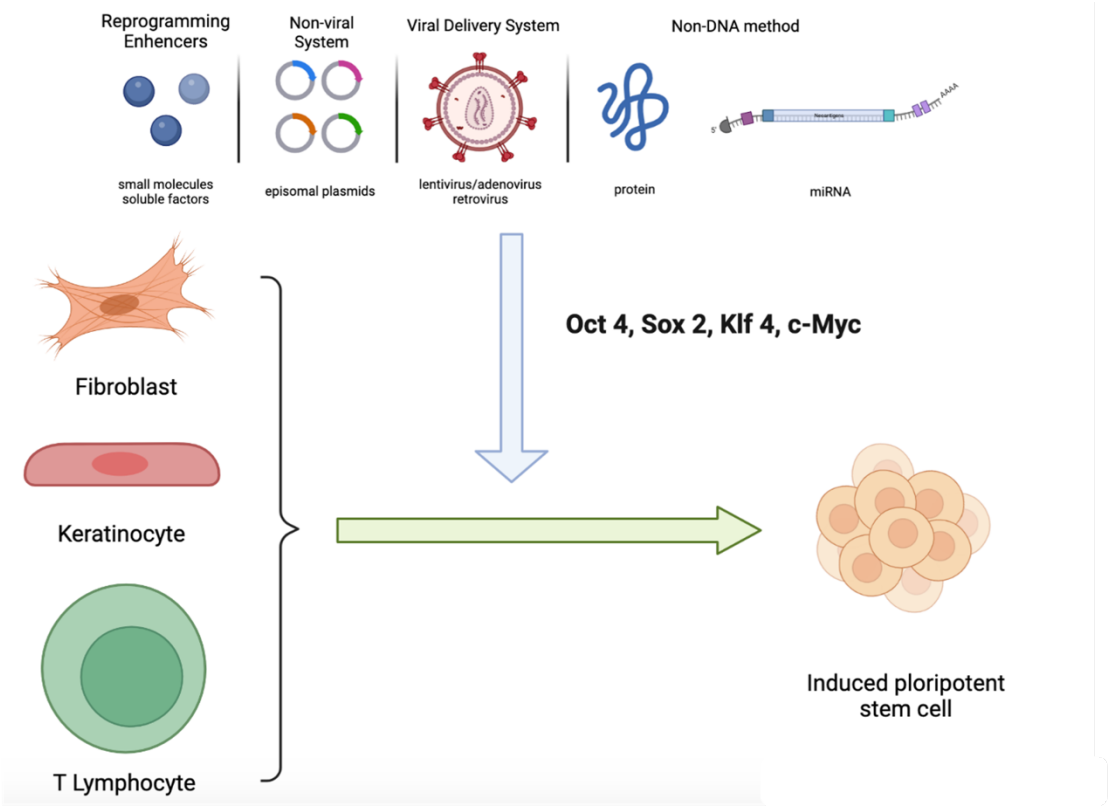

Figure 2. Strategies of reprogramming somatic cells into iPSCs.

Somatic cells can be reprogrammed into iPSCs by forcing the overexpression of the four TFs: *OCT4, SOX2, KLF4,* and *cMYC* by different approaches. Created with BioRender.com

Sendai virus (SeV) is a negative-sense single-stranded RNA (ssRNA) virus of the Paramyxoviridae family[39]. It contains of six genes coding for the viral proteins: NP (nucleocapsid protein), P (phosphoprotein), L (large protein) and the proteins essential for the fusion of the virus with the cell F (fusion protein), HN (Hemagglutinin-Neuraminidase) and the matrix (M protein). The ssRNA genome consists of six cistrons (NP, P, L, F, HN, M). Each cistron has its own initiation of transcription as well as its own termination signal and encodes one polypeptide each. SeV preparation for reprogramming can be obtained as a commercially available kit. The four TFs are cloned between the 3'end and the NP gene into the genome of a modified non-transmissible form of SeV in which the fusion gene (F) has been deleted. This prevents the production of infectious particles by infected cells[40].

The iPSCs used in this project were prepared using a reprogramming kit consisting of the above-mentioned modified SeV vectors. SeV infects cells by binding to sialic acid receptors present on the cell surface and replicates only in the cytoplasm of the infected cells. The sialic acid receptors are present on nearly all cell types, and therefore all somatic cells are prone to be used for reprogramming. Thus, the viral vectors introduce the four TFs (*OCT4, SOX2, KLF4* and *cMYC*) into the cells without integrating into the genome of host cells. According to the manufacturer's description, the virus is discharged from the cell after 6 to 7 passages, depending on the cell line[41].

1.2.3 Applications of human iPSCs in cardiovascular medicine

Cardiovascular disease remains the disease with the highest mortality rate world-wide accounting for 31% of all global deaths[42, 43]. Investigation of CMs is limited by the low or nearly non-existing proliferative potential of these cells. Direct isolation from healthy probands is no option and isolation from patient undergoing cardiovascular procedure would never result in sufficient numbers for further investigations. These circumstances lead to the absence of basic material for biological and medical demands which have to be given for researchers to study the mechanisms of heart disease. Thus, more effective diagnostic methods and appropriate treatment therapies are necessary. iPSCs provide an excellent solution for these problems. The cells can be reprogrammed from somatic cells and have no limitations with the respect to the cell source. iPSCs can be cultured and expanded with relatively simple methods and effectively differentiated into almost all kinds of human somatic cell types including CMs *in vitro*. The numerous iPSC-derived somatic cells are valuable tools for disease modeling, drug screening or toxicological analyses, and regenerative cell therapy. More importantly, the iPSCs can be obtained from individual persons, such as CHD patients, and differentiated into CMs for the study of disease mechanism, cellular disease model generation, and investigation of individualized drug sensitivities to potentially develop customized therapies.

1.3 Cardiac differentiation of iPSCs

1.3.1 Background of cardiac differentiation

The heart contains a subpopulation of multipotent SCs which have the capability of heart regeneration. However, only about 0.3 to 1% of the CMs can be replaced every year, and most of these renewal events occur in the first decade of life[44]. The very limited proliferation of CMs becomes an obstacle for the progress in several instances:

- Therapies for cardiovascular disease based on the transplantation of CMs or cardiomyogenic SCs to ameliorate the consequences of myocardial infarction (MI), characterized by a loss of myocardium due to oxygen and nutrient deficiency and the replacement with non-contractile scar tissue
- Cardiac disease modeling for CHD or dilated cardiomyopathy
- Pharmaceutical research to assess the benefit or toxic side-effect of heart-related drugs

The human SCs (hESCs or hiPSCs) can be expanded in large numbers and have the ability to generate the three germ layers of early embryos *in vitro*, enabling their differentiation into all cell types of human beings. These abilities of SCs can meet the researchers' requirement for high numbers of CMs.

Studies revealed that there are three central signaling pathways which play a critical role during the early stages of cardiogenesis: bone morphogenetic protein (BMP) pathway, Wingless/INT protein (Wnt) pathway, and the fibroblast growth factor (FGF) pathway[45]. By activating or inhibiting these pathways the researchers could induce cardiomyogenesis in SCs. This characteristic of SCs provides a new approach for researchers to obtain robust CMs *in vitro*.

In 2001, the research group of Kehat[46] reported successful differentiation of human ESCs into CMs by culturing ESCs in suspension and plating them to form three-dimensional aggregates, termed embryoid bodies (EBs), which comprise cells of the three embryonic germ layers. In this report, around 8.1% of EBs showed spontaneous contraction. Two years later, Beltrami et al.[47] identified a group of cardiac progenitor cells (CPCs) characterized by the expression of c-*KIT* with multi-directional differentiation ability. These cells could differentiate into CMs, smooth muscle cells (SMCs), and endothelial cells (ECs). Since Takahashi et al.[35] successfully reprogrammed human adult somatic cells into iPSCs in 2007, researchers began to utilize this new technology as a starting point for CM differentiation. In 2008, Mauritz et al.[48] generated murine CMs from iPSCs with the EB-based protocol and achieved around 55% of spontaneously beating EBs.

The studies of these pioneers opened a gate for follow-up researchers. In a manner of speaking, human iPSCs provide a renewable resource for the studies of cardiac development and function.

1.3.2 Current methods for cardiac differentiation

During the past decade, many successful protocols for iPSC-CMs differentiation have been reported[49-51]. These protocols can be divided into three types: 1) EB-mediated or spontaneous differentiation. 2) co-culture with stromal cells. 3) monolayer or direct cardiac differentiation.

For spontaneous differentiation, iPSCs are dissociated into single cells and cultured in suspension in medium containing fetal bovine serum (FBS). The cells will develop into three-dimensional aggregates and subsequently differentiate into the derivatives with three germ layers, termed EBs. With the addition of FBS and specific growth factors in the medium, the EBs can be induced to differentiate into CMs[52]. These initial protocols have the disadvantage that the efficiency of spontaneous differentiation is

poor with only 1 to 10 % of CMs[11, 53-55]. In addition, the differentiation medium contains animal products, like FBS which are not clearly defined. Such culture conditions result in difficulties of reproducibility. In order to raise the efficiency of differentiation and eliminate the use of undefined animal or human products, new protocols were developed. Serum-free defined media were used for CM differentiation such as APEL (StemCell Technologies)[56] and StemPro34 (Invitrogen)[57], growth factors including BTB-POZ and MATH domain 4 (BMP4), activin A, FGF2, which could improve the development of cardiac cells during differentiation. Meanwhile, spin EBs[58] or microwell EBs[59] methods were used in differentiation where the researchers could control the size of EBs.

Co-culture protocols, e.g., with visceral endodermal-like cells are used to optimize differentiation. In the embryonic stage, the visceral endoderm cells can promote the differentiation of cardiac precursor cells in adjacent mesoderm[60]. In 2003, Mummery et al. differentiated ESCs into CMs by co-culturing with visceral endodermal-like cells for the first time[61]. Two years later, Passier et al. refined this protocol[62].

Direct cardiac differentiation of iPSCs starts with cells plated on Matrigel-coated plates grown as monolayers. Subsequently, the iPSCs are exposed to certain growth factors, including BMP4, activin A, Wnt 3 and bFGF and others, in defined Roswell Park Memorial Institute (RPMI) medium supplemented with B27. In the classical protocol of direct cardiac differentiation, iPSCs are sequentially treated with activin A for 24 hours and then cultured in serum-free RPMI/B27 medium supplemented with BMP4[63]. The critical part of this protocol is the ratio of activin A to BMP4 and the time of addition and removal of these growth factors. Differentiation of iPSCs into CMs by modulating the Wnt signaling pathway is a further protocol of direct cardiac differentiation. Researchers could differentiate iPSCs by sequentially applying Wnt agonists and inhibitors[64]. These direct cardiac differentiation protocols are easy to handle, highly reproducible with a yield of more than 65% $TNNT2^{+}$ cells[65]. However, they need to adjust the growth factors temporally at the optimum concentration for each

cell line to induce the cardiac differentiation in comparable quantity and quality between the cell lines[66].

1.3.3 The effect of Wnt signaling pathways in cardiac differentiation

Wnt signaling pathways are a set of protein-based signal transduction pathways. Signals are transmitted to the interior of the cells by binding of ligands to the receptors on the cell surface[67]. Depending on the function, the Wnt signaling pathways can be separated into the Wnt/β-catenin signaling pathway (canonical Wnt pathway), the noncanonical planar cell polarity pathway, and the non-canonical Wnt/calcium pathway[68]. Among them, the Wnt/β-catenin pathway is one of the key regulating pathways which can be modulated in cardiogenesis.

The canonical Wnt signaling pathway displays a biphasic modulation effect during cardiogenesis. In the early stage of the embryo, Wnt/β-catenin could enhance the mesoderm formation[69] and increase the expansion of insulin gene enhancer protein 1 (Isl1) positive cardiovascular progenitors[70]. However, in the gastrula stage embryo, overexpression of Wnt/β-catenin signaling would block the development of CMs. The activation of Wnt/β-catenin signaling pathway will cause the accumulation of β-catenin in the nucleus which will interact with the TFs of the T-cell factor/lymphoid enhancer-binding factor (TCF/LEF) family[71] to co-activate target gene transcription. The β-catenin could be degraded by targeted ubiquitination by a protein complex, which comprises axin, adenomatosis polyposis coli (APC), protein phosphatase 2A (PP2A), glycogen synthase kinase 3 (GSK3), and casein kinase 1a (CK1a), and is afterwards digested within the proteasome[72, 73]. According to this characteristic, iPSC-CMs were generated by artificially enhancing the Wnt signaling pathway in the first stage to generate mesodermal cells, and subsequently inhibiting its activity after the formation of mesoderm[65, 74]. In my project, the small molecules CHIR99021 and Wnt-C59 were used for CM generation, which influence the Wnt/β-catenin signaling pathway in an agonistic and inhibitory way, respectively (Fig. 3).

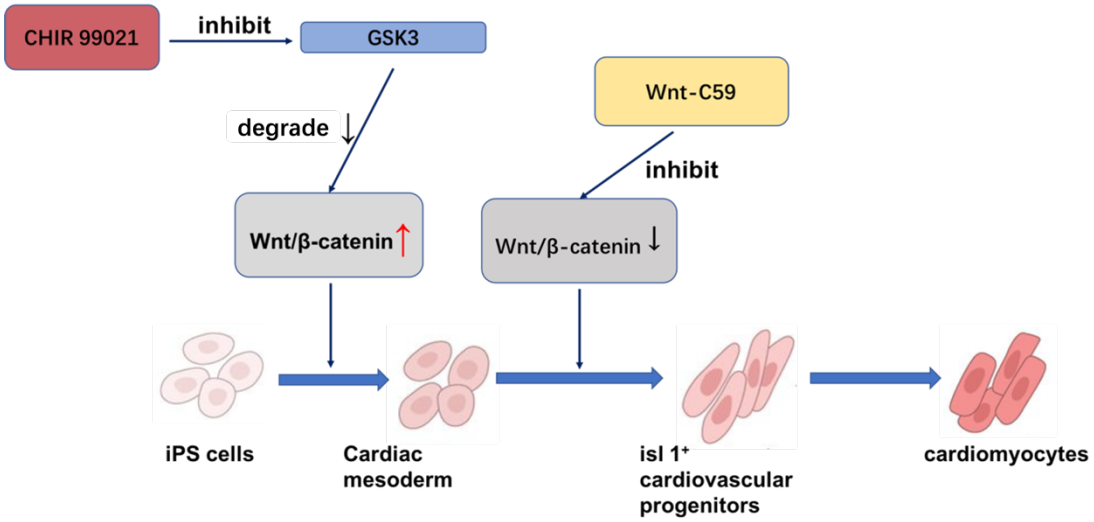

Figure 3. Direct differentiation by modulating the Wnt signaling pathway.

On day 0, CHIR 99021 can inhibit the digestion of GSK3 to Wnt/β-catenin, leading to accumulation of Wnt/β-catenin and iPSCs differentiation into cardiac mesoderm cells. Two days later, Wnt-C59 was added which can inhibit the function of the Wnt/β-catenin pathway. At this stage, cardiac mesoderm cells differentiate into cardiovascular progenitor cells. With extended culture period progenitor cells finally differentiate into CMs. Created with BioRender.com

1.4 The aim of this work

The aim of this project is the characterization of the iPSC lines derived from patients with HLHS and healthy controls and the production of highly enriched and pure CMs. The characterization of iPSCs includes: 1) Sendai footprint to guarantee completely virus-free lines were allowed for next experiment. 2) Endogenous expression of pluripotency factors. 3) Differentiation into cell types of all three germ layers. 4) Differentiation of the iPS lines with a direct cardiac differentiation protocol. The optimum conditions of the differentiation protocol have to be established for each individual iPSC line. It is an essential requirement to establish defined and reproducible conditions for production of CMs from HLHS and control lines to obtain CMs of high quality and quantity. Having characterized the iPSC lines and defined the conditions for their efficient cardiac differentiation, the generated iPSC-CMs shall prove their suitability in a downstream experiment such as the generation of engineered heart tissue.

(Fig.4)

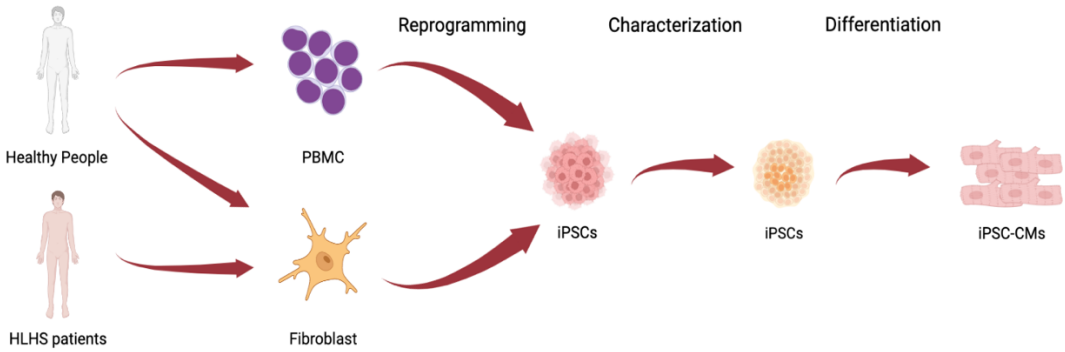

Figure 4. Workflow of this project.

Skin fibroblasts or PBMCs were obtained from HLHS patients and healthy people for iPSC reprogramming. Then the reprogrammed iPSCs were extensively characterized and differentiated into CMs. Created with BioRender.com

Materials

2.1 Used cell lines

Six iPSC lines were used in this project, including 3 lines from HLHS patients (experimental group with 2 males and 1 female) and 3 lines from healthy probands (control group with 2 males and 1 female). All iPSCs of HLHS lines were generated from skin fibroblasts of the patients. While one cell line of the control group was generated from skin fibroblasts, the other two lines were generated from PBMCs. The skin fibroblasts were established from a small biopsy. PBMCs were collected from the blood of the healthy probands, isolated by Ficoll-Paque density gradient centrifugation and stored in liquid nitrogen until reprogramming. All six iPSC lines were reprogrammed by non-integrating Sendai-Virus. Three iPSC lines were generated at the German Heart Center Munich (606, 612, S), the other three iPSC lines (375, H, C) were generated by the group of Dr. Moretti at the Klinikum rechts der Isar with the approvement of the local ethical committee at the respective institutions. All patients and probands have signed a written consent.

Table 1: HLHS iPSC lines used for the project

HLHS iPS lines	Sex	Diagnosis	reprogramming	Biological source
375	Male	HLHS, atresia of AV and MV	Sendai-Virus	Skin fibroblasts
606	Female	HLHS, atresia of AV and MV	Sendai-Virus	Skin fibroblasts
612	Male	HLHS, atresia of AV and MV	Sendai-Virus	Skin fibroblasts

iPS: induced pluripotent stem cell, HLHS: hypoplastic left heart syndrome, AV: aortic valve, MV: mitral valve

Table 2: Control iPSC lines used for the project

Control iPS lines	Sex	Diagnosis	reprogramming	Biological source

C	Female	Healthy	Sendai-Virus	Skin fibroblasts
H	Male	Healthy	Sendai-Virus	PBMC
S	Male	Healthy	Sendai-Virus	PBMC

iPS: induced pluripotent stem cell; PBMC: peripheral blood mononuclear cell.

2.2 Chemicals and reagents

In table 3 all chemicals and reagents used for my doctoral thesis are listed.

Table 3: Used chemicals and reagents

Designation	**order number**	**Manufacturer**
0.5 M EDTA (pH 8.0)	1109540	GIBCO
Agarose (PeqGOLD Universal)	35-1020	Peqlab
Albumin Human	SLBN8290V	SIGMA
Anti-alpha Myosin heavy chain (mouse IgG2)	MAB4470	Novus
Anti-cardiac troponin T [1C11] (mouse monoclonal IgG)	Ab8295	Abcam
Anti-cardiac troponin T-FITC	5160203052	Miltenyi Biotech
Anti-Connexin 40 (rabbit polyclonal IgG)	Ab38580	Abcam
Anti-Connexin 43 (mouse Ig G)	MAB3068	Merck Millipore
BD Perm/Wash Buffer (10 X)	6356786	BD Biosciences
Bovine Serum Albumin (BSA)	B14	ThermoFisher Scientific
CHIR99021	C-6556	LC Laboratories
Collagenase Type II	1775669	Life Technology
Corning Matrigel membrane matrix	7315687	CORNING

DAPI	Ab 104139	Abcam
dATP	R0141	ThermoFisher Scientific
dCTP	R0161	ThermoFisher Scientific
dGTP	R151	ThermoFisher Scientific
DNA Gel Loading Dye (6 X)	R0611	ThermoFisher Scientific
DEPC-Water (RNase free water)	4034	Peqlab
Dimethylsulfoxid	A994.2	Carl Roth
Dispase in Hanks' Balanced salt solution (5 U/mL)	07913	STEMCELL Technologies
DMEM/Ham's F12 Medium	0872F	Biochrom
DNase AWAY	7010	Molecular BioProduct
DNase Recombinant	15968900	Roche Diagnostics
DTT	Y00147	Invitrogen
dTTP	R0171	ThermoFisher Scientific
EDTA (4 mM)	CN 06.1	Carl Roth GmbH-Co.KG
FCS (EU approved origin, South America)	42G9273K	Gibco
Fixation and Permeabilization solution	6047882	BD Biosciences
Goat anti mouse IgG H&L (Alexa Flour 488)	Ab150113	Abcam
Goat-anti mouse Ig G H&L (Alexa Flour 555)	Ab 150114	Abcam
Goat-anti rabbit IgG H&L (Alexa Flour 488)	Ab 150077	Abcam
Goat serum	sc-2043	Santa Cruz Biotechnology
Goat serum	Sc45051	Santa Cruz Biotechnology
H_2O (bi-distilled)	R91051	H.Kerndl GmbH
H_2O (Millipore)		Merck Millipore
H_2O (VE)		Water purification system from DHM

Ham's F-12 Medium	0592F	Biochrom
Immersion oil	56822	Sigma Life Science
κ isotype control FITC (mouse IgM)	553474	BD Pharmingen
κ isotype control PerCP-Cyc5.5 (rat IgM)	560573	BD Pharmingen
L-Ascorbic acid 2-phosphate	SLBL2114V	SIGMA
MLC2a-FITC	130-106-191	Miltenyi-Biotec
MLC2v-APC	130-106-184	Miltenyi-Biotec
M-MLV Reverse Transcriptase	28025-013	invitrogen
Normal goat serum	Ab 7481	Abcam
Paraformaldehyde	0335.1	Carl Roth GmbH
PBS Dulbecco (10 X)	0410C	Biochrom
Penicillin-streptomycin (P/S) (100 X)	5020317	PanReac Applichem
Power SYBR Green (PCR Master Mix)	436759	ThermoFisher Scientific
Protector RNase Inhibitor	3335402001	Roche
Quantities DNA Marker (25 bp-500 bp)	240216	Biozym Scinetific GmbH
Quantities DNA Marker (GeneRuler, 50 bp)	SM0371	ThermoFisher Scientific
Random Primers (3 µg/µL)	48190-011	Invitrogen
ReLeSR™ (Enzyme-Free)	05872	STEMCELL Technologies
Rock inhibitor (Y-27632 2HCl)	16F71975	STEMCELL Technologies
RNase AWAY	7002	Molecular BioProducts
RPMI 1640 Medium	0732F	Biochrom
SOX-2 (1 mg/ml) (rabbit polyclonal IgG)	Ab137385	Abcam
TeSR™-E8™ basal Medium	05990	STEMCELL Technologies

Triton-X-100	3051.3	Carl Roth GmbH
Wnt C-59	S7037	Selleckchem

2.3 Consumables

All consumables used for my doctoral thesis are listed in table 4.

Table 4: Used consumables

Material	order number	Manufacturer
500 ml storage bottle	430282	CORNING
Disposable gloves (powder-free 100)	SSCR101	Sempermed
Nalgene Rapid Flow Filter	455-1000	ThermoFisher Scientific
6-well cell culture plate	E180134A	Bio-one
24-well cell culture plate	E16103N7	Bio-one
Millicell EZ slide (8-well Glass)	PEZGS0816	Merck Millipore
15/50 ml Falcon Tube	15417113	FALCON™
Pipette (0.1-10 µl, 1-100 µl, 100-1000 µl)	2149E-HR, 2065-HR, 2179-HR	ThermoFisher Scientific
10 ml pipette	7015	BD Falcon™
40 µm filter	542040	Greiner Bio-one
Rotilabo-spritzenfilter 0.22 µm	R6DA44688	Carl Roth GmbH
Cell scraper 24 cm	83.3950	SARSTEDT
Sprits Inject 25 ml	16H01C8	B Braun
Cryotube 1.0/1.8 ml	374081/347627	ThermoFisher Scientific
1.5 ml safe-lock tubes	0030121503	Eppendorf
Cryo 1°C Freezing Container	5100-0001	NALGENE™

Surphob Spitzen	VT0230	Biozym Scientific GmbH

2.4 Devices

In table 5 all devices used for my thesis are listed.

Table 5: Used devices

Devices	**Manufacturer**
EVOS Xl Core Microscope	ThermoFisher Scientific
Analytical balance	Kern & Sohn GmbH
BD LSRFortessa™	BD Biosciences
Fluorescence Microscope Axiovert 200M	ZEISS
Freezer -20°C	SIEMENS
Gel documentation device ChemDoc XR System	Bio-Rad Laboratories GmbH
HERAEUS Megafuge 16R centrifuge	ThermoFisher Scientific
HERA freezer -80°C	ThermoFisher Scientific
HERA Safe Hood	Heraeus Instruments
HERAcell 240i CO_2 incubator	ThermoFisher Scientific
Hettich Centrifuge Micro 220R	Andreas Hettich GmbH
Liquid nitrogen system	MESSER GRIESHEIM
Milli Q	Merck Millipore
NanoDrop 2000c Spectrophotometer	ThermoFisher Scientific
Pipetus	Hirschman Laborgeräte
PowerPac Basic gel electrophoresis device	Bio-Rad Laboratories GmbH
C1000 Touch Thermal Cycler	Biorad

Quant Studio 3	Applied Biosystems
Table centrifuge	Biozym
Table centrifuge 5417R	Eppendorf
Vortexer	Scientific Industries

2.5 Used Kits

In table 6 all used kits of my thesis work are listed.

Table 6: Used Kits

Material	Order number	Manufacturer
Fixation/permeabilization soluton kit	554714	BD Bioscience
M-MLV Reverse Transcriptase kit	28025-013	Invitrogen
peq GOLD DNase I Digest kit	12-1091-01	PeqLab
peq GOLD Total RNA kit	12-6834-02	PeqLab

2.6 Software

All utilized software is listed in table 7.

Table 7: Used software

Software	Company
Axio Vision (Version 4.8.2)	ZEISS
FlowJo 7.6.5	FlowJo LLC
NanoDrop 2000/2000c	ThermoFisher Scientific
Quantity One Chemidoc XRS (Version 4.6.9)	Bio-Rad Laboratories GmbH

Quant Studio Design & Analysis Software v1.4	Applied Biosystems by Thermo Fisher Scientific
SPSS 21.0	IBM SPSS, Inc

2.7 Manufactured solutions

All self-manufactured solutions are prepared as described in table 8.

Table 8: self-manufactured solutions

Solution	Preparation method
PBS/EDTA (0.5 mM)	50 µl EDTA (0.5 M) + 50 ml PBS (1X)
PBS (1 X)	10 ml PBS (10 X) + 90 ml Millipore H_2O
Dispase (1 U/ml)	5 ml dispase (5 U/ml) + 20 ml PBS (1X)
CDM3 Medium+P/S	500 ml RPMI 1640 medium + 250 mg Human Albumin + 1.5 ml P/S (100 X)
Collagenase II solution (400 U/ml)	1ml collagenase II solution (10,000 U/ml) + 24 ml PBS (1 X)
FACS-Buffer (PBS/0.5%BSA/4 mM EDTA)	1.0 g BSA + 1.2 ml EDTA (0.5 M) + 50 ml PBS (1X) Mix BSA, EDTA and PBS together and fill with 200 ml Millipore H_2O
PBS-T-Buffer (0.1%)	50 µl Triton-X-100 + 50 ml PBS (1X)
Bovine fibrinogen	200 mg/ml in NaCl 0.9% plus 0.5 µg/mg aprotinin
EHT culture medium	DMEM with 1% P/S, 10% horse serum, 10 µg/ml insulin, and 33 µg/ml aprotinin

2.8 Used primers

All used primers are listed in table 9.

Table 9: Used primers

gene	Accession number	5´→ 3´ (forward)	5´→ 3´ (reverse)
ACTA2	NM_001141945.2	**GTG ATC ACC ATC GGA AAT GAA**	**TCA TGA TGC TGT TGT AGG TGG T**

ACTB	NM_001101.3	**CCA ACC GCG AGA AGA TGA**	**CCA GAG GCG TAC AGG GAT AG**
AFP	NM_001134.2	**GTG CCA AGC TCA GGG TGT AG**	**CAG CCT CAA GTT GTT CCT CTG**
c-MYC	NM_002467.5	**CAC CAG CAG CGA CTC TGA**	**GAT CCA GAC TCT GAC CTT TTG C**
ISL1	NM_002202.2	**GCA GCC CAA TGA ACA AAA CTA A**	**CCG TCG TGT CTC TCT GGA CT**
KLF4	NM_001314052.1	**TCT TCG TGC ACC CAC TTG GG**	**CTG CTC AGC ACT TCC TCA AG**
KRT14	NM_000526.4	**CAC CTC TCC TCC TCC CAG TT**	**ATG ACC TTG GTG CGG ATT T**
NANOG	NM_024865.3	**TGC TTT GAA GCA TCC GAC TGT**	**GGT TGT TTG CCT TTG GGA CTG**
NKX2.5	NM_004387.3	**TTC TAT CCA CGT GCC TAC AGC**	**CTG TCT TCT CCA GCT CCA CC**
NPPA	NM_006172.3	**GAG CGG ACT GGG CTG TAA C**	**GGA GCC TCT TGC AGT CTG TC**
OCT4	NM_002701.5	**GGG ATG GCG TAC TGT GGG**	**GCA CCA GGG GTG ACG GTG**
REX1	NM_174900.4	**AGT AGT GCT CAC AGT CCA GCA G**	**TGT GCC CTT CTT GAA GGT TT**
SeV	M69046.1	**GGA TCA CTA GGT GAT ATC GAG C**	**ACC AGA CAA GAG TTT AAG AGA TAT GTA TC**
SOX2	NM_003106.3	**AGC AGA CTT CAC ATG TCC CAG**	**ACC GGG TTT TCT CCA TGC TGT**
TBX5	NM_000192.3	**TGA TCA TAA CCA AGG CTG GA**	**GAT TAA GGC CCG TCA CCT TC**
TNNT2	NM_000364.3	**ATG ATG CAT TTT GGG GGT TA**	**TCC TCC TCT CAG CCA GAA TC**

Methods

3.1 Human iPSC Culture

Prior to seeding of iPSCs, Matrigel (Corning, New York, NY) coated plates were prepared. Matrigel is a solubilized basement membrane product extracted from extracellular matrix protein-rich sarcoma of the Engelbreth-Holm-Swarm (EHS) mice. It contains all components of the extracellular basement membranes like laminin, collagen IV, heparan sulfate proteoglycan, and entactin/nidogen, but there is no cross-linking between these compositions, and they do not exhibit cross-linking as the basement membrane *in vivo*. The role of Matrigel is to facilitate the attachment of split cells to the surface of the culture dishes.

Matrigel was thawed at 4°C on ice for 1 hour before use. Once thawed, tubes were slightly mixed to ensure that the material is evenly dispersed. Matrigel was aliquoted into Eppendorf tubes sufficient to prepare 25 ml Matrigel/Ham's F12 (Biochrom GmbH, Berlin, Germany, final concentration 0.11 mg/ml) solution, which is the normal amount to prepare for one splitting procedure in our lab. 800 µl/well Matrigel solution in 6-well plates or 300 µl/well in 24-well plates have been used. It has to be guaranteed that the surface is completely covered by the Matrigel solution. Coated plates should be allowed to polymerize at room temperature (RT) for 2 hours or at 37°C for 30 min in the incubator (HERAcell 240i CO_2 incubator, Thermo Scientific, Waltram, MA) before use.

The iPSC lines for the project were provided by German Heart Center and the Klinikum rechts der Isar as frozen vials in liquid nitrogen (Liquid nitrogen system, Messer Griesheim, Bad Soden, Germany). Once the cryovial was removed from the liquid nitrogen, it was immediately immersed in a 37°C water bath until the cells began to thaw. Cells were transferred to a 15 ml falcon tube, which was filled up with 10 ml E8 culture medium (TeSR™-E8™ basal Medium, StemCell™ Technologies, Cologne, Germany) and then centrifuged at 1200 rpm (HERAEUS Megafuge 16R centrifuge, Thermo Scientific, Waltram, MA) for 8 min. After centrifugation, the supernatant was aspirated and the cell pellet was carefully resuspended with E8 culture medium,

supplemented with Y27632 ROCK inhibitor (StemCell™ Technologies, Cologne, Germany, final concentration 10 μM). Finally, the cell suspension was transferred to the cell culture plate. It has to be pointed out that the area of plating always corresponded to the area when the cells were frozen (e.g., one well of a 6-well plate).

For routine culture cells were incubated at 37°C and 5% CO2 in a humidified atmosphere. Normally the iPSCs were approximately 70% confluent within 5 days after the previous splitting at a ratio of 1 to 12. Nevertheless, despite being pluripotent, iPSCs tend to differentiate during cell culture and those differentiated fibroblast-like cells may arise around the edges of iPS colonies. Therefore, ReLeSR™ (StemCell™ Technologies, Cologne, Germany) was used as dissociating buffer for passaging of iPSCs. ReLeSR™ is an enzyme-free reagent which can selectively detach undifferentiated cells and easily generates aggregates of optimum size without manual scraping. iPSC passage was carried out according to the manufacturer's protocol. Cells were washed with PBS (1 X PBS Dulbecco, w/o Ca^{2+}, Biochrom GmbH, Berlin, Germany) twice and 1 ml ReLeSR™ buffer was added for 1 min at RT. Afterwards, ReLeSR™ buffer was aspirated, and the cells were incubated at 37°C for 3-5 min without any solution. After incubation, the cells were resuspended with E8 culture medium. The side of the plate was firmly tapped for 30-60 seconds to detach the colonies. Then the cell suspension was transferred to new Matrigel-coated plates (the splitting ratio 1:12).

3.2 Direct Cardiac Differentiation of Human iPSCs

A direct cardiac differentiation protocol was used to differentiate the iPSCs to CMs in 24-well plates. At least 3 confluent 6-well plates of iPSCs were used for differentiation in one 24-well plate. Two to three days after splitting from 6-well plates, cells generated a monolayer culture and were 100% confluent in the 24-well plate. During the differentiation, a chemically defined medium (CDM3 medium) was used which comprises three components: RPMI 1640 medium (with 2 mM glutamine, Biochrom GmbH, Berlin, Germany), *Oryza sativa*-derived recombinant human serum albumin (Sigma Aldrich, Darmstadt, Germany, final concentration 500 μg/ml), and freshly

prepared L-ascorbic acid 2-phosphate (AA2P, Sigma Aldrich, Darmstadt, Germany, final concentration 213 µg/ml). To induce the differentiation of iPSCs in cardiac direction, additional factors, so-called “small molecules”, were added on defined days. According to the protocol of Burridge et al.[64], the small molecules CHIR99021 and Wnt-C59 were used to generate CMs. CHIR99021 (LC Laboratories, Woburn, MA) was added on day 0 (D0) of differentiation for two days at a final concentration of 6 µM for activating the Wnt signaling pathway. On day 2 (D2), Wnt-C59 (Selleckchem, Houston, TX) was added at a final concentration of 2 µM for two days to inhibit the Wnt signaling pathway. On day 4, the culture medium was changed to CDM3 medium alone and was changed every other day until day 14 (Fig. 5).

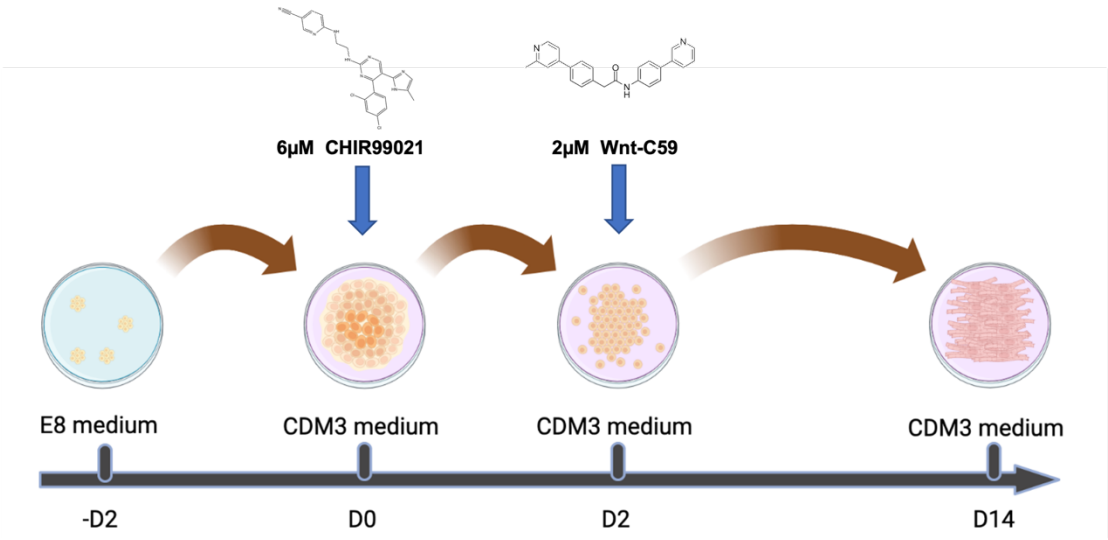

Figure 5. Schematic course of the directed differentiation.

Cells for direct cardiac differentiation were cultured on Matrigel coated 24-well plate. Differentiation stated on D0 with the addition of CHIR99021. On D2, the media changed to CDM3 containing Wnt-C59. By D4, the medium was changed every other day with CDM3 only. Created with BioRender.com

3.3 Spontaneous cardiac differentiation of human iPSCs

For spontaneous differentiation, iPSCs were cultured in Matrigel-coated 6-well plates in mTeSR1 medium (StemCell Technologies, Cologne, Germany) for 2 passages before differentiation. Assay was started at approximately 75% confluence of iPSCs.

The cells were detached with accutase, scraped off with a cell scraper, spun down at 1000 rpm for 10 min at RT and were resuspended with 4 ml mTeSR1 medium and transferred into a 6-well plate coated with 5% poly-hema (Sigma Aldrich, Darmstadt, Germany) . Cells were cultured in mTeSR1 medium for another three. By day 3 small aggregates, so-called embryoid bodies, had formed and the medium was replaced by cardiac differentiation medium, which was composed of DMEM/Ham's F12 (Biochrom GmbH, Berlin, Germany) supplemented with 20% FBS (EU approved origin, South America) (Gibco), 1% of 100x MEM non-essential amino acids (Invitrogen), 0.1 mM ß-mercaptoethanol (Sigma Aldrich, Darmstadt, Germany), 50 µg/ml vitamin C (Sigma Aldrich, Darmstadt, Germany) and 0.2% of 100x Pen/Strep (Thermo Scientific, Waltram, MA). These embryoid bodies were kept in cardiac differentiation medium in poly-hema coated plates till day 7. By day 7 large "embryoid bodies" had formed and were transferred onto 0.1% gelatin-coated (Sigma Aldrich, Darmstadt, Germany) 6-well plate (20~30 EBs per well). EBs were cultured in cardiac differentiation medium until day 21 with medium change every second day (Fig. 6). Normally the first beating area appeared around day 10-12.

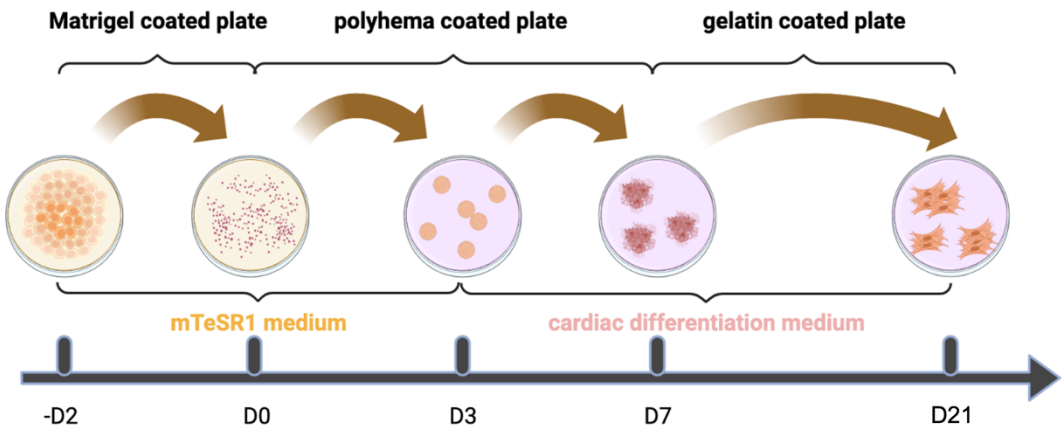

Figure 6. Schematic course of the spontaneous differentiation.

Cells for spontaneous differentiation were cultured on Martrigel-coated plate with mTeSR1 medium. Differentiation started by transferring iPSCs on poly-hema-coated plate for suspension culture. Since D3 the culture medium was changed to cardiac differentiation medium. On D7, the EBs were transferred on gelatin-coated plate and kept on culture till D21. Created with BioRender.com

3.4 iPSC-CM dissociation and Freezing

On day 14 of differentiation, iPSC-CMs were washed with PBS (1 X) for 5 min and digested with collagenase II (Thermo Scientific, Waltram, MA, final concentration 200 U/ml) for 3.5 hours to obtain a single-cell suspension. After dissociation, the cell suspension was transferred to a 15 ml Falcon tube and centrifuged at 100 X *g* for 15 min. Subsequently, the supernatant was aspirated and the iPSC-CMs were resuspended in 1 ml CDM3 medium. For cell counting, 10 µl suspension were diluted with 0.4% trypan blue (ThermoFisher Scientific, Waltram, MA) appropriately and counted in the Neubauer chamber (Thomas Scientific, Swedesboro, NJ) under the microscope (EVOS Xl Core, ThermoFisher Scientific, Waltram, MA). After cell counting, iPSC-CMs were centrifuged again and resuspended with freezing medium (90% FCS with 10% dimethylsulfoxide (DMSO, Carl Roth, Karlsruhe, Germany)) and transferred to 1.5 ml cryotubes. The CMs were kept in a cryobox (Cryo 1°C Freezing Container, NALGENE^{TM}, ThermoFisher Scientific, Waltram, MA) at -20°C for 2 hours and then transferred to -80°C refrigerator (HERA freezer -80°C, Thermo Scientific, Waltram, MA) overnight. The next day, the cells were transferred in liquid nitrogen.

3.5 Quantification of iPSC-CM using flow cytometry

Fluorescence-activated cell sorter (FACS) is a measuring device for the analysis and preparation of individual cells in suspension due to the different scattered light and fluorescence properties of the individual cells. This examination is also known as flow cytometry. In this project, flow cytometry was used to quantify the purification of the iPSC-CMs generated from HLHS and control lines.

Cardiac troponin T (cTnT) is part of the troponin complex in CMs, which is located on the thin filaments of the striated muscle. Alpha-myosin heavy chain (α-MHC) is an actin-based motor protein which binds to the A-band of thick filament of cardiac muscle myosin. In this project, cTnT and α-MHC were chosen as markers to assess the purity of iPSC-CMs. The CMs were stained with anti-cTnT antibody (clone 1C11, ab8295,

Abcam, Cambridge, MA) at a final concentration of 10 µg/ml and anti α-MHC (MAB4470, Novus Biologicals, Littleton, CO) at a final concentration of 2.5 µg/ml as the first antibody, respectively. As the secondary antibody goat anti-mouse IgG H&L (Alexa Flour 488, Abcam, Cambridge, MA) was used at a final concentration of 1 µg/ml.

On day 14 of differentiation, iPSC-CMs were dissociated into single cells as described above and centrifuged for 5 min at a low rotation of 100 x *g*. After centrifugation, the DNase solution (DNase I recombinant, Roche Diagnostics, Mannheim, Germany, final concentration 60 units/ml) was added and incubated at RT for 5 min. Then cells were fixed and permeabilized at RT for 20 min with 100 µl fixation / permeabilization solution (1 X, BD Biosciences, Franklin Lakes, NJ) and washed twice with 1 ml BD Perm/Wash buffer (BD Biosciences, Franklin Lakes, NJ). The primary antibodies, anti-Troponin T and anti-α-MHC, were added at a dilution of 1 to 200 in wash buffer according to the manufacturer's recommendation. First antibodies were incubated for 30 min on ice and washed with BD Perm/Wash buffer. Subsequently, the secondary fluorescent dye-labeled antibody goat anti-mouse IgG H&L Alexa Flour 488 (diluted 1:2000) was added and cells were incubated for 1 hour on ice in the dark. After incubation, all samples were washed twice and resuspended with 300 µl FACS buffer (PBS/0.5% BSA/4 mM EDTA). Finally, samples were evaluated by FACS instrument (BD LSRFortessa, BD Biosciences, Franklin Lakes, NJ) and data were analyzed with FlowJo 7.6.5 (Table 7).

3.6 Immunocytochemistry

Immunocytochemistry (ICC) is a technique to determine the localization of specific antigens in tissue or more detailed on single cells. By recognition of specific epitopes with the primary antibody, the distribution of a given protein can be visualized *in situ* after incubation with secondary fluorescence-labeled antibodies under a fluorescence microscope.

Cytochemical staining was performed to detect the presence of sarcomeric structures, such as Troponin T, α-actinin, α-MHC and gap junction proteins like connexin 40 and connexin 43, in iPSC-CMs on day 30 of differentiation. The primary antibodies were anti-Trop T (1C11) mouse IgG1 (ab8295, Abcam, Cambridge, MA), anti- α-MHC mouse IgG2b (MAB3370, Novus biological, Littleton, CO), anti-sarcomeric α-actinin mouse IgG1 (ab9465, Abcam, Cambridge, MA), anti-Connexin 40 rabbit IgG (ab38580, Abcam, Cambridge, MA), and anti-Connexin 43 mouse IgG1 (MAB3068, Merck Millipore, Darmstadt, Germany). The secondary antibody for Trop T, α-actinin, α-MHC, and connexin 43 was goat-anti-mouse IgG H&L Fluor 555 (ab150114, Abcam, Cambridge, MA) and the secondary antibody for connexin 40 was goat-anti-rabbit IgG AlexaFluor 488 (ab150077, Abcam, Cambridge, MA).

Staining of intracellular structures implicates fixation and permeabilization of the cells. By briefly washing the cells in PBS (1 X), the remaining medium was removed. Cells were fixed in 4% paraformaldehyde (Carl Roth GmbH, Karlsruhe, Germany) for TropT, α-Actinin and α-MHC staining for 10 min at RT. Connexin stainings implicated fixation with 100% acetone at -20°C for 10 min. Subsequently, samples were washed twice in PBS (1 X) buffer. Cells were permeabilized with 0.1% Triton-X-100 (PBS-T, Carl Roth GmbH, Karlsruhe, Germany) for 10 min at RT. All further washing steps during staining were done with 0.1% PBS-T. To reduce background staining, cells were incubated with serum of the species from which the secondary antibody was derived and the concentration was given in table 10. iPSC-CMs used for TropT, α-Actinin and α-MHC staining were incubated in 10% normal goat serum (Abcam, Cambridge, MA) in 0.1% PBS-T, while cells used for connexin 40 and connexin 43 staining were incubated in 5% normal goat serum in 0.1% PBS-T. All samples were incubated at RT for 60 min and washed twice with PBS-T. Subsequently, the primary antibodies were added to the cells using the conditions mentioned in table 10. After incubation with the first antibody for 1 hour at 4°C, cells were washed twice and stained with the corresponding secondary antibodies as mentioned in table 10 and incubated for 1 hour at RT in dark. Next, cells were washed twice with PBS and once with aq. bidest. Thereafter, the separation chamber was removed and slides were allowed to air dry in the dark. To visualize the cell nuclei a mounting medium containing 4,6-diamidino-2-

phenylindole (DAPI, Ab 104139, Abcam, Cambridge, MA) was used. Finally, slides were covered with coverslips.

Table 10. The antibodies used for immunochemistry staining.

Primary Antibodies	Dilution	Final concentration
Anti-cardiac Trop T	1:100	20 µg/ml
Anti-α-MHC	1:50	10 µg/ml
Anti-sarcomeric α-actinin	1:200	5 µg/ml
Anti-Connexin 40	1:100	10 µg/ml
Anti-Connexin 43	1:100	2.5 µg/ml
Secondary Antibodies	**Dilution**	**Final concentration**
Goat-anti-mouse IgG Alexa 555	1:500	4 µg/ml
Goat-anti-mouse IgG Alexa 488	1:500	4 µg/ml

Staining was evaluated by a fluorescence microscope (Axiovert 200M, Carl Zeiss, Oberkochen, Germany). The pictures were taken at 100x and 400x magnification.

3.7 Gene expression analysis of cardiac TFs

3.7.1 RNA extraction

For gene expression analysis, cells were harvest at several time-points during differentiation. From day 0 to day 14, cells were lysed with 100 µl RNA Lysis Buffer T (PeqLab, Erlangen, Germany) every second day. The isolation of RNA from the cells was carried out with peqGOLD Total RNA kit (PeqLab, Erlangen, Germany) according to the manufacturer's recommendation. In brief, the lysate was transferred onto a DNA removing column to get rid of genomic DNA by absorption to a matrix of silica gel and centrifuged for 1 min at 12000 x *g*. An equal volume of 70% ethanol (100 µl) was added to the flowthrough, and the solution was thoroughly vortexed and transferred onto an

RNA-binding column and centrifuged for 1 min at 10000 x *g*. The column was washed with 500 µl RNA Wash Buffer I and centrifuged for 1 min at 10000 x *g*. To digest residual genomic DNA of total RNA, DNase I was added, which cleaves DNA into small fragments. For this purpose, a DNase I reaction mixture was prepared (per sample: 73.5 µl DNase I digestion buffer + 1.5 µl RNase-free DNase I) at a final concentration of 4 units/ml, pipetted onto the RNA-binding column and incubated at RT for 15 min. Columns were sequentially washed with 400 µl RNA Wash Buffer I and 600 µl RNA Wash Buffer II. To remove residual ethanol the columns were centrifuged dry for 1 min at 10000 x *g*. Finally, 50 µl RNase-free water are added onto the matrix, columns are centrifuged for 1 min at 10000 x *g* and the eluted RNA is collected in a fresh 1.5 ml Eppendorf tube. After RNA extraction, the RNA concentration of the purified samples was measured using the NanoDrop spectrophotometer (Thermo Scientific, Waltram, MA) and stored at -20°C for cDNA synthesis.

3.7.2 cDNA synthesis

The cDNA (complementary DNA), which is synthesized from the purified RNA serves as a template for the downstream RT-PCR expression analyses. The cDNA was produced with an M-MLV Reverse Transcriptase Kit (Thermo Scientific, Waltram, MA). First, 1.5 µl 2'-deoxyribonucleoside5'-triphosphates (dNTPs, 10 mM), 1.5 µl random hexamer primers (250 ng), and 100 ng total RNA were mixed and filled up with RNase-free water to 19 µl. The mixture was heated to 65°C for 5 min in a conventional block cycler (Bio-Rad Laboratories, Hercules, CA). The second master mix consisted of 1 µl RNase-free (Peqlab, Erlangen, Germany), 6 µl First Strand Buffer (5x, Thermo Scientific, Waltram, MA), and 3 µl DTT (0.1 mM, Thermo Scientific, Waltram, MA) per sample. After addition of the second master mix, the samples were mixed and incubated in the block cycler (Bio-Rad Laboratories, Hercules, CA) for 2 min at 37° C. Finally, 1 µl of M-MLV Reverse Transcriptase (Thermo Scientific, Waltram, MA) was added to the samples to synthesize a single-stranded DNA complementary strand from the RNA using the following conditions in a block cycler:
10 min at 25° C
50 min at 37° C
15 min at 75° C

After incubation, the cDNA was stored at -20 °C until further use.

3.7.3 Real-Time Polymerase Chain Reaction

The real-time polymerase chain reaction (RT-PCR) is a technique for semi-quantitatively assess the expression of a gene of interest. A master mix was prepared for the RT-PCR that contains all the reagents required for the reaction (Table 11). The primers used in this project are shown in Table 9.

Table 11: Reaction setup for qRT-PCR of mRNA.

Reagents	Final concentration	Volume (µl)
Template cDNA	-	1
Power SYBR Green PCR Mastermix (2x)	1x	10
Primer forward (5 µM)	0.3 µM	1.2
Primer reverse (5 µM)	0.3 µM	1.2
PCR grade water	-	6.6
Total volume		20

The master mix prepared was mixed and distributed (19 µl per well) into individual wells of a 96-well plate. 1 µl cDNA sample to be amplified was added to each well. The plate was sealed with a film and centrifuged for 30 seconds (Mini Plate Spinner mps 1000, Labnet, Edison, NJ) in order to collect both the template and the master mix at the bottom of the plate. The RT-PCR was performed with Quant Studio 3 (Thermo Fisher, Waltram, MA). Programs for the RT-PCR runs were prepared using the Quant Studio Design & Analysis software (Thermo Fisher, Waltram, MA). The RT-PCR conditions are shown in Table 12.

Table 12: Thermocycling profile for RT-PCR.

Reaction step	Duration (S)	Temperature (°C)

Initial activation:	120	50°C
	600	95°C
40 cycles: denaturation	15	95°C
annealing, extension	60	60°C
melting curve	15 60	95°C 60°C 60 - 95°C at 0.15°C/sec
cooling	∞	4°C

The qRT-PCR is initially carried out on all samples with the primers specific for the *β-actin* gene. *β-actin* belongs to the group of so-called housekeeping genes, whose products are necessary for cell development and cell maintenance. These genes are detectable at any time and are expressed in large quantities in the cells. This enables to check the efficiency of cDNA synthesis. In addition, the *β-actin* values serve as a reference for evaluating the measurement results. Since it is assumed that housekeeping genes are not or at least hardly subject to regulation and are similarly expressed in all samples, *β-actin* can be used as a reference gene to estimate the relative change in gene expression.

3.7.4 Separation of amplified PCR fragments by gel electrophoresis

The agarose is dissolved in TBE buffer solution at a concentration of 2.0%, boiled in a microwave and supplemented with ethidium bromide. Then the agarose gel was poured into a gel chamber with a comb inserted for pockets. After the solidification, the comb was removed, and the gel chamber was placed into the electrode chamber. The samples (20 µl PCR reactions) were mixed with 4 µl 6 X loading dye solution and pipetted into the pockets. After applying all samples, 120 V were applied for 40 minutes. Due to the negative charge of the DNA, the samples migrate through the gel from the cathode to the anode. The mobility of the molecules depends on their size. Short DNA fragments migrate faster than long ones and thus the shortest strands in the gel migrate the furthest

towards the anode. For size determination of the electrophoresed fragments, appropriate molecular weight markers are run in a separate lane. The electrophoresed fragments were visualized under UV light with a gel electrophoresis documentation system (ChemiDoc Imaging System, Bio-Rad, Hercules, CA).

3.8 Statistics

Statistical calculations were performed with SPSS Statistics 21.0 (IBM SPSS, Armonk, NY). Data are presented as means and standard error or 95% confidence intervals as indicated. Error bars indicate standard deviations. Differences between groups were analyzed using One-way ANOVA test for paired comparisons. Continuous variables in distinct groups were compared with Student's t-test. Two-tailed P-values less than 0.05 were considered statistically significant.

Results

4.1 Characterization of human patient-specific and control iPSC lines

All six cell lines formed nice compact colonies (Fig. 6A to 11A), typical for human iPSCs. Further, a full characterization of the generated iPSC lines is essential.

Sendai footprinting was performed to guarantee the absence of the Sendai virus genome in the iPS clones. The positive control came from 1456 adipose fibroblasts, which had already been infected with Sendai virus. All six cell lines were checked and only those lines which were completely virus-free were allowed to be utilized for further experiments. Figures 6 B to 11 B illustrated the absence of Sendai-related sequences (181 bp) for each iPSC line. As an internal control, the housekeeping gene β-actin (96 bp) was amplified in each case to prove the presence of amplifiable cDNA. These results confirmed that all iPSC lines which were analyzed in this experiment were Sendai-free.

Another analysis was done to confirm that the iPSC endogenously express *OCT4, KLF4, SOX2, c-MYC, NANOG*, and *REX1*. In parallel, sequences of the housekeeping gene β-actin were amplified as well. Fig. 6 C to 11 C showed the expression of the pluripotency factors for each individual line. The expression of *OCT4* (148 bp)*, KLF4* (133 bp) and *SOX2* (191 bp), which were used for reprogramming, could be detected in all six iPSC lines. In contrast, *c-MYC* (101 bp) expression could only be detected in four cell lines but was absent in S and C line (Fig. 6C and 7C). In addition, the expression of two further pluripotency factors, *NANOG* (193 bp) and *REX1* (105 bp) could be detected in all cell lines. Next, the expression of NANOG, SOX2 and TRA1-81 was analyzed by ICC and a convincing fluorescent signal was detected in all six iPSC lines (Fig. 6 E to 11 E).

Another property of iPSC lines is the ability of differentiation into cell types of three germ layers. This capacity was validated during spontaneous differentiation by RT-PCR. Samples of iPSC lines were examined on day 0 and day 21 for the expression of marker genes indicative for each germ layer: *AFP* (endoderm), *ACTA2* (mesoderm), and *KRT14* (ectoderm). In all instances a strong increase of the expression of marker genes could be seen on day 21 of spontaneous differentiation (Fig. 6 D to 11 D). In another approach the differentiation competency of iPSCs was assessed in advance. iPSC-CMs were harvested on differentiated day 21 for detecting the cardiac-specific structural protein TNNT2 by ICC. Cells of all lines stained positively for TNNT2 (Fig. 6 F to 11 F).

Together, these results clearly indicated that the iPSCs used in this project were Sendai virus-free with confirmed pluripotent nature. These cells had differentiation competency and could be differentiated into cells of all three germlayers.

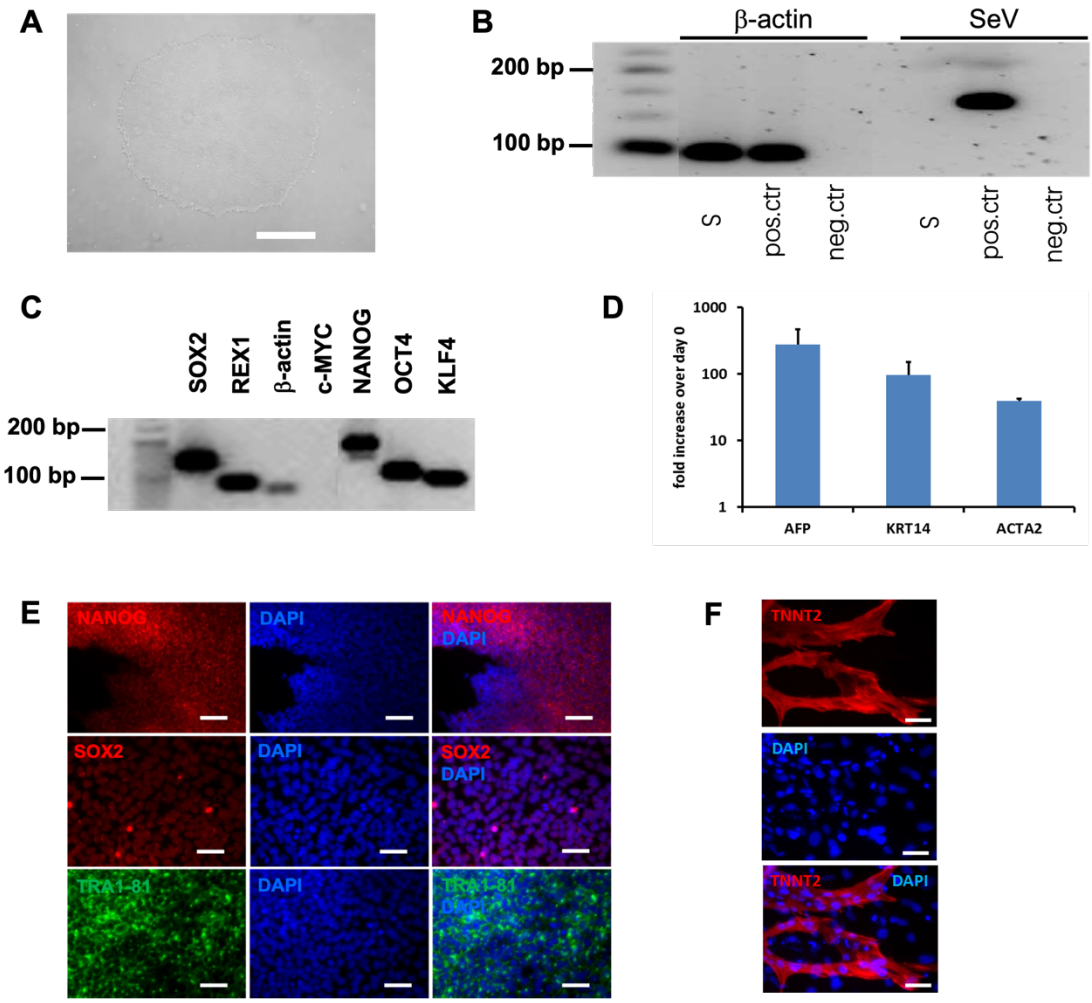

Figure 6. Characterization of S-line.

(A) Colony of iPSCs from S-line plated on Matrigel. (B) The RT-PCR showed Sendai virus-free in the S-line. (C) RT-PCR displayed the expression of *OCT4, KLF4, SOX2, c-MYC, NANOG, REX1,* and *β-actin* genes. (D) Relative expression of the three germ-layer genes *AFP, KRT14,* and *ACTA2* after spontaneous differentiation. (E) ICC showed the expression of the iPS-specific pluripotency factors, NANOG, SOX2, and TRA1-81. (F) ICC showed the expression of CM-specific protein TNNT2 after direct cardiac differentiation. Scale bars: A, 500 μm; E,100 μm; F, 20 μm

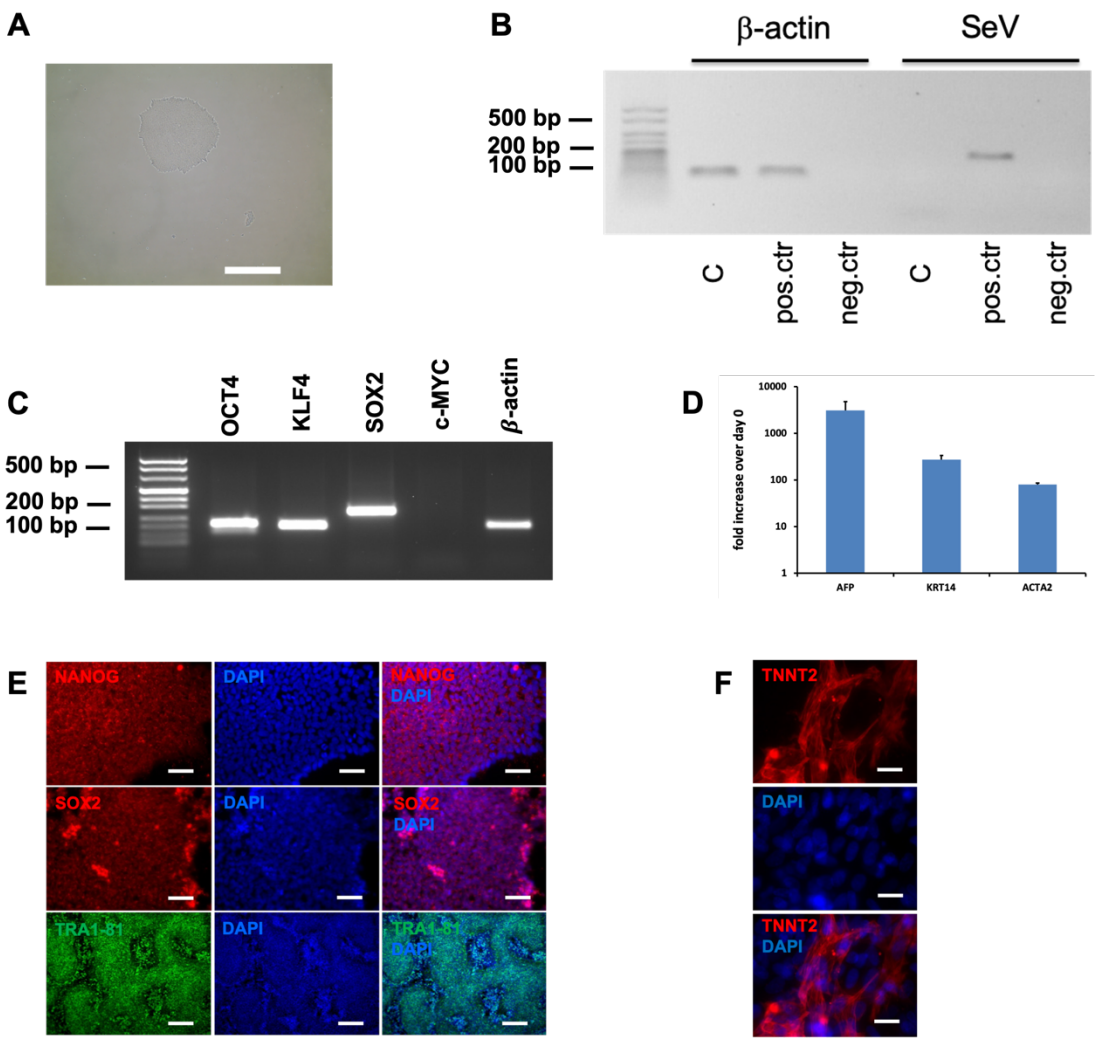

Figure 7. Characterization of C-line.

(A) Colony of iPSCs from C-line plated on Matrigel. (B) The RT-PCR showed Sendai virus-free in the C-line (C) RT-PCR displayed the expression of *OCT4, KLF4, SOX2, c-MYC,* and *NANOG* genes. (D) Relative expression of the three germ-layer genes *AFP, KRT14,* and *ACTA2* after spontaneous differentiation. (E) ICC showed the expression of the iPS-specific pluripotency factors, NANOG, SOX2, and TRA1-81. (F) ICC showed the expression of CM-specific protein TNNT2 after direct cardiac differentiation. Scale bars: A, 500 μm; E,100 μm; F, 20 μm

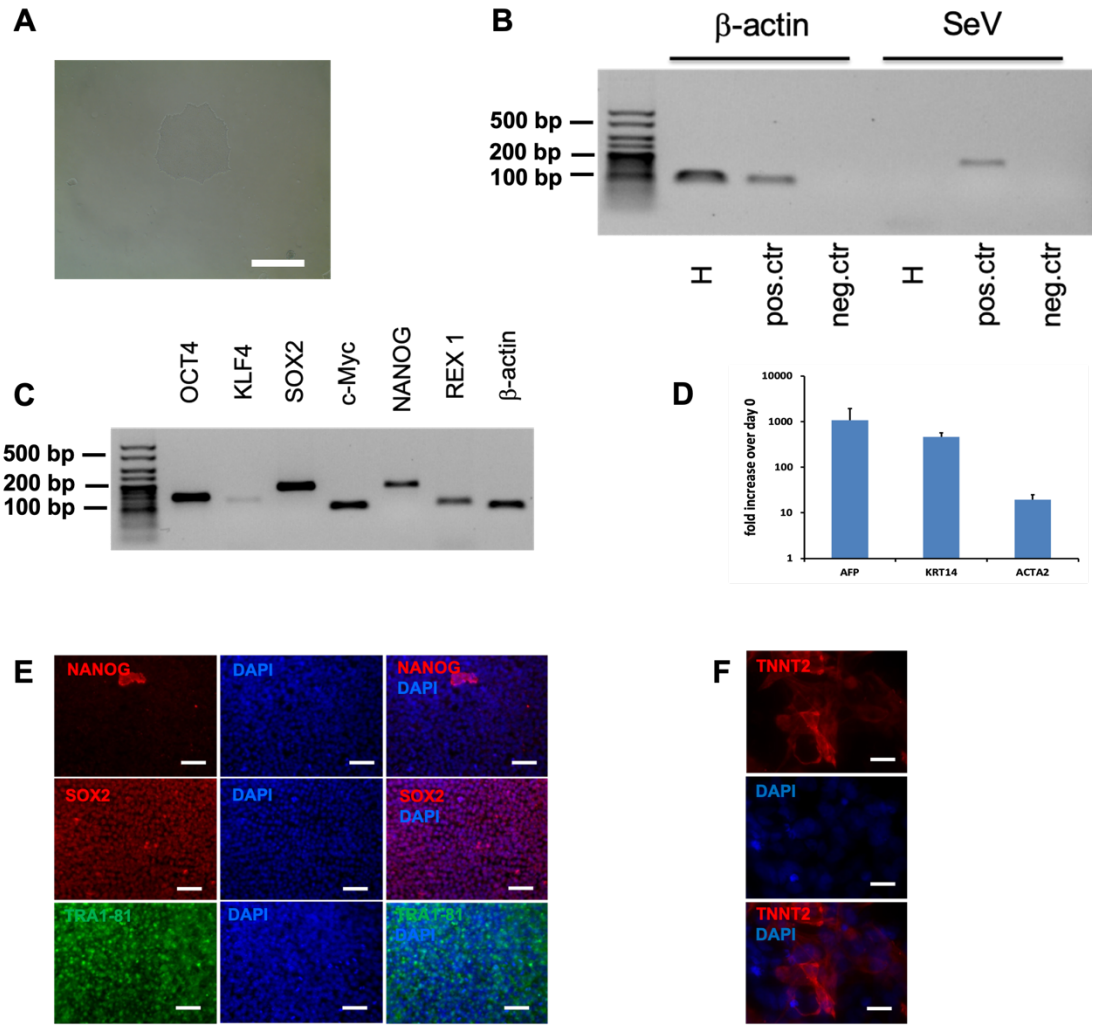

Figure 8. Characterization of H-line.

(A) Colony of iPSCs from H-line plated on Matrigel. (B) The RT-PCR showed Sendai virus-free in the H-line. (C) RT-PCR displayed the expression of *OCT4, KLF4, SOX2, c-MYC, NANOG, REX1,* and *β-actin* genes. (D) Relative expression of the three germ-layer genes *AFP, KRT14,* and *ACTA2* after spontaneous differentiation. (E) ICC showed the expression of the iPS-specific pluripotency factors, NANOG, SOX2, and TRA1-81. (F) ICC showed the expression of CM-specific protein TNNT2 after direct cardiac differentiation. Scale bars: A, 500 μm; E,100 μm; F, 20 μm

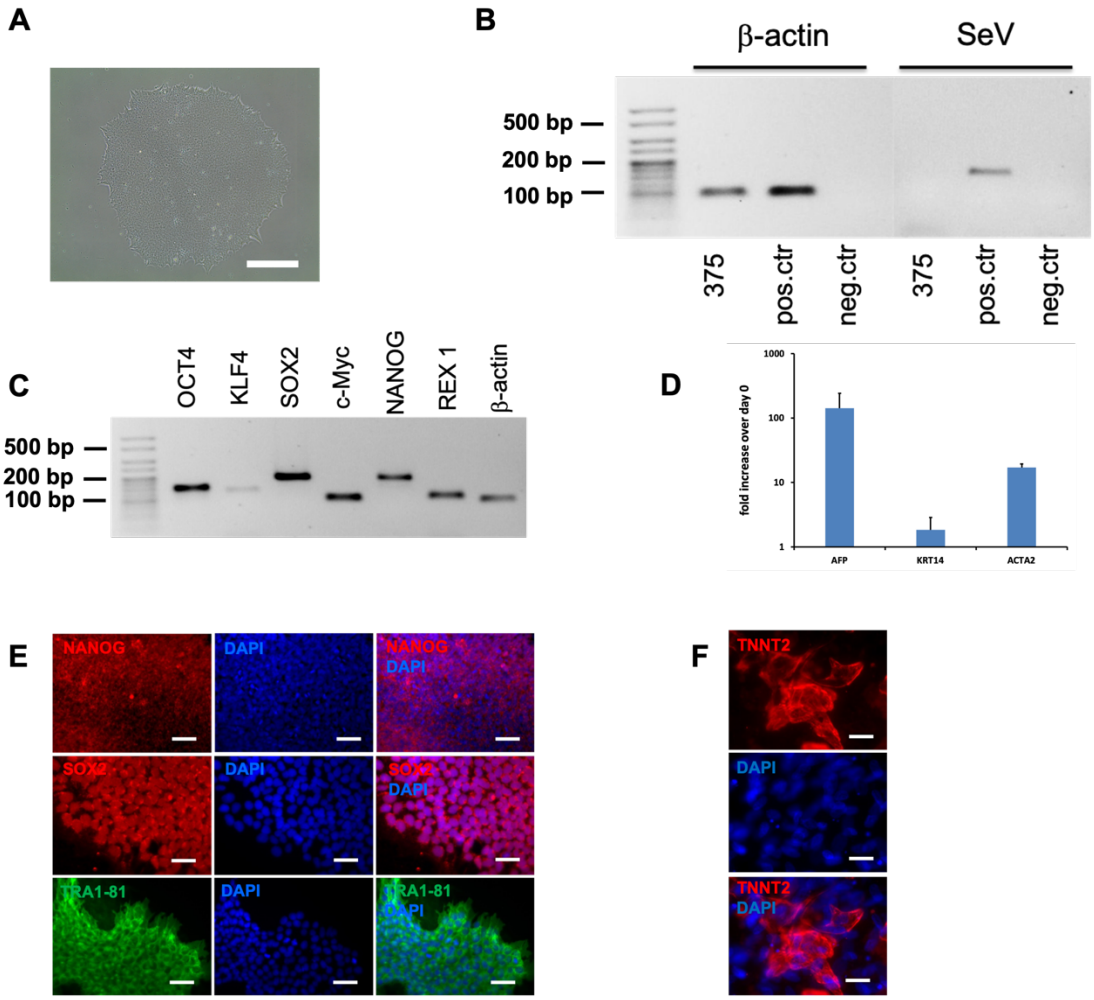

Figure 9. Characterization of 375-line.

(A) Colony of iPSCs from 375-line plated on Matrigel. (B) The RT-PCR showed Sendai virus-free in the 375-line. (C) RT-PCR displayed the expression of *OCT4, KLF4, SOX2, c-MYC, NANOG, REX1,* and *β-actin* genes. (D) Relative expression of the three germ-layer genes *AFP, KRT14,* and *ACTA2* after spontaneous differentiation. (E) ICC showed the expression of the iPS-specific pluripotency factors, NANOG, SOX2, and TRA1-81. (F) ICC showed the expression of CM-specific protein TNNT2 after direct cardiac differentiation. Scale bars: A, 500 μm; E,100 μm; F, 20 μm

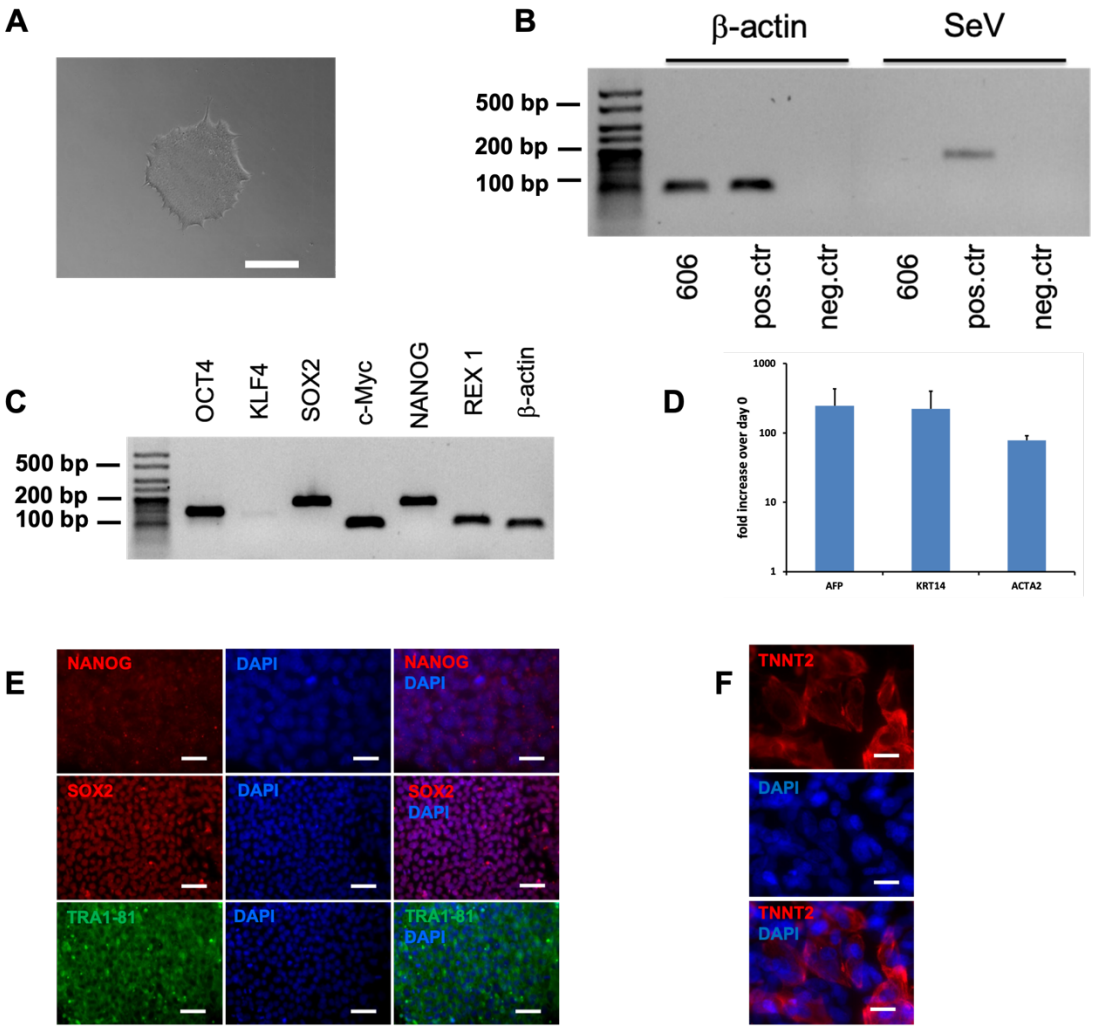

Figure 10. Characterization of 606-line.

(A) Colony of iPSCs from 606-line plated on Matrigel. (B) The RT-PCR showed Sendai virus-free in the 606-line . (C) RT-PCR displayed the expression of *OCT4, KLF4, SOX2, c-MYC, NANOG, REX1,* and *β-actin* genes. (D) Relative expression of the three germ-layer genes *AFP, KRT14,* and *ACTA2* after spontaneous differentiation. (E) ICC showed the expression of the iPS-specific pluripotency factors, NANOG, SOX2, and TRA1-81. (F) ICC showed the expression of CM-specific protein TNNT2 after direct cardiac differentiation. Scale bars: A, 500 μm; E,100 μm; F, 20 μm

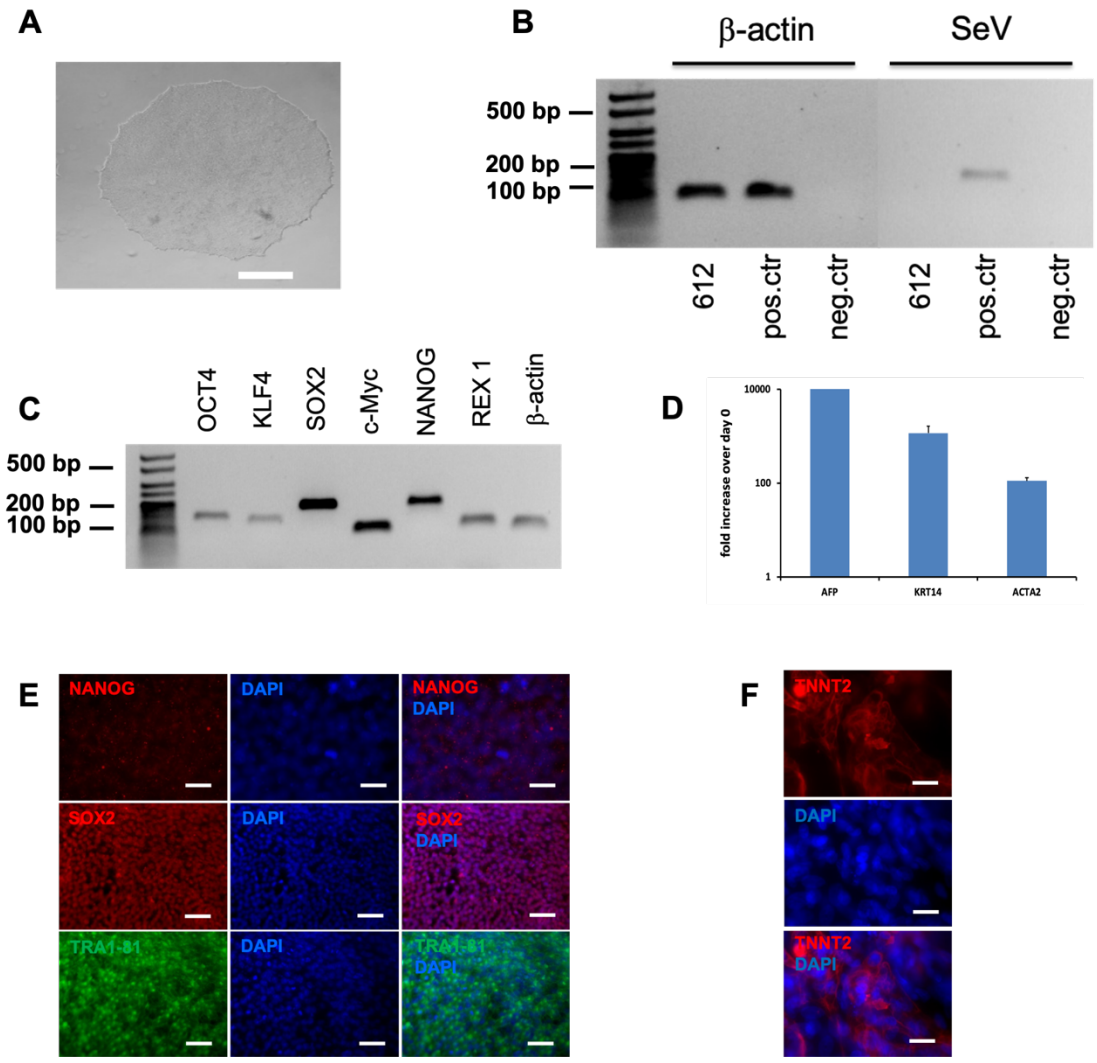

Figure 11. Characterization of 612-line.

(A) Colony of iPSCs from 612-line plated on Matrigel. (B) The RT-PCR showed Sendai virus-free in the 612-line. (C) RT-PCR displayed the expression of *OCT4, KLF4, SOX2, c-MYC, NANOG, REX1,* and *β-actin* genes. (D) Relative expression of the three germ-layer genes *AFP, KRT14,* and *ACTA2* after spontaneous differentiation. (E) ICC showed the expression of the iPS-specific pluripotency factors, NANOG, SOX2, and TRA1-81. (F) ICC showed the expression of CM-specific protein TNNT2 after direct cardiac differentiation. Scale bars: A, 500 μm; E,100 μm; F, 20 μm

4.2 Spontaneous differentiation of control- and HLHS-cell lines

A spontaneous differentiation protocol according to Moretti et al. [75] was performed with iPSCs derived from either healthy probands or HLHS patients. iPSCs were cultured in suspension to form EBs for 7 days on poly-hema-coated plates (Fig. 12 A and B). Thereafter, EBs were transplanted into gelatin-coated plates for further

differentiation at a defined density (20 to 30 EBs per 24-well) (Fig 12. C and D). Normally, the spontaneous contraction appeared around day 12 to 14 of differentiation (Fig 12. E and F). Approximately 10% of beating clusters could be seen in each well with seeded EBs on day 14.

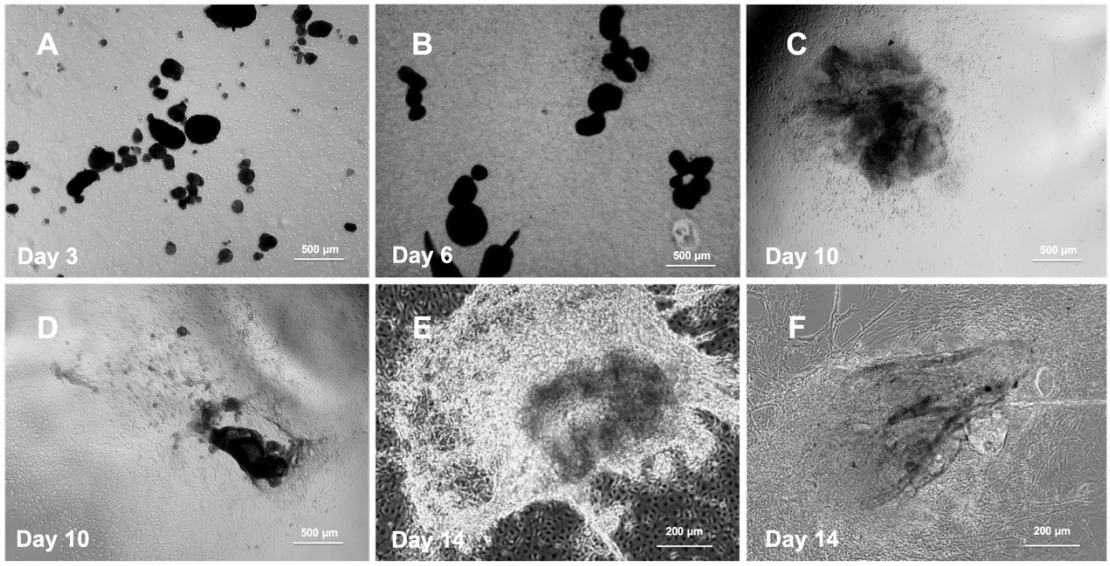

Figure 12. Spontaneous differentiation of S cell line iPSCs-CMs.

(A, B) Suspension culture to form EBs on day 3 and 6 in poly-hema-coated plate, respectively. (C, D) EBs transferred into gelatin-coated plate and spread out. (E, F) Upon differentiation iPSCs generated spontaneously beating areas with CM-like cells on day 14. Scalebar: A to D, 500 μm; E and F, 200 μm.

For the quantitative analysis of iPSC-CM after spontaneous differentiation, the presence of the Trop T and α-MHC in CMs were determined on day 14 by flow cytometry. The unstained CMs and CMs incubated with secondary antibody alone were used to determine the background fluorescence.

Fig. 13 A and B showed the representative plots of FACS results of iPSC-CMs from control- and HLHS-groups. For both Trop T and α-MHC frequencies of Alexa Fluor 488-positive cells were recorded. Fig. 13 C showed the summary of the FACS results on Troponin T for the two groups. The mean percentage of Trop T^+ cells in control and HLHS cell lines was 0.62% and 0.56%, respectively. The mean percentage of α-MHC^+ cells in control and HLHS cell lines was 43% and 56%, respectively. No statistically

significant difference of Trop T and α-MHC was evident between the two groups (Fig 13. D).

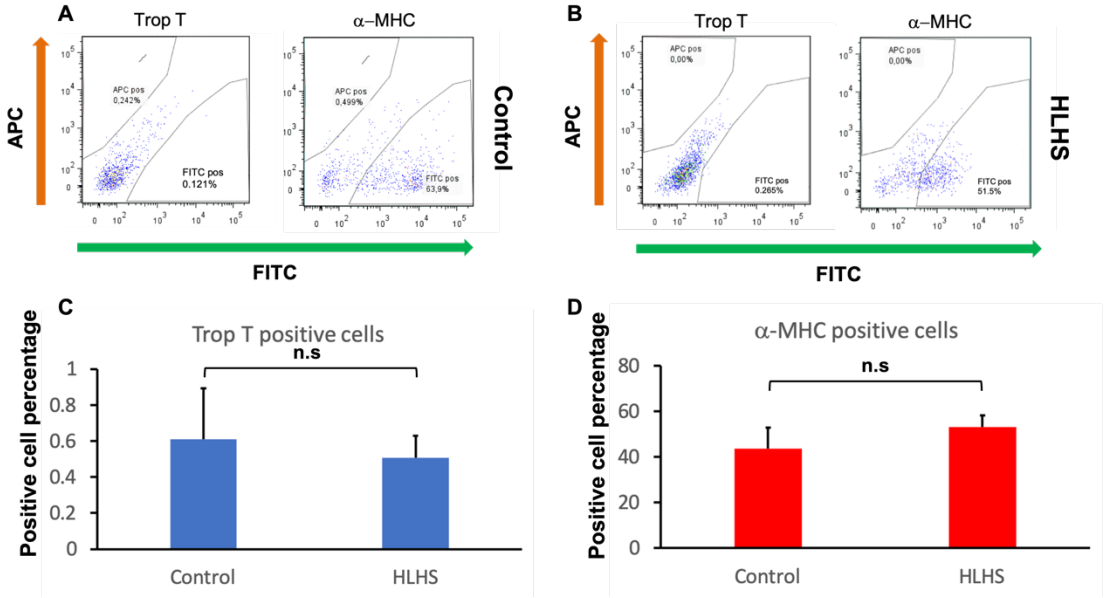

Figure 13. Quantitative analysis of CMs generated from control and HLHS iPSCs by spontaneous differentiation.

(A) Percentage of Troponin T^+ (0.121%) and α-MHC^+ cells (63.9%) in S-line (control group). (B) Percentage of Troponin T^+ (0.265%) and α-MHC^+ cells (51.5%) in 375-line (HLHS group). (C, D) No significant difference in Trop T^+ and α-MHC^+ cell percentage was observed between the two groups.

4.3 Establishment of protocol for direct cardiac differentiation

For this work, a protocol for iPSC culture and direct cardiac differentiation according to Burridge et al.[64] was used. Generally, the iPSCs were seeded at a 1:12 split ratio and cultured on Matrigel-coated 6-well plates (Fig. 14 A). Cells grew as flat, rounded colonies, typical of human iPSCs (Fig. 14 B). When reaching approximately 70% confluence, iPSCs were split to 24-well plate as single cells and cultured until 100% confluence (Fig. 14 C). After application of CHIR-99021 many cells died as expected (Fig. 14 D). Upon addition of Wnt-C59 on day 2 the cell culture recovered and regrew (Fig. 14 E). First beating cells could be seen between day 6 to 8 (Fig. 14 F), depending on the cell line. With ongoing culture, the contracting areas enlarged and covered the entire well. Ideally, cells across the whole well beat in a wave-like manner starting around day 10 (Fig. 14 G-H).

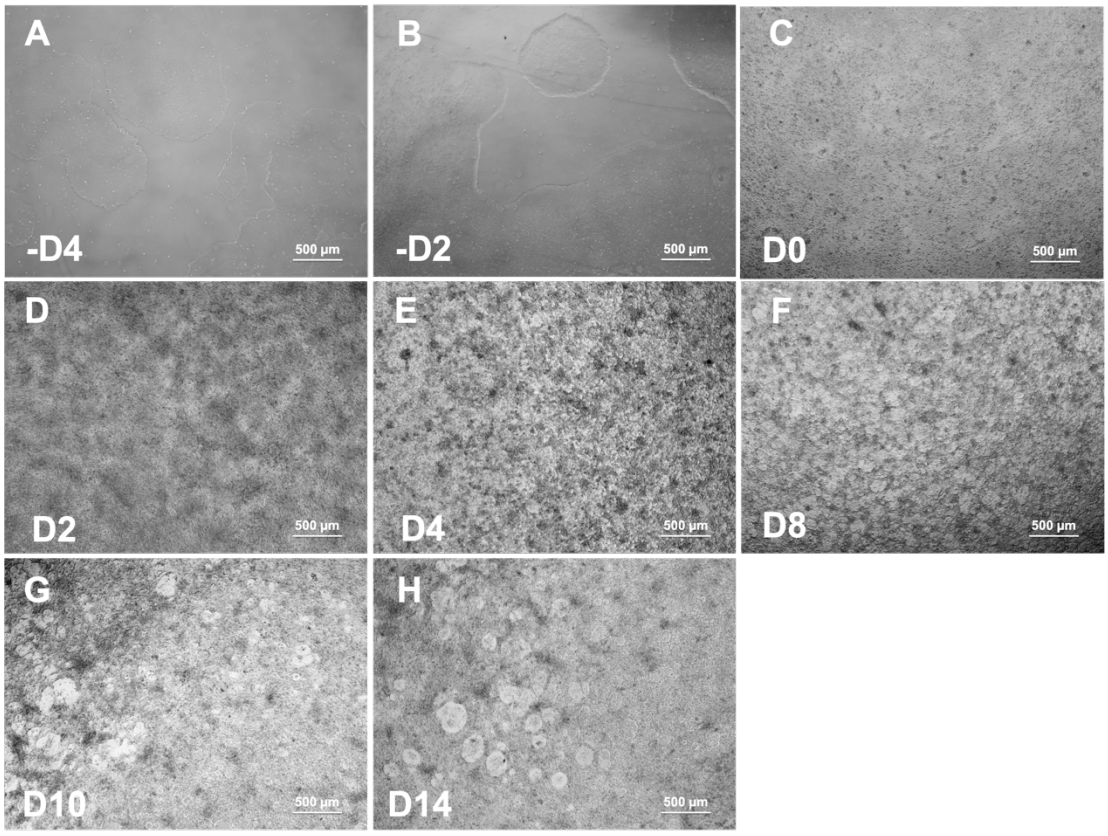

Figure 14. Morphology of iPSCs (H cell line) during the process of direct cardiac differentiation.

Representative images showing the morphology of H-line iPSCs during normal culture and the process of direct cardiac differentiation. (A and B) The iPSCs were routinely grown in 24-well plates with E8 medium. (C) Differentiation started with application of CHIR99021 when iPSCs were 100% confluent. (D) Addition of Wnt-C59 on day 2 of differentiation. (E to H) Cell morphology changes during the process of cardiac differentiation. Scalebars: 500 μm

Initially differentiation was performed in 6-well plates. However, the frequency of beating cells was inferior to that obtained in 24-well plates. Only the cells on the edge beat nicely, the other parts were dead or did not beat at all. Due to the result of these preliminary experiments, only 24-well plates were utilized for CM differentiation in all future experiments.

4.3.1 Determination of optimum CHIR-99021 concentration

According to the published protocol[64] iPSCs were treated with 6 µM CHIR99021 on day 0. Nevertheless, for some cell lines this concentration led to massive cell death within the first two days. Representative pictures are shown in Fig. 15 A and B. In other

cell lines the initially used concentration of CHIR99021 (6 µM) did not kill a large fraction of cells but also did not yield a high amount of beating cells (Fig. 15 C). This varying sensitivity of individual cell lines to CHIR99021 had also been mentioned in one of the publications by Burridge et al[64]. Therefore, multiple experiments were performed to define the optimum concentration for the six cell lines used in this thesis. The optimum concentration for each cell line was determined by incubation with graded concentrations of CHIR99021. Thereafter, each cell line was treated as indicated in Table 13 to obtain beating cells in all future experiments.

Table 13. Tested concentrations and finally used concentration (in bold) of CHIR99021 for the HLHS- and control iPSC lines.

Cell line	CHIR99021 concentration	Cell condition	Cell line	CHIR99021 concentration	Cell condition
	6 µM	dead		6 µM	dead
612	5 µM	dead	H	5 µM	dead
	4 µM	**beat**		**4 µM**	**beat**
	6 µM	dead		6 µM	dead
606	5 µM	dead	S	5 µM	dead
	4 µM	**beat**		**4 µM**	**beat**
	6 µM	dead		6 µM	dead
375	5 µM	dead	C	5 µM	dead
	4 µM	most dead		4 µM	most dead
	3 µM	**beat**		**3 µM**	**beat**

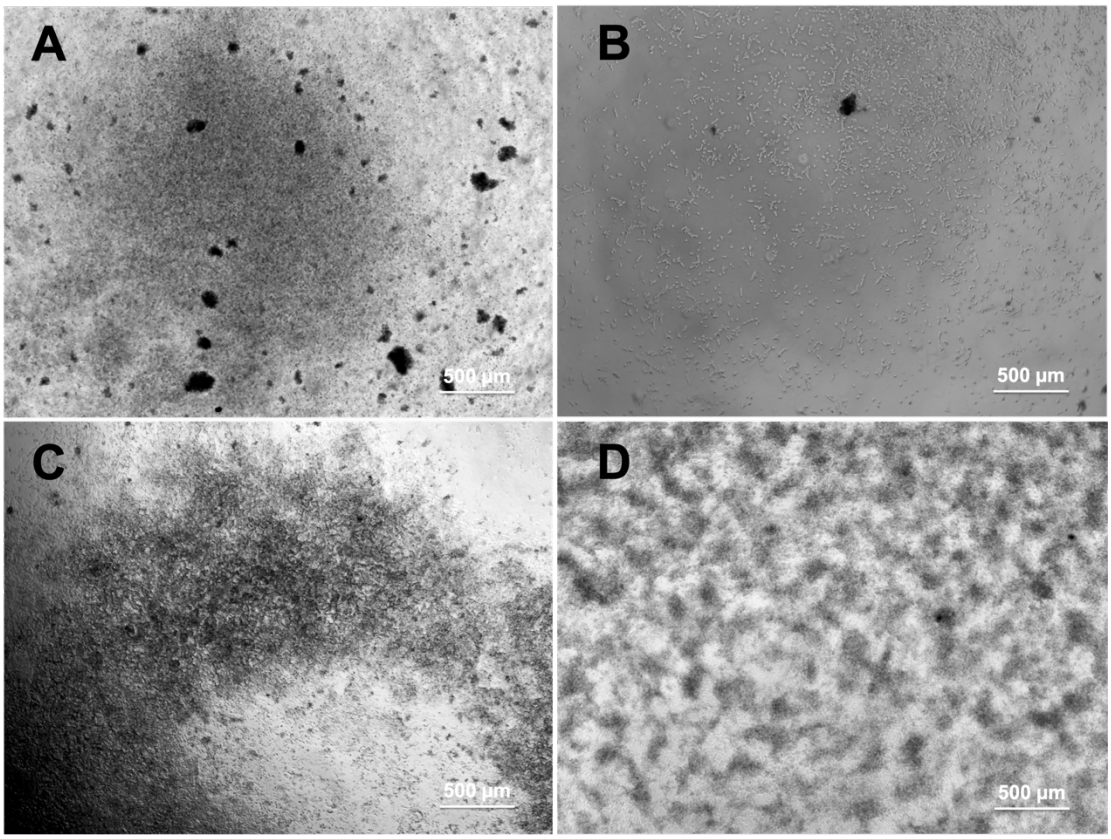

Figure 15. Representative documentation of the establishment of direct cardiac differentiation.

(A) Massive cell death at day 1 after addition of CHIR99021 using 6 µM CHIR99021 in 375-line. (B) Loss of cell monolayer after medium change with few cells remaining on day 2. (C) H-line on day 6 with 6 µM CHIR99021: only small areas of cells left. (D) 612-line on day 12 with 3 µM CHIR99021: most of the cells were alive and still attached but did not beat. Scalebars: 500 μm

4.3.2 Preferential beating and differentiation of the edges of the well

An interesting phenomenon was observed during differentiation that the initial beating parts always appeared on the edge of the well. Upon further culture, the beating area gradually spread to the entire well (Fig. 16 A to D). Furthermore, the cell density and morphology also changed around day 14. There were fewer cells on the edge of the well, and the cells elongated and generated a "fishing-net" structure (Fig. 16 E and F). The cell density was much higher in the middle of the well and the cells were beating as a monolayer (Fig. 16 B and C).

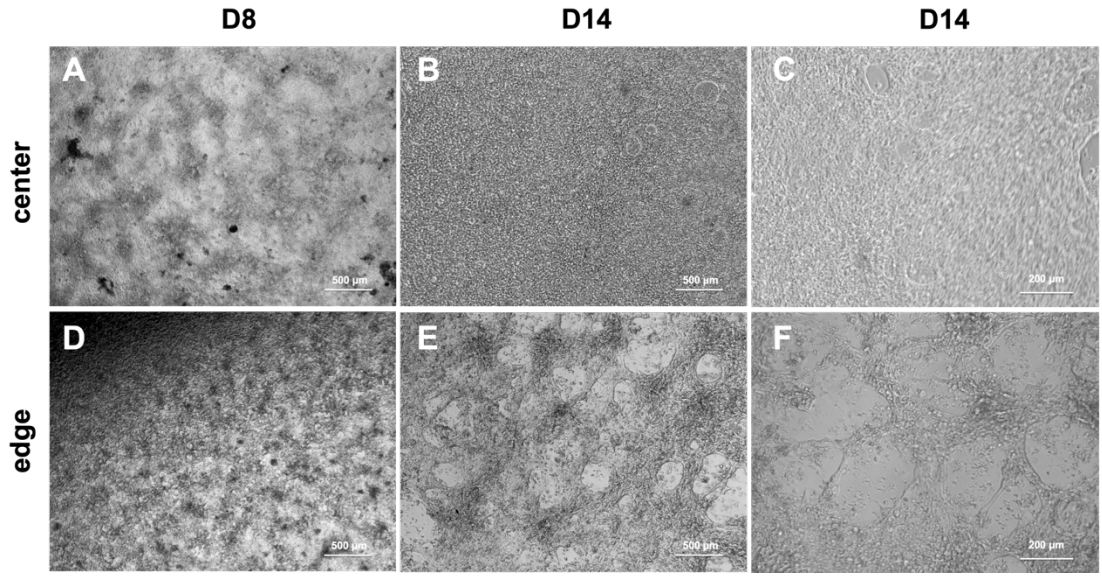

Figure 16. Comparison of CM morphology in the center and on the edge of the well during direct cardiac differentiation.

Representative images were taken from 375-line at different time points of differentiation. (A) Cells located in the center of the well on day 8. (B) Cells in the center on day 14 at 100 X magnification. (C) Cells in the center on day 14 at 400 X magnification. (D) Cells on the edge of the well on day 8. (E) Cells on the edge on day 14 at 100 X magnification. (F) Cells on the edge on day 14 at 400 X magnification. Scalebar: A, B, D, and E, 500 μm; C and F, 200 μm.

4.4 Gene expression of cardiac TFs during differentiation

For the investigation of the cardiac TFs expression during direct cardiac differentiation, samples were taken on days 0, 6, 8, 10 and 14. The gene expression of cardiac TFs as *NKX2.5, TBX5, ISLET1*, *NPPA* (down-stream target of *TBX 5*) as well as *TNNT2* (encoding cardiac Troponin T) were measured by qRT-PCR. Three differentiations per line were detected and for each time point, two samples were taken and measured in duplicate. The gene expression of the HLHS lines (375, 606, and 612) in the comparison with control lines (S, C, and H) is shown. Each value represents the average of six individual data. The figure shows the relative change of gene expression in the process of differentiation compared with day 0.

An elevated expression of all TFs could be observed during differentiation. The expression of *ISLET1* increased in the first six days and then peaked at a stable level with no significant difference between the two groups (Fig. 17 A). The expression of *NKX2.5* was significantly retarded in the HLHS lines until day 8 but caught up by day 10 to the values of the control group (Fig. 17 B). A tremendously lower expression of *TBX5* was seen in HLHS-derived iPSC-CMs throughout the whole differentiation which was highly significant at all time-points in control group (Fig. 17 C). Consistent with this result was the dramatically reduced expression of *NPPA*, a direct target gene of *TBX5*, in the HLHS-group throughout, also with continuous significance (Fig. 17 D). Finally, *TNNT2* expression, increased in parallel in both groups until day 8 and was slightly enhanced in the control group on day 10 (Fig. 17E). These results impressively demonstrate a dysregulation of certain TFs in iPSC-CM derived from HLHS-patients compared to those established from healthy probands.

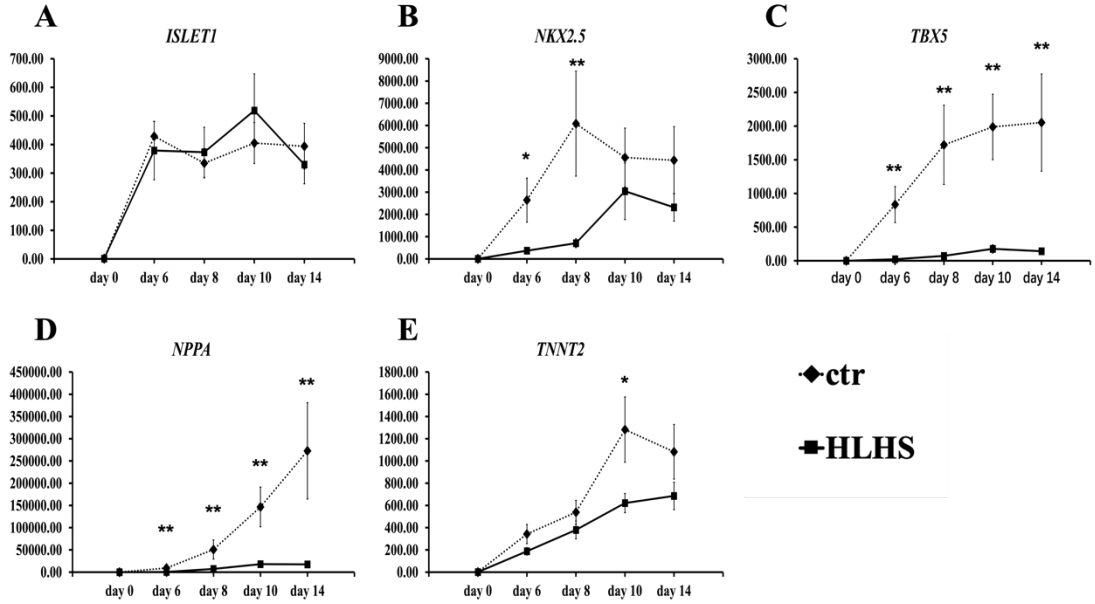

Figure 17. Relative change of the gene expression of *ISLET1, NKX2.5, TBX5, NPPA,* and *TNNT2* in direct cardiac differentiation.

(A) *ISLET1* gene was expressed in both groups and no significant difference was observed. (B) *NKX2.5* gene was highly expressed on day 6 and day 8 in control group and caught up by HLHS group on day 10. (C and D) the expression of *TBX5* and *NPPA* gene were significantly higher in control group from the beginning of differentiation. (E) The *TNNT2* expression increased in parallel and was enhanced on day 10 in control group. Results are presented as means ± SEM. The significance of differences was tested using the One-way ANOVA test. p-values <0.05 were statistically significant. p-values <0.05 are indicated as (*), p-values <0.01 are indicated as (**).

4.5 Immunocytochemical analysis of sarcomeric structures

Next, the development of sarcomeric structures in iPSC-CMs were analyzed. In all cases, iPSC-CMs used for immunochemical staining were replated around day 21 and stained on day 23. To evaluate sarcomeric structures, anti-α-actinin, anti-α-MHC, and anti-Trop T antibodies were utilized. In both control and HLHS lines sarcomeric structures could clearly be identified. Interestingly, no differences between both groups were evident (Fig. 18 A, B and C).

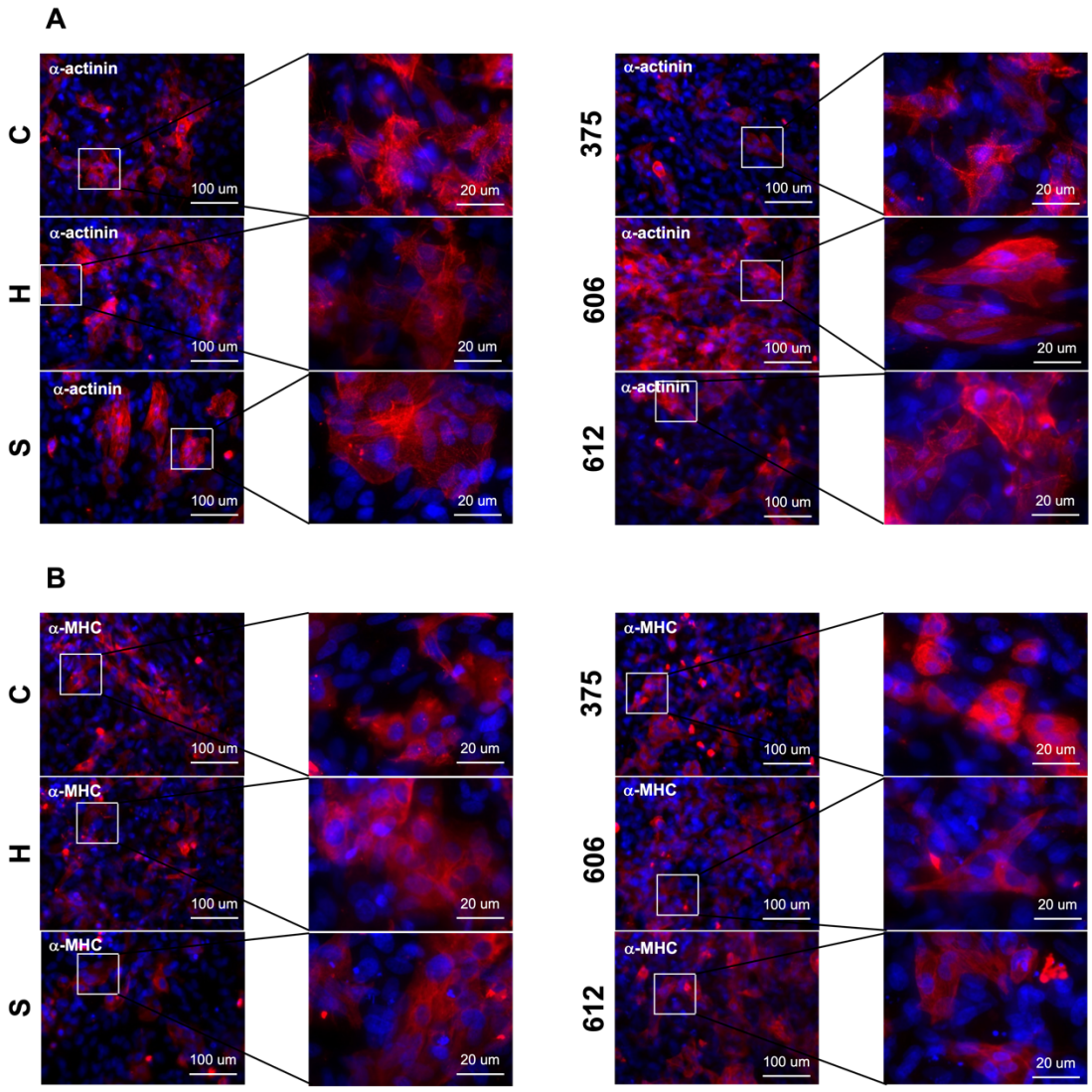

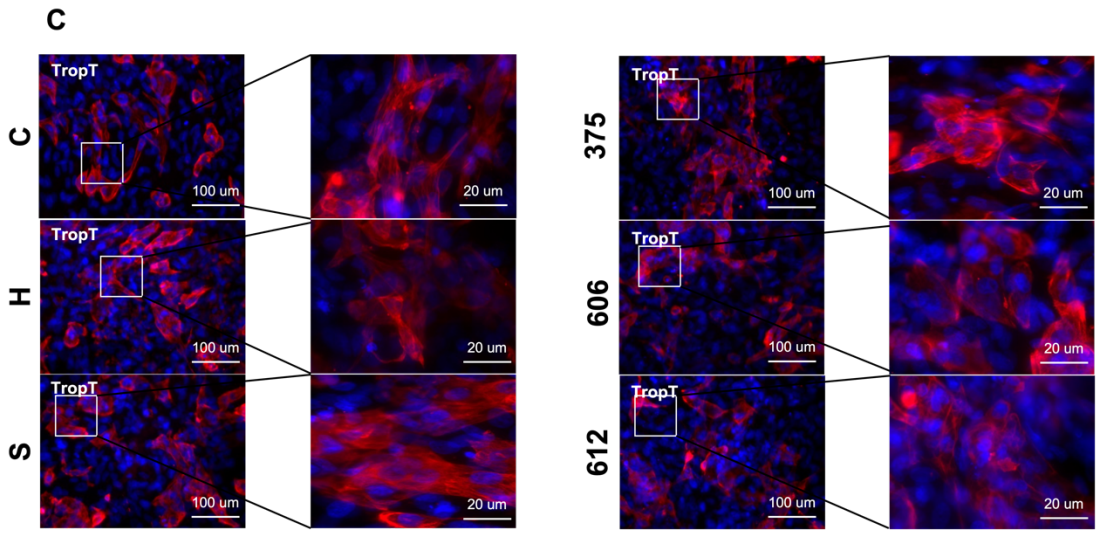

Figure 18. Characterization of sarcomeric structures of iPSC-CMs.

Representative immunofluorescence images of day 14 iPSC-CMs for the control lines (left) and HLHS lines (right). Sarcomeres were marked by α-actinin (A), α-MHC (B), and Trop T (C). Scale bars, 100 µm and 20 µm for magnified.

In addition, the presence and distribution of connexins were analyzed to get an idea whether the intercellular connection at the gap junctions may show any differences. To that end two connexins (CX40 and CX43) were investigated in further detail. Both molecules are expressed in the mammalian heart though with a different distribution. In both control and HLHS lines the gap junctions could be clearly identified and there was no major difference between both groups (Fig. 19 A and B)

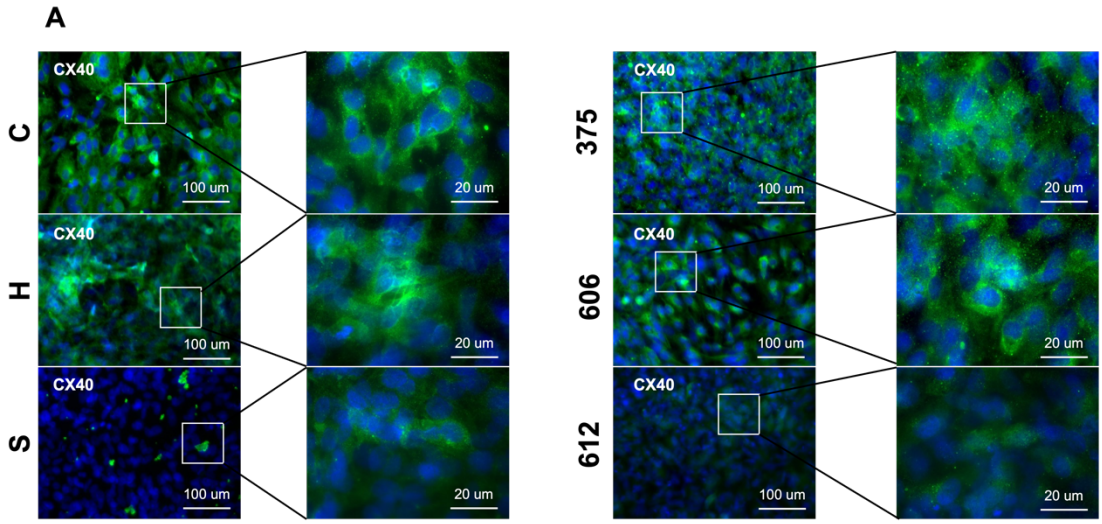

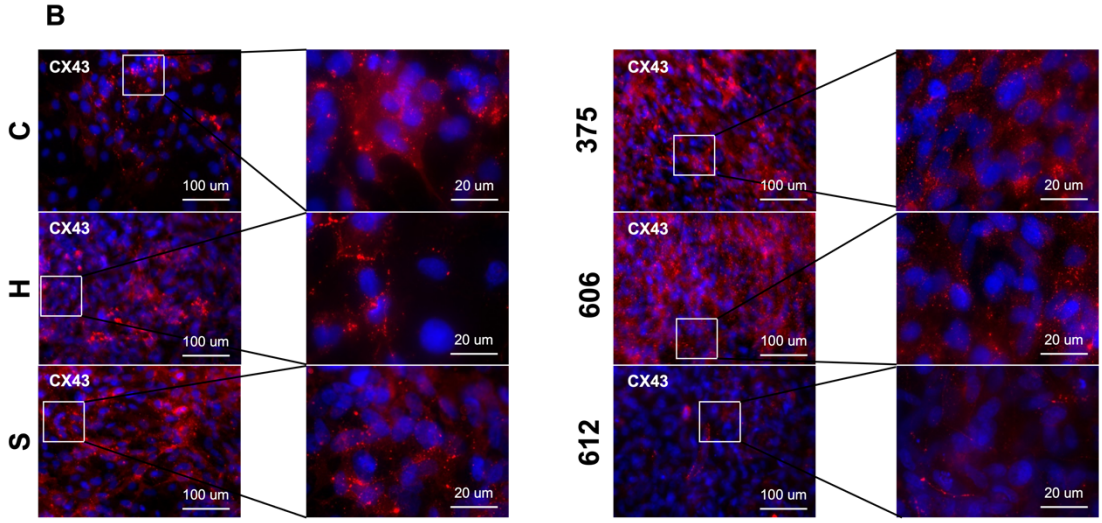

Figure 19. Connexin proteins staining of iPSC-CMs.

Immunofluorescence images showing the connexin proteins CX40 (A) and CX43 (B) in representative iPSC-CMs for the control lines (left) and HLHS lines (right). Scale bars, 100 µm and 20 µm for magnified.

4.6 Quantification and purification analysis of iPSC-CMs

For the pilot experiment, iPSC-CMs were intended to generate engineered heart tissue (EHT), which required a certain quality of iPSC-CMs. A previous study indicates [76] that in preparations with less than 60% CMs no detectable beating amplitude will be generated. To ensure high quality of iPSC-CMs preparations, the presence of the cardiac sarcomere proteins TNNT2 and α-MHC in iPSC-CMs were determined quantitatively at day 14 by flow cytometry. The unstained iPSC-CMs and iPSC-CMs incubated with secondary antibody alone were used to determine the background fluorescence.

Fig.20 A and B shows representative plots of FACS results of iPSC-CMs. For both TNNT2 and α-MHC frequencies of positive cells were recorded which were clearly higher than the required 60%, evidenced by the AlexaFluor 488 signal of the $TNNT^{+}$ and $\alpha\text{-}MHC^{+}$ cells.

These FACS analyses were repeatedly performed and the summary of the frequency of TNNT2^{+} and α-MHC^{+} cells is shown in Fig. 20 C and D. The mean percentage of TNNT2^{+} cells in H, C, and S control cell lines are 67.03 ± 8.22%, 75.90 ± 7.35%, and 73.2 ± 11.61%, respectively. These results were close to the HLHS group (375-line, 79.10 ± 10.89%; 612-line, 67.40 ± 5.19%; 612-line, 73.27 ± 18.40%). The values of α-MHC^{+} cells were 91.80 ± 4.79%, 77.60 ± 10.18%, and 95.33 ± 2.58% in H-, C-, and S-line, respectively. In HLHS group, the values were 95.15 ± 1.34%, 93.53 ± 2.85%, and 92.03 ± 4.50% in H-, C-, and S-line, respectively (Fig. 20 C). The percentage of TNNT 2^{+} cells in all cell lines was well over the required 60% cutoff. Likewise, a frequency of more than 75% of α-MHC^{+} cells was detected. Therefore, these proportions of TNNT2^{+} and α-MHC^{+} cells definitely meet the requirements for the generation of EHTs with these cell populations. In addition, the percentage of TNNT2^{+} and α-MHC^{+} cells across all cell lines between both groups was compared. A Student's t-test revealed no significant differences (Fig. 20 D) suggesting that cardiac differentiation has worked equally well in both HLHS and control lines, at least with respect to the number and frequency of iPSC-CMs.

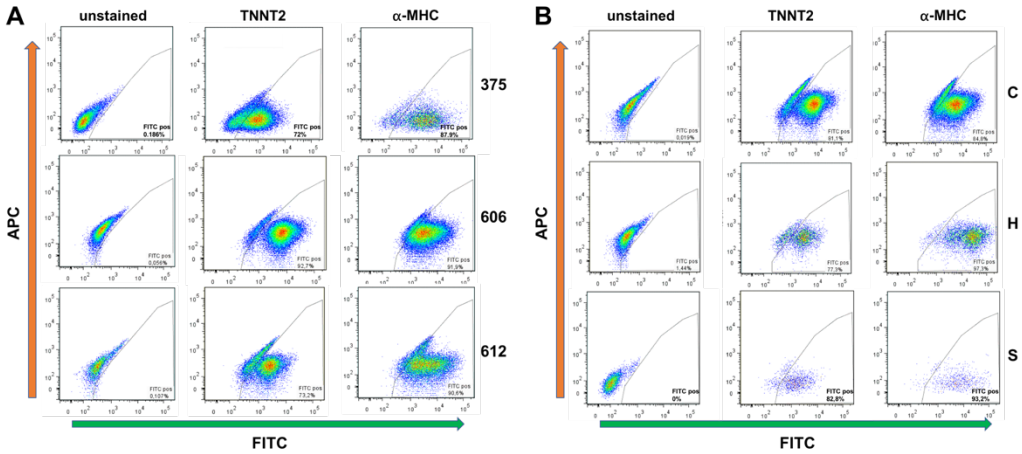

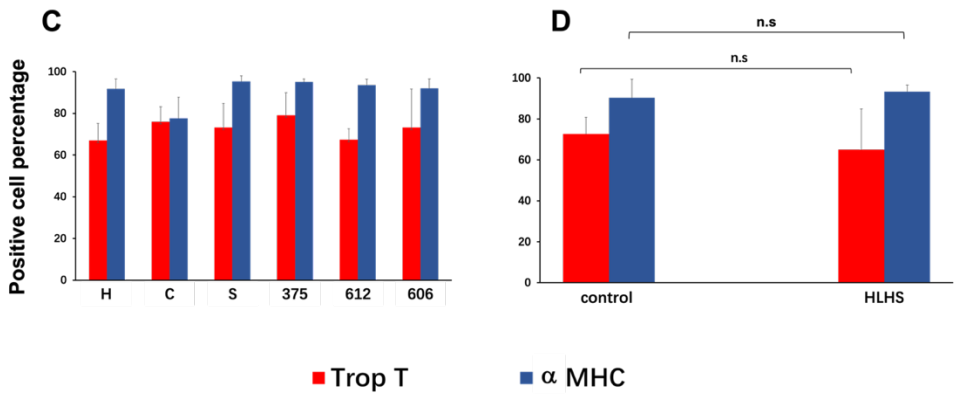

Figure 20. Representative FACS results of each cell line.

The anti-TNNT2 and anti-α-MHC antibodies were stained with a AlexaFluor 488-labeled secondary antibody. The $TNNT2^+$ and $\alpha\text{-}MHC^+$ cells show a signal for AlexaFluor 488 in HLHS group (A) and control group (B). For each line, the left panel shows the unstained cell population, the middle panel represents the $TNNT2^+$ cell population, and the right panel illustrates the $\alpha\text{-}MHC^+$ cell population. (C) Summarized results of FACS for each cell line. (D) No significant differences were observed for $TNNT2^+$ and $\alpha\text{-}MHC^+$ cell frequency between HLHS and control group. All values are presented as the mean ± SEM. Significance of differences was tested using the unpaired Student's t-test. P-values <0.05 were statistically significant. n.s: not significant.

4.7 Determination of physical parameters of EHT in a pilot experiment

4.7.1 Determination of physical parameters in EHTs

As a pilot study, the iPSC-CMs were utilized for generation of EHTs. This experiment was performed at the Universitätsklinikum Hamburg-Eppendorf as part of a collaboration with the group of Arne Hansen. The EHT generation protocol is robust, reproducible, and simple and allows measurements in a 24-well format with limited numbers of cells[77]. Spontaneous contraction was observed around day 4 to day 6. The contractile force analysis was evaluated on day 11 after EHT casting, which was performed by a video-optical recording system (Fig. 21 A and C). Fig. 21 B shows the morphology of EHTs on day 11.

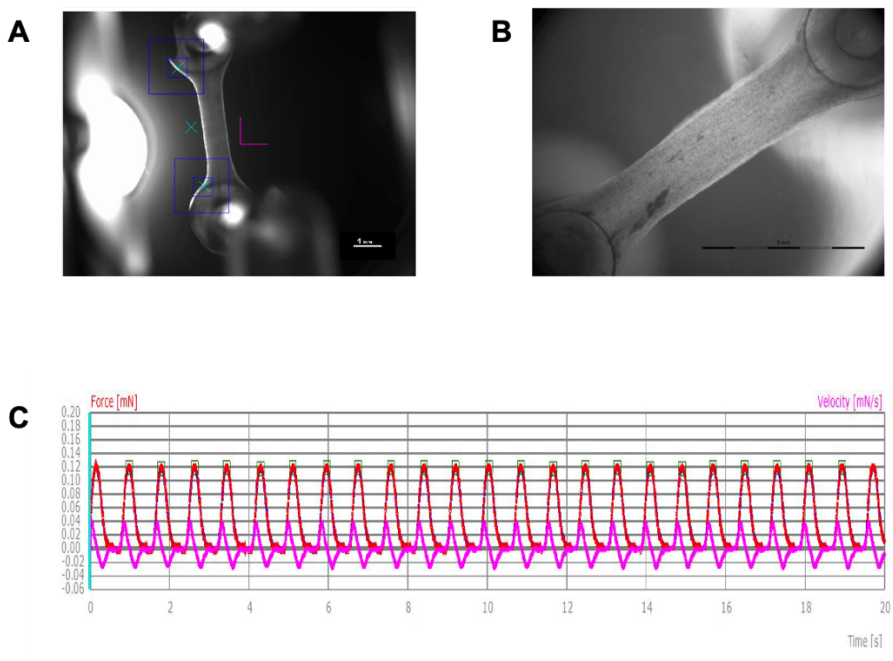

Figure 21. The spontaneous beating of EHTs from H-line on 11 days after casting.

(A) Camera view of an EHT during the measurement. (B) The morphology of EHT on day 11. (C) The contractile parameters of the EHT. Red line shows the force parameter (mN), and the pink line reveals the velocity (mN/s). Scale bar, 1 mm.

4.7.2 Subtypes and proliferation capacity of iPSC-CMs in EHTs

In order to establish the iPSC-CMs subtypes in EHTs, histochemical staining with α-actinin combined with two isoforms of myosin light chain 2 (MLC2a and MLC2v) was performed for the EHTs. MLC2a and MLC2v were used as markers to detect atrial and ventricular subtypes, respectively. The histochemical staining results showed that α-actinin stained iPSC-CMs scattered in the EHT (Fig. 22 A) and both atrial and ventricular subtype of CMs were found in EHTs (Fig. 22 B and C).

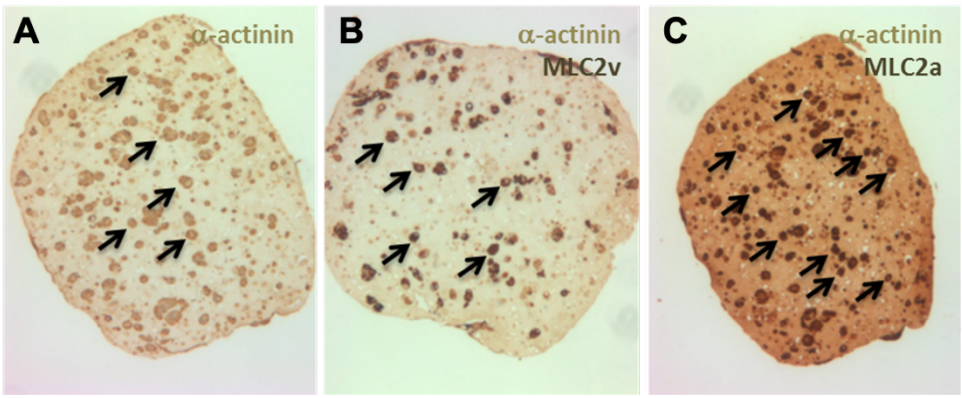

Figure 22. Immunohistochemical staining of iPSC-CM subtypes for EHT.

(A) The black arrows show the iPSC-CMs stained with α-actinin. (B) The black arrows illustrate the ventricular-like iPSC-CMs stained with α-actinin and MLC2v. (C) The black arrows reveal the atrial-like iPSC-CMs stained with α-actinin and MLC2a.

Next, proliferation of iPSC-CMs in EHTs was analyzed. The Ki67 protein is a cellular marker for proliferation. It is expressed in the active cell cycle (G_1, S, G_2, and mitosis) but not in resting cells (G_0)[78]. Phospho-histone 3 (PH3) is an immunomarker specific for cells undergoing mitosis[79]. Therefore, anti-Ki67 and anti-PH3 antibodies were used to assess the proliferative capacity of CMs. The results showed that some CMs in EHT still had the ability of proliferation (Fig. 23), indicating that the iPSC-CMs used for EHT generation were immature.

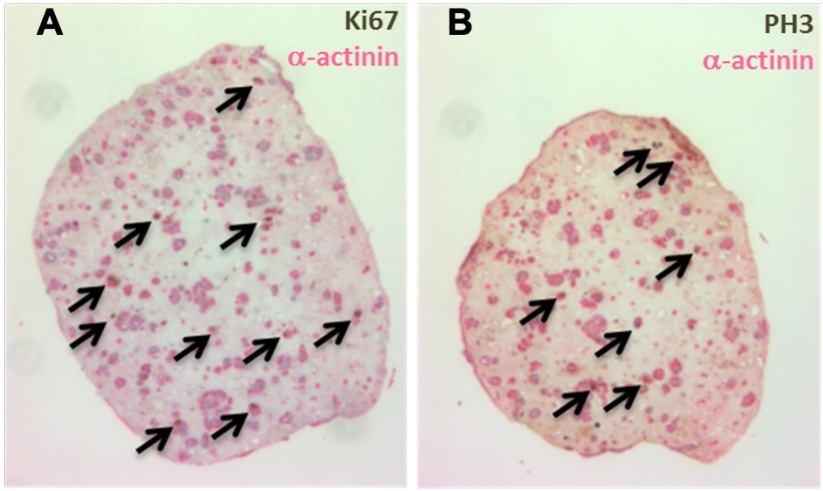

Figure 23. Proliferation staining of iPSC-CMs for EHT.

The pink areas represented iPSC-CMs stained with α-actinin (A) Combined staining of α-actinin and Ki67. Black arrows depict the CMs stained with Ki67. (B) Combined staining of α-actinin and PH3. Black arrows illustrate the CMs stained with PH3.

Discussion

HLHS is a rare congenital heart disease with a wide pathophysiological basis. The cause of HLHS is considered to be multifactorial, owing to multiple genetic and environmental factors. Historically, the "flow theory" was believed to best conceptualize the etiology of HLHS. Nevertheless, a previously published article indicated that the morphology of LV was not correlated to the degree of valvar stenosis [13]. Our published research revealed that *de novo* mutations which drive cardiomyogenesis were strongly associated with the formation of HLHS [22]. The purpose of this project is the encompassed characterization of HLHS-iPSC lines and the establishment of defined and reproducible conditions for the production of CMs of high quality and quantity, which are the indispensable basis to shed light on the potential impairment and/or dysfunction of HLHS-CM compared to control-CMs.

5.1 Characterization of the generated iPSC lines

With the help of Sendai virus transduction, fibroblasts or PBMCs from the HLHS patients and healthy probands were reprogrammed into iPSCs. Due to the same genetic background with the HLHS patients, these cells could serve as an ideal *in vitro* disease model. The advantage of transduction with the Sendai virus is its non-integrative characteristic. The reprogramming factors are introduced into the cell without any integration of viral sequences into the host genome. This approach prevents the potential destruction or dysregulation of relevant genes or pathways, which is a major advantage over the use of retro- or lentiviruses.

The Sendai virus, which carries the Yamanaka factors *OCT4, KLF4, SOX2*, and c-*MYC*, was used for reprogramming the somatic cells to iPSCs. These TFs induce a dramatic change in the gene program of the somatic cells and start an endogenous program which is very similar to that of ESCs. After complete and successful reprogramming, the iPSCs should be able to express the TFs endogenously and independently maintain their pluripotent status.

Thus, the first step of my research was to prove the successful reprogramming of the six generated iPSC lines. Sendai-virus footprinting was carried out at different passages to check for the absence of viral sequences (Fig. 6-11 B). This was quite variable in the different cell lines. The S-line was already free of Sendai virus after passage 4, while 612-line required 12 passages to be virus-free. These differences may be a consequence of intrinsic biological properties of individual cell lines and such discrepancies are also reported by others[80, 81].

Having confirmed the absence of viral sequences in all six cell lines, the next goal was to prove the pluripotency status of the generated iPSC lines. The pluripotency of the lines was confirmed by positive endogenous expression of *OCT4, KLF4, SOX2*, *c-MYC*, *NANOG* and *REX1* (Fig. 6-11, C). Furthermore, NANOG, SOX2, and TRA1-81 expression were also observed by immunofluorescence staining (Fig. 6-11, E).

The generation of iPSCs in this study included Sendai virus containing the c-*MYC* gene. But I found that c-*MYC* expression could be observed in 4 of six lines and was absent in S- and C-line (Fig. 6-7, C). Several cellular studies have shown a role of the myc proteins in proliferation, growth, apoptosis, and differentiation [82, 83] [84]. However, accumulating evidence strongly suggests c-*MYC* does not contribute too much in the process of reprogramming cells and is not required for the maintenance of the pluripotent state of the iPSCs [35, 85]. Moreover, *c-MYC* is a gene associated with oncogenic potential[86] and cell apoptosis [87]. Therefore, the role of *c-MYC* may be just a switch to initiate cell reprogramming rather than a stabilizer of pluripotency.
iPSCs were similar to ESCs in morphology, proliferation and gene and surface antigen expression. These cells should have to ability to differentiate into cell types of the three germ layers (endoderm, mesoderm, and ectoderm). The markers, *AFP, KRT14*, and *ACTA2* were consistently expressed at a much higher level upon spontaneous differentiation (Fig. 6-11, D), though to a different extent. This result can be expected and is inherent for such an approach which does not favor the differentiation into a specific cell type.

5.2 Efficient differentiation of iPSC into CMs

5.2.1 Optimum CHIR99021 concentration in direct cardiac differentiation

In a first step the spontaneous differentiation protocol was used to assess its potential to generate iPSC-CMs. Indeed, few contracting clusters could be seen around day 12 to 14 (Fig. 12). Flow cytometric analysis showed that only a minor fraction of Trop T^+ or α-MHC^+ cells were recorded (Fig. 13). This result underlines that this protocol yields CMs with poor efficiency. In addition, the culture medium used for differentiation contains FBS which is not clearly defined.

During the last decade, many strategies of cardiac differentiation have been established and applied for biological and clinical research. The protocol used in this project was based on the publication of Burridge et al.[65]. The culture medium called CDM3 had a standard basal medium (RPMI 1640) with only two clearly defined components: recombinant human serum albumin and L-ascorbic acid 2-phosphate. Secondly, this approach used two molecules (CHIR99021, Wnt-C59) which modulate the Wnt signaling pathway and were added at defined concentrations and timepoints. This tremendously favors the conditions towards generation of CMs while other cell types were present as an only very minor fraction.

In this work, CHIR99021 was used to inhibit GSK3 during direct cardiac differentiation, leading to the accumulation of β-catenin and induction of the undifferentiated iPSCs to progress to the mesodermal stage. Subsequently, a small molecule Wnt/β-catenin signaling inhibitor, Wnt-C59 was used to block the expression of Wnt signals and promote the development of CMs (Fig. 3). With this protocol, it was possible to generate at least >60% Trop T positive (TNNT2+) cells prior to purification (Fig. 20).

During my studies, I found that the addition of CHIR99021 caused large extent of cell death (Fig. 15), quite similar to the results of Burridge and colleagues who also claim a massive cell death after the treatment of CHIR99021[64]. The fraction of dead cells varied in individual lines as did the concentration of CHIR99021 necessary to induce effective differentiation of CMs[64]. GSK3 is a serine/threonine protein kinase. It is a component of a multi-protein complex which can degrade the β-catenin protein[88]. With the addition of CHIR99021, the biological activity of GSK3 is blocked, leading to the accumulation of β-catenin, promoting the activation of the Wnt/β-catenin signaling pathway. In addition, GSK3 has been shown to be related to some apoptotic signaling pathways and its overexpression could result in apoptosis[89].

Owing to the toxicity of CHIR99021 I have performed multiple experiments applying different concentrations to specify optimum conditions for the efficient generation of CMs for each cell line. This approach successfully defined the optimum concentration of CHIR99021 for each of the six cell lines used in this project (Table 13).

5.2.2 High cell density promotes cardiac differentiation

Another major factor critical for a successful differentiation is the cell seeding density. According to the protocol of Burridge et al. iPSCs can efficiently be differentiated once the cells have reached 65% to 85% confluence[64]. During the establishment of the protocol two phenomena were observed: firstly, the iPSCs started to undergo spontaneous apoptosis since they could not reach a confluent state. Secondly, with lower confluence in the beginning the subsequent cardiac differentiation was very inefficient. To circumvent these difficulties, in my research the iPSCs were cultured in 6-well plates till 70% confluence and were then split into 24-well plates at 100% confluence (Fig. 14). Under these conditions the efficiency of differentiation was satisfying.

This is in good agreement to previously published reports which indicated that rising cell density could improve the differentiation efficiency[90] [91] [92]. This might be due to the fact that a high cell density could maintain the cell-cell interaction, intracellular signal transmission and synthesis of extracellular matrix (ECM) at a high level[93, 94]. Meanwhile, because of highly proliferative property, iPSCs have a relatively short G1 cell cycle[95]. G1 phase plays an important role in the response of cells to chemicals that induce differentiation. Lengthening G1 phase contributes to early stem cell differentiation[96]. At high cell seeding density, environmental components, especially space and nutrients, limited the proliferative capacity of stem cells. With the G1 phase prolonged, the response of cells to chemical molecules is enhanced, resulting in a better efficiency of cell differentiation. Moreover, Kim and colleagues[97] illustrated that the initial cell seeding density could influence the temporal gene expression profiles of endogenous growth factors. Rising cell density could increase the *BMP-2, FGF-2*, and *TGF-β2* expression, which promote stem cells to mesodermal lineages and influence the early cardiomyogenic differentiation[98] [99] [100].

It should also be noted that exceeding optimum cell density may lead to reduced cell function or may even cause cell apoptosis. This might be due to contact-inhibition, lack of oxygen and nutrients, and inefficient waste removal[101].

5.2.3 Spatial structure is conducive to cell differentiation

Interestingly, the initial beating areas preferentially appeared on the edge of the well and upon further culture, the beating area gradually spread to the entire well. Furthermore, the cell density and morphology were also different between the edge and center of the well. This phenomenon was observed in both HLHS and control iPSC lines (Fig.16).

The reason of this phenomenon may be attributed to the spatial structure of cells. After cell-splitting, there were cells seeding on the wall of the well forming a three-

dimensional structure with the cells in the corner. One might speculate that the somehow 3D spatial structure can mimic the complexity and organization of real organs to some extent, especially the microenvironment and intercellular connection[102]. Many publications have illustrated that 3D structure could have an influence on cell morphology[103], proliferation[104], and differentiation[105]. Moreover, a 3D system can promote iPSC-CMs which display more mature characteristics[106]. Brannvall and colleagues have shown that neural stem cells cultured in 3D scaffolds generated 5-fold more neurons and expressed markers of mature nerve cells at an earlier time point compared to cells cultured in 2D culture systems[107]. Similar results were also found in cholangiocytes[108], lung fibroblasts[109], and CMs[103, 110]. In this study, due to the 3D environment, the cells located at the edge of the wells were more likely to differentiate into contractile CMs than the cells sitting in the center. In line with that, the visible initial beating area always appeared at the edge of the well.

5.3 Intercellular communication

Gap junctions are one of the intercellular signal transmission mechanisms, which directly connect the cytoplasm of two cells[111]. In cardiovascular system, gap junctions play a major role in the rapid electrical transmission between CMs[111]. Meanwhile, the gap junctions are important for the velocity and safety of electrical propagation between CMs[112]. It enables electrical signals to be transmitted in an orderly manner to adjacent CMs. The gap junctions also exist between iPSCs3 and influence the cell homeostasis, morphogenesis, and differentiation[113, 114]. Several studies have demonstrated that *CX43* mRNA is highly expressed in hESCs[115]. Furthermore, Beckmann et al. confirmed the presence of gap junctions in undifferentiated hiPSCs by using freeze-fracture replica immunogold labeling[116]. In this study, the expression of CX40 and CX43 were analyzed, both important components of the gap junction channel. The iPSC-CMs in both groups clearly expressed CX40 and CX43 (Fig.19). After the appearance of initial contracting parts during the cardiac differentiation, the electrical signal should be transmitted to surrounding cells via the gap junctions, possibly stimulating iPSC-CM differentiation. Thus, upon differentiation it could be seen that the beating area spread from initial part to the whole well and beating like “wave”.

In some publications, obvious reduction of *CX43* expression[117] and induction of *CX40* expression[118] were found in the HLHS-iPSC-CMs compared to control. However, in my research, no significant difference between the two groups (Fig.19, B and C) was observed, suggesting a comparable maturation status of CMs in both experimental groups.

5.4 The differences in gene expression of HLHS-derived iPSCs during myocardial differentiation

In my research, the transcription of some genes was suppressed during the direct cardiac differentiation of HLHS derived iPSCs, which are related to the development of HLHS (Fig. 17).

NKX2.5 is a member of NK 2 family and plays a critical role in cardiogenesis. *NKX2.5* regulates the expression of genes associated with proliferation, migration, and heart development [119]. Therefore, *NKX2.5* mutations may cause a series of heart disease. The first documented *NKX2.5* mutation associated with HLHS was reported in 2003[120]. After that, several studies in murine model and humans have shown the relationship between *NKX2.5* and HLHS [15, 120-122]. In particular, changes in *NKX2.5-Hand 1* transcriptional pathway affect the development of LV in cardiogenesis [123]. In this study, HLHS-derived iPS lines showed a clearly delayed expression of *NKX2.5* (Fig. 17 B), indicating the gene expression of HLHS-iPSCs *in vitro* was similar to that of HLHS patients during cardiogenesis.

TBX5 is a member of T-box transcription factor family and plays a key role in determining the morphogenesis and development of the heart [124]. It is located on chromosome 12 (12q24.1), with a total length of 2133 bp, containing 8 coding exons and encoding 518 amino acids [125]. *TBX5* mutation has been identified as a factor

strongly related to Holt-Oram syndrome (HOS) [126]. Since 2004, it was found to be associated to other non-HOS CHD like ASD, VSD, and AV block[127]. *TBX5* has positive function in cardiogenesis and CM maturation[128]. The expression of *TBX5* in human LV is second only to that in atrium and originates from the first heart field prior to cardiac morphogenesis[129]. Researchers have shown that interaction between *TBX5* and *Baf60c* and *Brg1*, members of the SWI/SNF family, participates in the regulation of chromatin remodeling, affecting the differentiation of mesodermal cells into CMs[130]. In addition, *TBX5* and *NKX2.5* interact to control cardiac conduction system gene expression[128] and promote CM maturation[131, 132].

NPPA, encoding atrial natriuretic factor (ANF), is expressed in atrial and ventricular cells during embryonic and neonatal stage. But the expression is downregulated after birth. *NPPA* is a stress-induced gene and can be activated by MI, salt-sensitive hypertension, and cardiac hypertrophy[133, 134]. Furthermore, *NPPA* is also an important marker for myocardial chamber differentiation and congenital heart defects[132]. *TBX5* is a direct regulator of *NPPA* and can bind sites on the promoters of *NPPA* in a dosage-dependent manner[135]. The expression of *NPPA* was significantly decreased in *TBX5* knockout mice[128]. *TBX5* can activate *NPPA* expression by binding to NPPA promotor through the C-terminal domain. In addition, *TBX5* and *NKX2.5* form a heterodimer complex through the N-terminal domain and then interact with *NPPA* promotor for *NPPA* activation[136]. In my research, the expression of *TBX5* and *NPPA* was almost consistent, which was quite low in the HLHS group (Fig. 17 C and D). This result is similar to that of Bruneau[128].

The LIM-homeodomain transcription factor Islet1 (Isl1) is known as a core marker of cardiac progenitor cell (CPC) and is required for proliferation, expansion, and migration of CPCs. The cardiac progenitor cell population in the visceral mesoderm can be divided into first heart field (FHF) and second heart field (SHF) according to the fate of differentiation [137]. Cells in FHF eventually differentiate into left ventricle and part of atrium, and cells in SHF differentiate into right ventricle, outflow tract, and the

remaining atrium [138]. Studies have shown that *Isl1* is already expressed in the common CPC population, but the role of *Isl1* in FHF differentiation is not critical compared with its role in SHF[139, 140]. *Isl1*-knockout heart failed to form the RV and outflow tract, while the LV marker, as *Tbx5*, *Hand1*, and *Fgf10*, still can be detected[141]. In this research, I found the expression of *ISL1* had no difference between the HLHS and control group (Fig. 17 A). Moreover, *Isl1* is direct target of Wnt/β-catenin signaling pathway[142]. The usage of Wnt promoter and inhibitor (CHIR99021 and Wnt-C59) may also affect the expression of *ISL1* in my study.

Troponin T plays a crucial role in the contraction of striated muscle. It is encoded by three type-specific isoforms including *TNNT1* (slow skeletal muscle), *TNNT2* (cardiac muscle), and *TNNT3* (fast skeletal muscle)[143]. A previous study indicated that the expression of *TNNT2* in HLHS derived iPSC was significantly lower, and the expression could be restored after the combination of TFs (*NKX2-5*, *NOTCH1*, and *HAND1*) with *TNNT2* promoter[15]. In my research, I found that the *TNNT 2* expression increased in parallel in both groups until day 8 and was slightly enhanced in the control group on day 10 (Fig. 17 E). Furthermore, the results of ICC (Fig. 18) and flowcytometry (Fig. 20 D) also showed no significant differences between the two groups. The expression of *TNNT2* in the control group peaked on day 10 and gradually decreased thereafter, which was quite similar to the result of Burridge[65]. In the HLHS group, the expression of *TNNT2* continued to rise in the first 14 days of differentiation. This might be because the reduced expression of multiple TFs, like *TBX5*, *NPPA*, and *NKX2.5*, caused a delay of *TNNT2* expression in HLHS-derived iPSCs. But more research is needed obtain a better understanding of the interaction between the TFs and *TNNT2*.

5.5 EHT formation

EHTs or engineered cardiac tissues are SC-derived CMs cultured in a three-dimensional scaffold *in vitro*, able to mimic the *in vivo* contraction of heart tissue. The first artificial contracting tissue has been created much earlier than the term engineered tissue was introduced. In the late 1950ies, Moscana[144] generated spontaneously

beating spheroid aggregates from embryonic chicken cardiac myocytes. In 1997, Eschenhagen and colleagues[145] successfully generated the contracting strip, which was the first "real" EHT, by culturing a mixture of embryonic chicken CMs and collagen solution in a slide with two Velcro-coated glass tubes. Presently, tremendous progress has been made during the two decades after the first generation of EHTs. Cell culture has been extended from embryonic chicken CMs to human CMs which were derived from ESCs or iPSCs. New biomaterial scaffolds were created for better retention and maturation of CMs[146]. This progress and success lead to a broad application spectrum for EHTs.

As a pilot study, the CMs which were differentiated from iPSCs were used for the generation of EHTs. For this approach it is important to generate a cell population which consists of more than 60% CMs. The analyses above have confirmed that this requirement could be overfulfilled in the direct cardiac differentiation assay (Fig. 20 C). Spontaneous contraction of the EHTs could be observed around day 4 to day 6 and it was possible to determine several physical parameters such as contractile force, velocity, rate, and rhythm with the video-optical recording system[77].

For a better understanding of the iPSC-CMs subtype in the EHTs, immunohistochemical staining of MLC2a and MLC2v was performed. MLC2a and MLC2v are two different isoforms of the cardiac myosin light chain. Generally, MLC2a is thought to be expressed in all chambers (atria and ventricles) and immature CMs, while MLC2v is rather a marker for ventricular CMs[147, 148]. Thus, MLC2a and MLC2v were used as markers to determine the subtype and developmental stage of CMs[149]. Fikru and colleagues' research illustrated that during differentiation of iPSCs into CMs the MLC2a is expressed at an early stage. Afterwards, MLC2a expression gradually decreased with MLC2v expression increased, and a large number of iPSC-CMs expressed both MLC2a and MLC2v[150]. In this study, both MLC2a- and MLC2v-positive CMs could be found in the EHTs after 3 weeks of culture (Fig. 22). Thus, the EHT approach successfully generated CMs which had differentiated into the atrial or ventricular direction.

It is well accepted and known that adult CMs have a very low incidence of proliferation (0.3% to 1%)[151]. The highest proliferation of CMs is seen during the prenatal stage[152], which means that compared with adult CMs, premature or immature CMs have a higher proliferative ability (Fig. 23). The staining of proliferative markers, Ki67 and PH3, showed that there is a tendency that part of CMs in the EHTs display a proliferative capacity (Fig. 24).

Conclusion

HLHS is a very severe congenital heart disease characterized by aortic and/or mitral valve stenosis or atresia with significant hypoplastic left ventricle, and hypoplasia of the ascending aorta and aortic arch. The patient-specific derived iPSC provides an approach for modeling HLHS *in vitro* and they allow the study of pathophysiology of HLHS.

Direct cardiac differentiation modulated by small molecular has been proved to be an easy-to-handle protocol with a satisfactory output. In this study, CHIR99021 and Wnt-C59 were used to modulate the Wnt/β-catenin signaling pathway for the cardiac differentiation of hiPSCs. During cell differentiation, I found that cell death was heavily affected by the concentration of CHIR99021 and initial cell seeding density confirming similar observations of other research groups. This is due to the role of CHIR99021 in regulating cell apoptosis and each cell line has a different sensitivity to the concentration of CHIR99021. Therefore, the definition of an appropriate concentration of CHIR99021 for each cell line is crucial to obtain an effective cardiac differentiation.

In the study of modeling HLHS with patient-specific iPSC-CMs, I found no significant differences in the differentiation efficiency, sarcomeric and connexin proteins between the HLHS- and control groups, in the first sight. Nevertheless, there are differences in the expression of essential cardiac transcription factors, especially the *TBX5* and its direct target gene *NPPA*, which were quite low expressed in HLHS-iPSCs during differentiation.

As a pilot study, the iPSC-CMs were used for the generation of EHTs. Spontaneous contraction of the EHTs could be observed and several physical parameters such as contractile force, velocity, rate, and rhythm was recorded by the video-optical recording system. Furthermore, the subtype and proliferative activity were detected in the EHTs.

These results showed that the iPSC-CMs-generated EHTs could be used to study the differentiation and maturation of HLHS-CMs under spatial 3D culture and external force.

References

[1] J. I. Hoffman, and S. Kaplan, "The incidence of congenital heart disease," *J Am Coll Cardiol,* vol. 39, no. 12, pp. 1890-900, Jun 19, 2002.

[2] D. van der Linde, E. E. Konings, M. A. Slager, M. Witsenburg, W. A. Helbing, J. J. Takkenberg, and J. W. Roos-Hesselink, "Birth prevalence of congenital heart disease worldwide: a systematic review and meta-analysis," *J Am Coll Cardiol,* vol. 58, no. 21, pp. 2241-7, Nov 15, 2011.

[3] P. C. Helm, H. Kaemmerer, G. Breithardt, E. J. Sticker, R. Keuchen, R. Neidenbach, G. P. Diller, O. Tutarel, and U. M. M. Bauer, "Transition in Patients with Congenital Heart Disease in Germany: Results of a Nationwide Patient Survey," *Front Pediatr,* vol. 5, pp. 115, 2017.

[4] C. I. Tchervenkov, H. L. Walters, 3rd, and V. F. Chu, "Congenital Heart Surgery Nomenclature and Database Project: double outlet left ventricle," *Ann Thorac Surg,* vol. 69, no. 4 Suppl, pp. S264-9, Apr, 2000.

[5] M. Yabrodi, and C. W. Mastropietro, "Hypoplastic left heart syndrome: from comfort care to long-term survival," *Pediatr Res,* vol. 81, no. 1-2, pp. 142-149, Jan, 2017.

[6] H. Lahm, P. Schon, S. Doppler, M. Dressen, J. Cleuziou, M. A. Deutsch, P. Ewert, R. Lange, and M. Krane, "Tetralogy of Fallot and Hypoplastic Left Heart Syndrome - Complex Clinical Phenotypes Meet Complex Genetic Networks," *Curr Genomics,* vol. 16, no. 3, pp. 141-58, Jun, 2015.

[7] A. Lindinger, G. Schwedler, and H. W. Hense, "Prevalence of congenital heart defects in newborns in Germany: Results of the first registration year of the PAN Study (July 2006 to June 2007)," *Klin Padiatr,* vol. 222, no. 5, pp. 321-6, Sep, 2010.

[8] C. D. Morris, J. Outcalt, and V. D. Menashe, "Hypoplastic left heart syndrome: natural history in a geographically defined population," *Pediatrics,* vol. 85, no. 6, pp. 977-83, Jun, 1990.

[9] M. K. Metcalf, and J. Rychik, "Outcomes in Hypoplastic Left Heart Syndrome," *Pediatr Clin North Am,* vol. 67, no. 5, pp. 945-962, Oct, 2020.

[10] M. D. K. David J Barron, Ben Davies, John G C Wright, Timothy J Jones,

William J Brawn, "Hypoplastic left heart syndrome," *Lancet,* vol. 374, no. 9689, pp. 551-564, 2009.

[11] A. Sharma, G. Li, K. Rajarajan, R. Hamaguchi, P. W. Burridge, and S. M. Wu, "Derivation of highly purified cardiomyocytes from human induced pluripotent stem cells using small molecule-modulated differentiation and subsequent glucose starvation," *J Vis Exp*, no. 97, Mar 18, 2015.

[12] A. T. Hattam, "A potentially curative fetal intervention for hypoplastic left heart syndrome," *Med Hypotheses,* vol. 110, pp. 132-137, Jan, 2018.

[13] A. Crucean, A. Alqahtani, D. J. Barron, W. J. Brawn, R. V. Richardson, J. O'Sullivan, R. H. Anderson, D. J. Henderson, and B. Chaudhry, "Re-evaluation of hypoplastic left heart syndrome from a developmental and morphological perspective," *Orphanet J Rare Dis,* vol. 12, no. 1, pp. 138, Aug 10, 2017.

[14] D. A. Lara, M. K. Ethen, M. A. Canfield, W. N. Nembhard, and S. A. Morris, "A population-based analysis of mortality in patients with Turner syndrome and hypoplastic left heart syndrome using the Texas Birth Defects Registry," *Congenital Heart Disease,* vol. 12, no. 1, pp. 105-112, 2017.

[15] J. Kobayashi, M. Yoshida, S. Tarui, M. Hirata, Y. Nagai, S. Kasahara, K. Naruse, H. Ito, S. Sano, and H. Oh, "Directed differentiation of patient-specific induced pluripotent stem cells identifies the transcriptional repression and epigenetic modification of NKX2-5, HAND1, and NOTCH1 in hypoplastic left heart syndrome," *PLoS One,* vol. 9, no. 7, pp. e102796, 2014.

[16] S. C. Glidewell, S. D. Miyamoto, P. D. Grossfeld, D. E. Clouthier, C. D. Coldren, R. S. Stearman, and M. W. Geraci, "Transcriptional Impact of Rare and Private Copy Number Variants in Hypoplastic Left Heart Syndrome," *Clin Transl Sci,* vol. 8, no. 6, pp. 682-9, Dec, 2015.

[17] R. Redon, S. Ishikawa, K. R. Fitch, L. Feuk, G. H. Perry, T. D. Andrews, H. Fiegler, M. H. Shapero, A. R. Carson, W. Chen, E. K. Cho, S. Dallaire, J. L. Freeman, J. R. Gonzalez, M. Gratacos, J. Huang, D. Kalaitzopoulos, D. Komura, J. R. MacDonald, C. R. Marshall, R. Mei, L. Montgomery, K. Nishimura, K. Okamura, F. Shen, M. J. Somerville, J. Tchinda, A. Valsesia, C. Woodwark, F. Yang, J. Zhang, T. Zerjal, J. Zhang, L. Armengol, D. F. Conrad,

X. Estivill, C. Tyler-Smith, N. P. Carter, H. Aburatani, C. Lee, K. W. Jones, S. W. Scherer, and M. E. Hurles, "Global variation in copy number in the human genome," *Nature,* vol. 444, no. 7118, pp. 444-54, Nov 23, 2006.

[18] X. Zhao, Y. Wang, and X. Sun, "The functions of microRNA-208 in the heart," *Diabetes Res Clin Pract,* vol. 160, pp. 108004, Feb, 2020.

[19] X. Zhang, S. Dong, Q. Jia, A. Zhang, Y. Li, Y. Zhu, S. Lv, and J. Zhang, "The microRNA in ventricular remodeling: the miR-30 family," *Biosci Rep,* vol. 39, no. 8, Aug 30, 2019.

[20] J. Yuan, H. Liu, W. Gao, L. Zhang, Y. Ye, L. Yuan, Z. Ding, J. Wu, L. Kang, X. Zhang, X. Wang, G. Zhang, H. Gong, A. Sun, X. Yang, R. Chen, Z. Cui, J. Ge, and Y. Zou, "MicroRNA-378 suppresses myocardial fibrosis through a paracrine mechanism at the early stage of cardiac hypertrophy following mechanical stress," *Theranostics,* vol. 8, no. 9, pp. 2565-2582, 2018.

[21] C. C. Sucharov, J. Sucharov, A. Karimpour-Fard, K. Nunley, B. L. Stauffer, and S. D. Miyamoto, "Micro-RNA expression in hypoplastic left heart syndrome," *J Card Fail,* vol. 21, no. 1, pp. 83-8, Jan, 2015.

[22] M. Krane, M. Dressen, G. Santamaria, I. My, C. M. Schneider, T. Dorn, S. Laue, E. Mastantuono, R. Berutti, H. Rawat, R. Gilsbach, P. Schneider, H. Lahm, S. Schwarz, S. A. Doppler, S. Paige, N. Puluca, S. Doll, I. Neb, T. Brade, Z. Zhang, C. Abou-Ajram, B. Northoff, L. M. Holdt, S. Sudhop, M. Sahara, A. Goedel, A. Dendorfer, F. V. Y. Tjong, M. E. Rijlaarsdam, J. Cleuziou, N. Lang, C. Kupatt, C. Bezzina, R. Lange, N. E. Bowles, M. Mann, B. D. Gelb, L. Crotti, L. Hein, T. Meitinger, S. Wu, D. Sinnecker, P. J. Gruber, K. L. Laugwitz, and A. Moretti, "Sequential Defects in Cardiac Lineage Commitment and Maturation Cause Hypoplastic Left Heart Syndrome," *Circulation,* vol. 144, no. 17, pp. 1409-1428, Oct 26, 2021.

[23] W. I. Norwood, P. Lang, and D. D. Hansen, "Physiologic repair of aortic atresia-hypoplastic left heart syndrome," *N Engl J Med,* vol. 308, no. 1, pp. 23-6, Jan 6, 1983.

[24] C. E. Greenleaf, J. M. Urencio, J. D. Salazar, and A. Dodge-Khatami, "Hypoplastic left heart syndrome: current perspectives," *Translational Pediatrics,* vol. 5, no. 3, pp. 142-147, 2016.

[25] L. J. Kleinsmith, and G. B. Pierce, Jr., "Multipotentiality of Single Embryonal

Carcinoma Cells," *Cancer Res,* vol. 24, pp. 1544-51, Oct, 1964.

[26] J. A. Ankrum, J. F. Ong, and J. M. Karp, "Mesenchymal stem cells: immune evasive, not immune privileged," *Nat Biotechnol,* vol. 32, no. 3, pp. 252-60, Mar, 2014.

[27] E. Dzierzak, and N. A. Speck, "Of lineage and legacy: the development of mammalian hematopoietic stem cells," *Nat Immunol,* vol. 9, no. 2, pp. 129-36, Feb, 2008.

[28] J. E. Ferguson, 3rd, R. W. Kelley, and C. Patterson, "Mechanisms of endothelial differentiation in embryonic vasculogenesis," *Arterioscler Thromb Vasc Biol,* vol. 25, no. 11, pp. 2246-54, Nov, 2005.

[29] P. D. Lewis, "Mitotic activity in the primate subependymal layer and the genesis of gliomas," *Nature,* vol. 217, no. 5132, pp. 974-5, Mar 9, 1968.

[30] Z. Li, "CD133: a stem cell biomarker and beyond," *Exp Hematol Oncol,* vol. 2, no. 1, pp. 17, Jul 1, 2013.

[31] S. Mitalipov, and D. Wolf, "Totipotency, pluripotency and nuclear reprogramming," *Adv Biochem Eng Biotechnol,* vol. 114, pp. 185-99, 2009.

[32] W. Zakrzewski, M. Dobrzynski, M. Szymonowicz, and Z. Rybak, "Stem cells: past, present, and future," *Stem Cell Res Ther,* vol. 10, no. 1, pp. 68, Feb 26, 2019.

[33] S. He, D. Nakada, and S. J. Morrison, "Mechanisms of stem cell self-renewal," *Annu Rev Cell Dev Biol,* vol. 25, pp. 377-406, 2009.

[34] K. Takahashi, and S. Yamanaka, "Induction of pluripotent stem cells from mouse embryonic and adult fibroblast cultures by defined factors," *Cell,* vol. 126, no. 4, pp. 663-76, Aug 25, 2006.

[35] K. Takahashi, K. Tanabe, M. Ohnuki, M. Narita, T. Ichisaka, K. Tomoda, and S. Yamanaka, "Induction of pluripotent stem cells from adult human fibroblasts by defined factors," *Cell,* vol. 131, no. 5, pp. 861-72, Nov 30, 2007.

[36] J. B. Gurdon, T. R. Elsdale, and M. Fischberg, "Sexually mature individuals of Xenopus laevis from the transplantation of single somatic nuclei," *Nature,* vol. 182, no. 4627, pp. 64-5, Jul 5, 1958.

[37] T. Zhou, C. Benda, S. Dunzinger, Y. Huang, J. C. Ho, J. Yang, Y. Wang, Y.

Zhang, Q. Zhuang, Y. Li, X. Bao, H. F. Tse, J. Grillari, R. Grillari-Voglauer, D. Pei, and M. A. Esteban, "Generation of human induced pluripotent stem cells from urine samples," *Nat Protoc,* vol. 7, no. 12, pp. 2080-9, Dec, 2012.

[38] Y. H. Loh, S. Agarwal, I. H. Park, A. Urbach, H. Huo, G. C. Heffner, K. Kim, J. D. Miller, K. Ng, and G. Q. Daley, "Generation of induced pluripotent stem cells from human blood," *Blood,* vol. 113, no. 22, pp. 5476-9, May 28, 2009.

[39] P. Faisca, and D. Desmecht, "Sendai virus, the mouse parainfluenza type 1: a longstanding pathogen that remains up-to-date," *Res Vet Sci,* vol. 82, no. 1, pp. 115-25, Feb, 2007.

[40] M. Nakanishi, and M. Otsu, "Development of Sendai virus vectors and their potential applications in gene therapy and regenerative medicine," *Curr Gene Ther,* vol. 12, no. 5, pp. 410-6, Oct, 2012.

[41] M. Hayes, and N. Zavazava, "Strategies to generate induced pluripotent stem cells," *Methods Mol Biol,* vol. 1029, pp. 77-92, 2013.

[42] M. Writing Group, D. Mozaffarian, E. J. Benjamin, A. S. Go, D. K. Arnett, M. J. Blaha, M. Cushman, S. R. Das, S. de Ferranti, J. P. Despres, H. J. Fullerton, V. J. Howard, M. D. Huffman, C. R. Isasi, M. C. Jimenez, S. E. Judd, B. M. Kissela, J. H. Lichtman, L. D. Lisabeth, S. Liu, R. H. Mackey, D. J. Magid, D. K. McGuire, E. R. Mohler, 3rd, C. S. Moy, P. Muntner, M. E. Mussolino, K. Nasir, R. W. Neumar, G. Nichol, L. Palaniappan, D. K. Pandey, M. J. Reeves, C. J. Rodriguez, W. Rosamond, P. D. Sorlie, J. Stein, A. Towfighi, T. N. Turan, S. S. Virani, D. Woo, R. W. Yeh, M. B. Turner, C. American Heart Association Statistics, and S. Stroke Statistics, "Heart Disease and Stroke Statistics-2016 Update: A Report From the American Heart Association," *Circulation,* vol. 133, no. 4, pp. e38-360, Jan 26, 2016.

[43] R. Estruch, E. Ros, J. Salas-Salvado, M. I. Covas, D. Corella, F. Aros, E. Gomez-Gracia, V. Ruiz-Gutierrez, M. Fiol, J. Lapetra, R. M. Lamuela-Raventos, L. Serra-Majem, X. Pinto, J. Basora, M. A. Munoz, J. V. Sorli, J. A. Martinez, M. A. Martinez-Gonzalez, and P. S. Investigators, "Primary prevention of cardiovascular disease with a Mediterranean diet," *N Engl J Med,* vol. 368, no. 14, pp. 1279-90, Apr 4, 2013.

[44] E. Tzahor, and K. D. Poss, "Cardiac regeneration strategies: Staying young

at heart," *Science,* vol. 356, no. 6342, pp. 1035-1039, Jun 9, 2017.

[45] E. N. Olson, and M. D. Schneider, "Sizing up the heart: development redux in disease," *Genes Dev,* vol. 17, no. 16, pp. 1937-56, Aug 15, 2003.

[46] I. Kehat, D. Kenyagin-Karsenti, M. Snir, H. Segev, M. Amit, A. Gepstein, E. Livne, O. Binah, J. Itskovitz-Eldor, and L. Gepstein, "Human embryonic stem cells can differentiate into myocytes with structural and functional properties of cardiomyocytes," *J Clin Invest,* vol. 108, no. 3, pp. 407-14, Aug, 2001.

[47] A. P. Beltrami, L. Barlucchi, D. Torella, M. Baker, F. Limana, S. Chimenti, H. Kasahara, M. Rota, E. Musso, K. Urbanek, A. Leri, J. Kajstura, B. Nadal-Ginard, and P. Anversa, "Adult cardiac stem cells are multipotent and support myocardial regeneration," *Cell,* vol. 114, no. 6, pp. 763-76, Sep 19, 2003.

[48] W. H. Zimmermann, "Biomechanical regulation of in vitro cardiogenesis for tissue-engineered heart repair," *Stem Cell Res Ther,* vol. 4, no. 6, pp. 137, 2013.

[49] M. E. Kupfer, W. H. Lin, V. Ravikumar, K. Qiu, L. Wang, L. Gao, D. B. Bhuiyan, M. Lenz, J. Ai, R. R. Mahutga, D. Townsend, J. Zhang, M. C. McAlpine, E. G. Tolkacheva, and B. M. Ogle, "In Situ Expansion, Differentiation, and Electromechanical Coupling of Human Cardiac Muscle in a 3D Bioprinted, Chambered Organoid," *Circ Res,* vol. 127, no. 2, pp. 207-224, Jul 3, 2020.

[50] S. K. Yadav, and P. K. Mishra, "Isolation, Characterization and Differentiation of Mouse Cardiac Progenitor Cells," *Methods Mol Biol,* vol. 1842, pp. 183-191, 2018.

[51] M. Wang, W. Ling, C. Xiong, D. Xie, X. Chu, Y. Li, X. Qiu, Y. Li, and X. Xiao, "Potential Strategies for Cardiac Diseases: Lineage Reprogramming of Somatic Cells into Induced Cardiomyocytes," *Cell Reprogram,* vol. 21, no. 2, pp. 63-77, Apr, 2019.

[52] C. L. Mummery, J. Zhang, E. S. Ng, D. A. Elliott, A. G. Elefanty, and T. J. Kamp, "Differentiation of Human Embryonic Stem Cells and Induced Pluripotent Stem Cells to Cardiomyocytes," *Circulation Research,* vol. 111, no. 3, pp. 344-358, 2012.

[53] I. Batalov, and A. W. Feinberg, "Differentiation of Cardiomyocytes from

Human Pluripotent Stem Cells Using Monolayer Culture," *Biomark Insights,* vol. 10, no. Suppl 1, pp. 71-6, 2015.

[54] K. R. Boheler, J. Czyz, D. Tweedie, H.-T. Yang, S. V. Anisimov, and A. M. Wobus, "Differentiation of Pluripotent Embryonic Stem Cells Into Cardiomyocytes," *Circulation Research,* vol. 91, no. 3, pp. 189-201, 2002.

[55] S. Tohyama, F. Hattori, M. Sano, T. Hishiki, Y. Nagahata, T. Matsuura, H. Hashimoto, T. Suzuki, H. Yamashita, Y. Satoh, T. Egashira, T. Seki, N. Muraoka, H. Yamakawa, Y. Ohgino, T. Tanaka, M. Yoichi, S. Yuasa, M. Murata, M. Suematsu, and K. Fukuda, "Distinct Metabolic Flow Enables Large-Scale Purification of Mouse and Human Pluripotent Stem Cell-Derived Cardiomyocytes," *Cell Stem Cell,* vol. 12, no. 1, pp. 127-137, 2013.

[56] L. Yang, M. H. Soonpaa, E. D. Adler, T. K. Roepke, S. J. Kattman, M. Kennedy, E. Henckaerts, K. Bonham, G. W. Abbott, R. M. Linden, L. J. Field, and G. M. Keller, "Human cardiovascular progenitor cells develop from a KDR+ embryonic-stem-cell-derived population," *Nature,* vol. 453, no. 7194, pp. 524-8, May 22, 2008.

[57] D. A. Elliott, S. R. Braam, K. Koutsis, E. S. Ng, R. Jenny, E. L. Lagerqvist, C. Biben, T. Hatzistavrou, C. E. Hirst, Q. C. Yu, R. J. Skelton, D. Ward-van Oostwaard, S. M. Lim, O. Khammy, X. Li, S. M. Hawes, R. P. Davis, A. L. Goulburn, R. Passier, O. W. Prall, J. M. Haynes, C. W. Pouton, D. M. Kaye, C. L. Mummery, A. G. Elefanty, and E. G. Stanley, "NKX2-5(eGFP/w) hESCs for isolation of human cardiac progenitors and cardiomyocytes," *Nat Methods,* vol. 8, no. 12, pp. 1037-40, Oct 23, 2011.

[58] M. Costa, M. Dottori, K. Sourris, P. Jamshidi, T. Hatzistavrou, R. Davis, L. Azzola, S. Jackson, S. M. Lim, M. Pera, A. G. Elefanty, and E. G. Stanley, "A method for genetic modification of human embryonic stem cells using electroporation," *Nat Protoc,* vol. 2, no. 4, pp. 792-6, 2007.

[59] E. S. Ng, R. P. Davis, L. Azzola, E. G. Stanley, and A. G. Elefanty, "Forced aggregation of defined numbers of human embryonic stem cells into embryoid bodies fosters robust, reproducible hematopoietic differentiation," *Blood,* vol. 106, no. 5, pp. 1601-3, Sep 1, 2005.

[60] T. Brade, L. S. Pane, A. Moretti, K. R. Chien, and K. L. Laugwitz, "Embryonic heart progenitors and cardiogenesis," *Cold Spring Harb Perspect Med,*

vol. 3, no. 10, pp. a013847, Oct 1, 2013.

[61] C. Mummery, D. Ward-van Oostwaard, P. Doevendans, R. Spijker, S. van den Brink, R. Hassink, M. van der Heyden, T. Opthof, M. Pera, A. B. de la Riviere, R. Passier, and L. Tertoolen, "Differentiation of human embryonic stem cells to cardiomyocytes: role of coculture with visceral endoderm-like cells," *Circulation,* vol. 107, no. 21, pp. 2733-40, Jun 3, 2003.

[62] R. Passier, D. W. Oostwaard, J. Snapper, J. Kloots, R. J. Hassink, E. Kuijk, B. Roelen, A. B. de la Riviere, and C. Mummery, "Increased cardiomyocyte differentiation from human embryonic stem cells in serum-free cultures," *Stem Cells,* vol. 23, no. 6, pp. 772-80, Jun-Jul, 2005.

[63] S. L. Paige, T. Osugi, O. K. Afanasiev, L. Pabon, H. Reinecke, and C. E. Murry, "Endogenous Wnt/beta-catenin signaling is required for cardiac differentiation in human embryonic stem cells," *PLoS One,* vol. 5, no. 6, pp. e11134, Jun 15, 2010.

[64] P. W. Burridge, A. Holmstrom, and J. C. Wu, "Chemically Defined Culture and Cardiomyocyte Differentiation of Human Pluripotent Stem Cells," *Curr Protoc Hum Genet,* vol. 87, pp. 21 3 1-21 3 15, Oct 6, 2015.

[65] P. W. Burridge, E. Matsa, P. Shukla, Z. C. Lin, J. M. Churko, A. D. Ebert, F. Lan, S. Diecke, B. Huber, N. M. Mordwinkin, J. R. Plews, O. J. Abilez, B. Cui, J. D. Gold, and J. C. Wu, "Chemically defined generation of human cardiomyocytes," *Nat Methods,* vol. 11, no. 8, pp. 855-60, Aug, 2014.

[66] X. Lian, C. Hsiao, G. Wilson, K. Zhu, L. B. Hazeltine, S. M. Azarin, K. K. Raval, J. Zhang, T. J. Kamp, and S. P. Palecek, "Robust cardiomyocyte differentiation from human pluripotent stem cells via temporal modulation of canonical Wnt signaling," *Proc Natl Acad Sci U S A,* vol. 109, no. 27, pp. E1848-57, Jul 3, 2012.

[67] R. Nusse, "Wnt signaling in disease and in development," *Cell Res,* vol. 15, no. 1, pp. 28-32, Jan, 2005.

[68] H. Zhang, H. Zhang, Y. Zhang, S. S. Ng, F. Ren, Y. Wang, Y. Duan, L. Chen, Y. Zhai, Q. Guo, and Z. Chang, "Dishevelled-DEP domain interacting protein (DDIP) inhibits Wnt signaling by promoting TCF4 degradation and disrupting the TCF4/beta-catenin complex," *Cell Signal,* vol. 22, no. 11, pp. 1753-60, Nov, 2010.

[69] S. Ueno, G. Weidinger, T. Osugi, A. D. Kohn, J. L. Golob, L. Pabon, H. Reinecke, R. T. Moon, and C. E. Murry, "Biphasic role for Wnt/beta-catenin signaling in cardiac specification in zebrafish and embryonic stem cells," *Proc Natl Acad Sci U S A,* vol. 104, no. 23, pp. 9685-90, Jun 5, 2007.

[70] Y. Qyang, S. Martin-Puig, M. Chiravuri, S. Chen, H. Xu, L. Bu, X. Jiang, L. Lin, A. Granger, A. Moretti, L. Caron, X. Wu, J. Clarke, M. M. Taketo, K. L. Laugwitz, R. T. Moon, P. Gruber, S. M. Evans, S. Ding, and K. R. Chien, "The renewal and differentiation of Isl1+ cardiovascular progenitors are controlled by a Wnt/beta-catenin pathway," *Cell Stem Cell,* vol. 1, no. 2, pp. 165-79, Aug 16, 2007.

[71] J. Tian, H. He, and G. Lei, "Wnt/beta-catenin pathway in bone cancers," *Tumour Biol,* vol. 35, no. 10, pp. 9439-45, Oct, 2014.

[72] D. P. Minde, Z. Anvarian, S. G. Rudiger, and M. M. Maurice, "Messing up disorder: how do missense mutations in the tumor suppressor protein APC lead to cancer?," *Mol Cancer,* vol. 10, pp. 101, Aug 22, 2011.

[73] D. P. Minde, M. Radli, F. Forneris, M. M. Maurice, and S. G. Rudiger, "Large extent of disorder in Adenomatous Polyposis Coli offers a strategy to guard Wnt signalling against point mutations," *PLoS One,* vol. 8, no. 10, pp. e77257, 2013.

[74] X. Lian, J. Zhang, S. M. Azarin, K. Zhu, L. B. Hazeltine, X. Bao, C. Hsiao, T. J. Kamp, and S. P. Palecek, "Directed cardiomyocyte differentiation from human pluripotent stem cells by modulating Wnt/β-catenin signaling under fully defined conditions," *Nature Protocols,* vol. 8, no. 1, pp. 162-175, 2012.

[75] A. Moretti, M. Bellin, C. B. Jung, T. M. Thies, Y. Takashima, A. Bernshausen, M. Schiemann, S. Fischer, S. Moosmang, A. G. Smith, J. T. Lam, and K. L. Laugwitz, "Mouse and human induced pluripotent stem cells as a source for multipotent Isl1+ cardiovascular progenitors," *FASEB J,* vol. 24, no. 3, pp. 700-11, Mar, 2010.

[76] K. Breckwoldt, D. Letuffe-Breniere, I. Mannhardt, T. Schulze, B. Ulmer, T. Werner, A. Benzin, B. Klampe, M. C. Reinsch, S. Laufer, A. Shibamiya, M. Prondzynski, G. Mearini, D. Schade, S. Fuchs, C. Neuber, E. Kramer, U. Saleem, M. L. Schulze, M. L. Rodriguez, T. Eschenhagen, and A. Hansen,

"Differentiation of cardiomyocytes and generation of human engineered heart tissue," *Nat Protoc,* vol. 12, no. 6, pp. 1177-1197, Jun, 2017.

[77] S. Schaaf, A. Shibamiya, M. Mewe, A. Eder, A. Stohr, M. N. Hirt, T. Rau, W. H. Zimmermann, L. Conradi, T. Eschenhagen, and A. Hansen, "Human engineered heart tissue as a versatile tool in basic research and preclinical toxicology," *PLoS One,* vol. 6, no. 10, pp. e26397, 2011.

[78] T. Scholzen, and J. Gerdes, "The Ki-67 protein: from the known and the unknown," *J Cell Physiol,* vol. 182, no. 3, pp. 311-22, Mar, 2000.

[79] D. Verduzco, and J. F. Amatruda, "Analysis of cell proliferation, senescence, and cell death in zebrafish embryos," *Methods Cell Biol,* vol. 101, pp. 19-38, 2011.

[80] H. Ye, and Q. Wang, "Efficient Generation of Non-Integration and Feeder-Free Induced Pluripotent Stem Cells from Human Peripheral Blood Cells by Sendai Virus," *Cell Physiol Biochem,* vol. 50, no. 4, pp. 1318-1331, 2018.

[81] T. M. Schlaeger, L. Daheron, T. R. Brickler, S. Entwisle, K. Chan, A. Cianci, A. DeVine, A. Ettenger, K. Fitzgerald, M. Godfrey, D. Gupta, J. McPherson, P. Malwadkar, M. Gupta, B. Bell, A. Doi, N. Jung, X. Li, M. S. Lynes, E. Brookes, A. B. Cherry, D. Demirbas, A. M. Tsankov, L. I. Zon, L. L. Rubin, A. P. Feinberg, A. Meissner, C. A. Cowan, and G. Q. Daley, "A comparison of non-integrating reprogramming methods," *Nat Biotechnol,* vol. 33, no. 1, pp. 58-63, Jan, 2015.

[82] P. S. Knoepfler, "Why myc? An unexpected ingredient in the stem cell cocktail," *Cell Stem Cell,* vol. 2, no. 1, pp. 18-21, Jan 10, 2008.

[83] H. J. Lim, J. Kim, C. H. Park, S. A. Lee, M. R. Lee, K. S. Kim, J. Kim, and Y. S. Bae, "Regulation of c-Myc Expression by Ahnak Promotes Induced Pluripotent Stem Cell Generation," *J Biol Chem,* vol. 291, no. 2, pp. 752-61, Jan 8, 2016.

[84] M. Couillard, and M. Trudel, "C-myc as a modulator of renal stem/progenitor cell population," *Dev Dyn,* vol. 238, no. 2, pp. 405-14, Feb, 2009.

[85] R. Sridharan, J. Tchieu, M. J. Mason, R. Yachechko, E. Kuoy, S. Horvath, Q. Zhou, and K. Plath, "Role of the murine reprogramming factors in the

induction of pluripotency," *Cell,* vol. 136, no. 2, pp. 364-77, Jan 23, 2009.

[86] D. Dominguez-Sola, C. Y. Ying, C. Grandori, L. Ruggiero, B. Chen, M. Li, D. A. Galloway, W. Gu, J. Gautier, and R. Dalla-Favera, "Non-transcriptional control of DNA replication by c-Myc," *Nature,* vol. 448, no. 7152, pp. 445-51, Jul 26, 2007.

[87] T. Sumi, N. Tsuneyoshi, N. Nakatsuji, and H. Suemori, "Apoptosis and differentiation of human embryonic stem cells induced by sustained activation of c-Myc," *Oncogene,* vol. 26, no. 38, pp. 5564-76, Aug 16, 2007.

[88] V. S. Li, S. S. Ng, P. J. Boersema, T. Y. Low, W. R. Karthaus, J. P. Gerlach, S. Mohammed, A. J. Heck, M. M. Maurice, T. Mahmoudi, and H. Clevers, "Wnt signaling through inhibition of beta-catenin degradation in an intact Axin1 complex," *Cell,* vol. 149, no. 6, pp. 1245-56, Jun 8, 2012.

[89] R. S. Jope, and G. V. Johnson, "The glamour and gloom of glycogen synthase kinase-3," *Trends Biochem Sci,* vol. 29, no. 2, pp. 95-102, Feb, 2004.

[90] W. Liu, Z. Ren, K. Lu, C. Song, E. C. W. Cheung, Z. Zhou, and G. Chen, "The Suppression of Medium Acidosis Improves the Maintenance and Differentiation of Human Pluripotent Stem Cells at High Density in Defined Cell Culture Medium," *Int J Biol Sci,* vol. 14, no. 5, pp. 485-496, 2018.

[91] S. Srimasorn, M. Kirsch, S. Hallmeyer-Ellgner, D. Lindemann, A. Storch, and A. Hermann, "Increased Neuronal Differentiation Efficiency in High Cell Density-Derived Induced Pluripotent Stem Cells," *Stem Cells Int,* vol. 2019, pp. 2018784, 2019.

[92] B. K. Gage, T. D. Webber, and T. J. Kieffer, "Initial cell seeding density influences pancreatic endocrine development during in vitro differentiation of human embryonic stem cells," *PLoS One,* vol. 8, no. 12, pp. e82076, 2013.

[93] H. K. Wilson, S. G. Canfield, M. K. Hjortness, S. P. Palecek, and E. V. Shusta, "Exploring the effects of cell seeding density on the differentiation of human pluripotent stem cells to brain microvascular endothelial cells," *Fluids Barriers CNS,* vol. 12, pp. 13, May 21, 2015.

[94] M. M. Najafabadi, V. Bayati, M. Orazizadeh, M. Hashemitabar, and F.

Absalan, "Impact of Cell Density on Differentiation Efficiency of Rat Adipose-derived Stem Cells into Schwann-like Cells," *Int J Stem Cells,* vol. 9, no. 2, pp. 213-220, Nov 30, 2016.

[95] E. Stead, J. White, R. Faast, S. Conn, S. Goldstone, J. Rathjen, U. Dhingra, P. Rathjen, D. Walker, and S. Dalton, "Pluripotent cell division cycles are driven by ectopic Cdk2, cyclin A/E and E2F activities," *Oncogene,* vol. 21, no. 54, pp. 8320-33, Nov 28, 2002.

[96] A. Calder, I. Roth-Albin, S. Bhatia, C. Pilquil, J. H. Lee, M. Bhatia, M. Levadoux-Martin, J. McNicol, J. Russell, T. Collins, and J. S. Draper, "Lengthened G1 phase indicates differentiation status in human embryonic stem cells," *Stem Cells Dev,* vol. 22, no. 2, pp. 279-95, Jan 15, 2013.

[97] K. Kim, D. Dean, A. G. Mikos, and J. P. Fisher, "Effect of Initial Cell Seeding Density on Early Osteogenic Signal Expression of Rat Bone Marrow Stromal Cells Cultured on Cross-Linked Poly(propylene fumarate) Disks," *Biomacromolecules,* vol. 10, no. 7, pp. 1810-1817, 2009.

[98] M. J. Goumans, A. Zwijsen, P. Ten Dijke, and S. Bailly, "Bone Morphogenetic Proteins in Vascular Homeostasis and Disease," *Cold Spring Harb Perspect Biol,* vol. 10, no. 2, Feb 1, 2018.

[99] T. Kawai, T. Takahashi, M. Esaki, H. Ushikoshi, S. Nagano, H. Fujiwara, and K. Kosai, "Efficient cardiomyogenic differentiation of embryonic stem cell by fibroblast growth factor 2 and bone morphogenetic protein 2," *Circ J,* vol. 68, no. 7, pp. 691-702, Jul, 2004.

[100] M. Azhar, J. Schultz Jel, I. Grupp, G. W. Dorn, 2nd, P. Meneton, D. G. Molin, A. C. Gittenberger-de Groot, and T. Doetschman, "Transforming growth factor beta in cardiovascular development and function," *Cytokine Growth Factor Rev,* vol. 14, no. 5, pp. 391-407, Oct, 2003.

[101] H. Zhou, M. D. Weir, and H. H. Xu, "Effect of cell seeding density on proliferation and osteodifferentiation of umbilical cord stem cells on calcium phosphate cement-fiber scaffold," *Tissue Eng Part A,* vol. 17, no. 21-22, pp. 2603-13, Nov, 2011.

[102] C. Liu, A. Oikonomopoulos, N. Sayed, and J. C. Wu, "Modeling human diseases with induced pluripotent stem cells: from 2D to 3D and beyond,"

Development, vol. 145, no. 5, Mar 8, 2018.

[103] C. Pontes Soares, V. Midlej, M. E. de Oliveira, M. Benchimol, M. L. Costa, and C. Mermelstein, "2D and 3D-organized cardiac cells shows differences in cellular morphology, adhesion junctions, presence of myofibrils and protein expression," *PLoS One,* vol. 7, no. 5, pp. e38147, 2012.

[104] T. Xu, P. Molnar, C. Gregory, M. Das, T. Boland, and J. J. Hickman, "Electrophysiological characterization of embryonic hippocampal neurons cultured in a 3D collagen hydrogel," *Biomaterials,* vol. 30, no. 26, pp. 4377-83, Sep, 2009.

[105] D. Simao, M. M. Silva, A. P. Terrasso, F. Arez, M. F. Q. Sousa, N. Z. Mehrjardi, T. Saric, P. Gomes-Alves, N. Raimundo, P. M. Alves, and C. Brito, "Recapitulation of Human Neural Microenvironment Signatures in iPSC-Derived NPC 3D Differentiation," *Stem Cell Reports,* vol. 11, no. 2, pp. 552-564, Aug 14, 2018.

[106] E. Giacomelli, M. Bellin, L. Sala, B. J. van Meer, L. G. Tertoolen, V. V. Orlova, and C. L. Mummery, "Three-dimensional cardiac microtissues composed of cardiomyocytes and endothelial cells co-differentiated from human pluripotent stem cells," *Development,* vol. 144, no. 6, pp. 1008-1017, Mar 15, 2017.

[107] K. Brannvall, K. Bergman, U. Wallenquist, S. Svahn, T. Bowden, J. Hilborn, and K. Forsberg-Nilsson, "Enhanced neuronal differentiation in a three-dimensional collagen-hyaluronan matrix," *J Neurosci Res,* vol. 85, no. 10, pp. 2138-46, Aug 1, 2007.

[108] F. Sampaziotis, M. C. de Brito, P. Madrigal, A. Bertero, K. Saeb-Parsy, F. A. C. Soares, E. Schrumpf, E. Melum, T. H. Karlsen, J. A. Bradley, W. T. Gelson, S. Davies, A. Baker, A. Kaser, G. J. Alexander, N. R. F. Hannan, and L. Vallier, "Cholangiocytes derived from human induced pluripotent stem cells for disease modeling and drug validation," *Nat Biotechnol,* vol. 33, no. 8, pp. 845-852, Aug, 2015.

[109] D. C. Wilkinson, J. A. Alva-Ornelas, J. M. Sucre, P. Vijayaraj, A. Durra, W. Richardson, S. J. Jonas, M. K. Paul, S. Karumbayaram, B. Dunn, and B. N. Gomperts, "Development of a Three-Dimensional Bioengineering

Technology to Generate Lung Tissue for Personalized Disease Modeling," *Stem Cells Transl Med,* vol. 6, no. 2, pp. 622-633, Feb, 2017.

[110] T. G. Otsuji, J. Bin, A. Yoshimura, M. Tomura, D. Tateyama, I. Minami, Y. Yoshikawa, K. Aiba, J. E. Heuser, T. Nishino, K. Hasegawa, and N. Nakatsuji, "A 3D sphere culture system containing functional polymers for large-scale human pluripotent stem cell production," *Stem Cell Reports,* vol. 2, no. 5, pp. 734-45, May 6, 2014.

[111] P. D. Lampe, and A. F. Lau, "The effects of connexin phosphorylation on gap junctional communication," *Int J Biochem Cell Biol,* vol. 36, no. 7, pp. 1171-86, Jul, 2004.

[112] S. Rohr, "Role of gap junctions in the propagation of the cardiac action potential," *Cardiovasc Res,* vol. 62, no. 2, pp. 309-22, May 1, 2004.

[113] Y. Jiang, S. Habibollah, K. Tilgner, J. Collin, T. Barta, J. Y. Al-Aama, L. Tesarov, R. Hussain, A. W. Trafford, G. Kirkwood, E. Sernagor, C. G. Eleftheriou, S. Przyborski, M. Stojkovic, M. Lako, B. Keavney, and L. Armstrong, "An induced pluripotent stem cell model of hypoplastic left heart syndrome (HLHS) reveals multiple expression and functional differences in HLHS-derived cardiac myocytes," *Stem Cells Transl Med,* vol. 3, no. 4, pp. 416-23, Apr, 2014.

[114] M. Oyamada, K. Takebe, A. Endo, S. Hara, and Y. Oyamada, "Connexin expression and gap-junctional intercellular communication in ES cells and iPS cells," *Frontiers in Pharmacology,* vol. 4, 2013.

[115] B. Bhattacharya, J. Cai, Y. Luo, T. Miura, J. Mejido, S. N. Brimble, X. Zeng, T. C. Schulz, M. S. Rao, and R. K. Puri, "Comparison of the gene expression profile of undifferentiated human embryonic stem cell lines and differentiating embryoid bodies," *BMC Dev Biol,* vol. 5, pp. 22, Oct 5, 2005.

[116] A. Beckmann, M. Schubert, N. Hainz, A. Haase, U. Martin, T. Tschernig, and C. Meier, "Ultrastructural demonstration of Cx43 gap junctions in induced pluripotent stem cells from human cord blood," *Histochem Cell Biol,* vol. 146, no. 5, pp. 529-537, Nov, 2016.

[117] E. A. Mahtab, A. C. Gittenberger-de Groot, R. Vicente-Steijn, H. Lie-Venema, M. E. Rijlaarsdam, M. G. Hazekamp, and M. M. Bartelings, "Disturbed myocardial connexin 43 and N-cadherin expressions in

hypoplastic left heart syndrome and borderline left ventricle," *J Thorac Cardiovasc Surg,* vol. 144, no. 6, pp. 1315-22, Dec, 2012.

[118] L. Miquerol, A. Bellon, N. Moreno, S. Beyer, S. M. Meilhac, M. Buckingham, D. Franco, and R. G. Kelly, "Resolving cell lineage contributions to the ventricular conduction system with a Cx40-GFP allele: a dual contribution of the first and second heart fields," *Dev Dyn,* vol. 242, no. 6, pp. 665-77, Jun, 2013.

[119] H. Wang, Y. Liu, S. Han, Y. Zi, Y. Zhang, R. Kong, Z. Liu, Z. Cai, C. Zhong, W. Liu, L. Li, and L. Jiang, "Nkx2-5 Regulates the Proliferation and Migration of H9c2 Cells," *Med Sci Monit,* vol. 26, pp. e925388, Aug 11, 2020.

[120] D. A. Elliott, E. P. Kirk, T. Yeoh, S. Chandar, F. McKenzie, P. Taylor, P. Grossfeld, D. Fatkin, O. Jones, P. Hayes, M. Feneley, and R. P. Harvey, "Cardiac homeobox gene NKX2-5 mutations and congenital heart disease: associations with atrial septal defect and hypoplastic left heart syndrome," *J Am Coll Cardiol,* vol. 41, no. 11, pp. 2072-6, Jun 4, 2003.

[121] M. Khatami, M. Mazidi, S. Taher, M. M. Heidari, and M. Hadadzadeh, "Novel Point Mutations in the NKX2.5 Gene in Pediatric Patients with Non-Familial Congenital Heart Disease," *Medicina (Kaunas),* vol. 54, no. 3, Jun 19, 2018.

[122] J. Yin, J. Qian, G. Dai, C. Wang, Y. Qin, T. Xu, Z. Li, H. Zhang, and S. Yang, "Search of Somatic Mutations of NKX2-5 and GATA4 Genes in Chinese Patients with Sporadic Congenital Heart Disease," *Pediatr Cardiol,* vol. 40, no. 1, pp. 17-22, Jan, 2019.

[123] H. Yamagishi, C. Yamagishi, O. Nakagawa, R. P. Harvey, E. N. Olson, and D. Srivastava, "The combinatorial activities of Nkx2.5 and dHAND are essential for cardiac ventricle formation," *Dev Biol,* vol. 239, no. 2, pp. 190-203, Nov 15, 2001.

[124] A. Yamak, R. O. Georges, M. Sheikh-Hassani, M. Morin, H. Komati, and M. Nemer, "Novel exons in the tbx5 gene locus generate protein isoforms with distinct expression domains and function," *J Biol Chem,* vol. 290, no. 11, pp. 6844-56, Mar 13, 2015.

[125] M. Xin, E. N. Olson, and R. Bassel-Duby, "Mending broken hearts: cardiac development as a basis for adult heart regeneration and repair," *Nat Rev*

Mol Cell Biol, vol. 14, no. 8, pp. 529-41, Aug, 2013.

[126] C. T. Basson, D. R. Bachinsky, R. C. Lin, T. Levi, J. A. Elkins, J. Soults, D. Grayzel, E. Kroumpouzou, T. A. Traill, J. Leblanc-Straceski, B. Renault, R. Kucherlapati, J. G. Seidman, and C. E. Seidman, "Mutations in human TBX5 [corrected] cause limb and cardiac malformation in Holt-Oram syndrome," *Nat Genet,* vol. 15, no. 1, pp. 30-5, Jan, 1997.

[127] S. M. Reamon-Buettner, and J. Borlak, "TBX5 mutations in non-Holt-Oram syndrome (HOS) malformed hearts," *Hum Mutat,* vol. 24, no. 1, pp. 104, Jul, 2004.

[128] B. G. Bruneau, G. Nemer, J. P. Schmitt, F. Charron, L. Robitaille, S. Caron, D. A. Conner, M. Gessler, M. Nemer, C. E. Seidman, and J. G. Seidman, "A murine model of Holt-Oram syndrome defines roles of the T-box transcription factor Tbx5 in cardiogenesis and disease," *Cell,* vol. 106, no. 6, pp. 709-21, Sep 21, 2001.

[129] W. P. Devine, J. D. Wythe, M. George, K. Koshiba-Takeuchi, and B. G. Bruneau, "Early patterning and specification of cardiac progenitors in gastrulating mesoderm," *Elife,* vol. 3, Oct 8, 2014.

[130] J. K. Takeuchi, X. Lou, J. M. Alexander, H. Sugizaki, P. Delgado-Olguin, A. K. Holloway, A. D. Mori, J. N. Wylie, C. Munson, Y. Zhu, Y. Q. Zhou, R. F. Yeh, R. M. Henkelman, R. P. Harvey, D. Metzger, P. Chambon, D. Y. Stainier, K. S. Pollard, I. C. Scott, and B. G. Bruneau, "Chromatin remodelling complex dosage modulates transcription factor function in heart development," *Nat Commun,* vol. 2, pp. 187, Feb 8, 2011.

[131] H. S. Jeong, E. S. Jung, Y. J. Sim, S. J. Kim, J. W. Jang, K. S. Hong, W. Y. Lee, H. M. Chung, K. T. Park, Y. S. Jung, C. H. Kim, and K. S. Kim, "Fbxo25 controls Tbx5 and Nkx2-5 transcriptional activity to regulate cardiomyocyte development," *Biochim Biophys Acta,* vol. 1849, no. 6, pp. 709-21, Jun, 2015.

[132] B. G. Bruneau, "Atrial natriuretic factor in the developing heart: a signpost for cardiac morphogenesis," *Can J Physiol Pharmacol,* vol. 89, no. 8, pp. 533-7, Aug, 2011.

[133] Y. Li, C. Wang, T. Li, L. Ma, F. Fan, Y. Jin, and J. Shen, "The whole transcriptome and proteome changes in the early stage of myocardial

infarction," *Cell Death Discov,* vol. 5, pp. 73, 2019.

[134] W. Song, H. Wang, and Q. Wu, "Atrial natriuretic peptide in cardiovascular biology and disease (NPPA)," *Gene,* vol. 569, no. 1, pp. 1-6, Sep 10, 2015.

[135] W. M. Hoogaars, A. Tessari, A. F. Moorman, P. A. de Boer, J. Hagoort, A. T. Soufan, M. Campione, and V. M. Christoffels, "The transcriptional repressor Tbx3 delineates the developing central conduction system of the heart," *Cardiovasc Res,* vol. 62, no. 3, pp. 489-99, Jun 1, 2004.

[136] Y. Hiroi, S. Kudoh, K. Monzen, Y. Ikeda, Y. Yazaki, R. Nagai, and I. Komuro, "Tbx5 associates with Nkx2-5 and synergistically promotes cardiomyocyte differentiation," *Nat Genet,* vol. 28, no. 3, pp. 276-80, Jul, 2001.

[137] M. Miyamoto, H. Gangrade, and E. Tampakakis, "Understanding Heart Field Progenitor Cells for Modeling Congenital Heart Diseases," *Curr Cardiol Rep,* vol. 23, no. 5, pp. 38, Mar 11, 2021.

[138] O. Elmas, "Effects of electromagnetic field exposure on the heart: a systematic review," *Toxicol Ind Health,* vol. 32, no. 1, pp. 76-82, Jan, 2016.

[139] K. L. Laugwitz, A. Moretti, L. Caron, A. Nakano, and K. R. Chien, "Islet1 cardiovascular progenitors: a single source for heart lineages?," *Development,* vol. 135, no. 2, pp. 193-205, Jan, 2008.

[140] R. Ilagan, R. Abu-Issa, D. Brown, Y. P. Yang, K. Jiao, R. J. Schwartz, J. Klingensmith, and E. N. Meyers, "Fgf8 is required for anterior heart field development," *Development,* vol. 133, no. 12, pp. 2435-45, Jun, 2006.

[141] C. L. Cai, X. Liang, Y. Shi, P. H. Chu, S. L. Pfaff, J. Chen, and S. Evans, "Isl1 identifies a cardiac progenitor population that proliferates prior to differentiation and contributes a majority of cells to the heart," *Dev Cell,* vol. 5, no. 6, pp. 877-89, Dec, 2003.

[142] L. Lin, L. Cui, W. Zhou, D. Dufort, X. Zhang, C. L. Cai, L. Bu, L. Yang, J. Martin, R. Kemler, M. G. Rosenfeld, J. Chen, and S. M. Evans, "Beta-catenin directly regulates Islet1 expression in cardiovascular progenitors and is required for multiple aspects of cardiogenesis," *Proc Natl Acad Sci U S A,* vol. 104, no. 22, pp. 9313-8, May 29, 2007.

[143]I. A. Katrukha, "Human cardiac troponin complex. Structure and functions," *Biochemistry (Mosc),* vol. 78, no. 13, pp. 1447-65, Dec, 2013.

[144] A. A. Moscona, "Tissues from dissociated cells," *Sci Am,* vol. 200, no. 5, pp. 132-4 passim, May, 1959.

[145] T. Eschenhagen, C. Fink, U. Remmers, H. Scholz, J. Wattchow, J. Weil, W. Zimmermann, H. H. Dohmen, H. Schafer, N. Bishopric, T. Wakatsuki, and E. L. Elson, "Three-dimensional reconstitution of embryonic cardiomyocytes in a collagen matrix: a new heart muscle model system," *FASEB J,* vol. 11, no. 8, pp. 683-94, Jul, 1997.

[146] F. Khan, and M. Tanaka, "Designing Smart Biomaterials for Tissue Engineering," *Int J Mol Sci,* vol. 19, no. 1, Dec 21, 2017.

[147] S. W. Kubalak, W. C. Miller-Hance, T. X. O'Brien, E. Dyson, and K. R. Chien, "Chamber specification of atrial myosin light chain-2 expression precedes septation during murine cardiogenesis," *J Biol Chem,* vol. 269, no. 24, pp. 16961-70, Jun 17, 1994.

[148] T. X. O'Brien, K. J. Lee, and K. R. Chien, "Positional specification of ventricular myosin light chain 2 expression in the primitive murine heart tube," *Proc Natl Acad Sci U S A,* vol. 90, no. 11, pp. 5157-61, Jun 1, 1993.

[149] F. B. Bedada, M. Wheelwright, and J. M. Metzger, "Maturation status of sarcomere structure and function in human iPSC-derived cardiac myocytes," *Biochim Biophys Acta,* vol. 1863, no. 7 Pt B, pp. 1829-38, Jul, 2016.

[150] F. B. Bedada, S. S. Chan, S. K. Metzger, L. Zhang, J. Zhang, D. J. Garry, T. J. Kamp, M. Kyba, and J. M. Metzger, "Acquisition of a quantitative, stoichiometrically conserved ratiometric marker of maturation status in stem cell-derived cardiac myocytes," *Stem Cell Reports,* vol. 3, no. 4, pp. 594-605, Oct 14, 2014.

[151] K. E. Yutzey, "Cardiomyocyte Proliferation: Teaching an Old Dogma New Tricks," *Circ Res,* vol. 120, no. 4, pp. 627-629, Feb 17, 2017.

[152] O. Bergmann, R. D. Bhardwaj, S. Bernard, S. Zdunek, F. Barnabe-Heider, S. Walsh, J. Zupicich, K. Alkass, B. A. Buchholz, H. Druid, S. Jovinge, and J. Frisen, "Evidence for cardiomyocyte renewal in humans," *Science,* vol. 324, no. 5923, pp. 98-102, Apr 3, 2009.

Articles

1. **Zhang Z**, Huang J, Wang Y, Shen W. Transcriptome analysis revealed a two-step transformation of vascular smooth muscle cells to macrophage-like cells. *Atherosclerosis*. 2022;346:26-35. doi:10.1016/j.atherosclerosis.2022.02.021

2. **Zhang, Z**, Mannhardt, I, Dressen, M. , Neb, I. , Doppler, S. , & M.-A, D. , et al. 5331functional analysis of induced pluripotent stem cell-derived cardiomyocytes from patients with hypoplastic left heart syndrome in engineered heart tissues. European Heart Journal(suppl_1), suppl_1. (2018)

3. Krane M, Dreßen M, Santamaria G, My I, Schneider CM, Dorn T, Laue S, Mastantuono E, Berutti R, Rawat H, Gilsbach R, Schneider P, Lahm H, Schwarz S, Doppler SA, Paige S, Puluca N, Doll S, Neb I, Brade T, **Zhang Z**, Abou-Ajram C, Northoff B, Holdt LM, Sudhop S, Sahara M, Goedel A, Dendorfer A, Tjong FVY, Rijlaarsdam ME, Cleuziou J, Lang N, Kupatt C, Bezzina C, Lange R, Bowles NE, Mann M, Gelb BD, Crotti L, Hein L, Meitinger T, Wu S, Sinnecker D, Gruber PJ, Laugwitz KL, Moretti A. Sequential Defects in Cardiac Lineage Commitment and Maturation Cause Hypoplastic Left Heart Syndrome. Circulation. 2021 Oct 26;144(17):1409-1428. doi: 10.1161/CIRCULATIONAHA.121.056198. Epub 2021 Oct 25. PMID: 34694888; PMCID: PMC8542085.

4. Hoelscher SC, Stich T, Diehm A, Lahm H, Dreßen M, **Zhang Z**, Neb I, Aherrahrou Z, Erdmann J, Schunkert H, Santamaria G, Cuda G, Gilsbach R, Hein L, Lange R, Hassel D, Krane M, Doppler SA. miR-128a Acts as a Regulator in Cardiac Development by Modulating Differentiation of Cardiac Progenitor Cell Populations. Int J Mol Sci. 2020 Feb 10;21(3):1158. doi: 10.3390/ijms21031158. PMID: 32050579; PMCID: PMC7038042.

5. Lahm H, Jia M, Dreßen M, Wirth F, Puluca N, Gilsbach R, Keavney BD, Cleuziou J, Beck N, Bondareva O, Dzilic E, Burri M, König KC, Ziegelmüller JA, Abou-Ajram C, Neb I, **Zhang Z**, Doppler SA, Mastantuono E, Lichtner P, Eckstein G, Hörer J, Ewert P, Priest JR, Hein L, Lange R, Meitinger T, Cordell HJ, Müller-Myhsok B,

Krane M. Congenital heart disease risk loci identified by genome-wide association study in European patients. J Clin Invest. 2021 Jan 19;131(2):e141837. doi: 10.1172/JCI141837. PMID: 33201861; PMCID: PMC7810487.

Acknowledgements

Here I would like to thank all the people around me for their friendly support and help in my experiments and dissertation. Without their help my dissertation would not have been possible.

First and foremost, I would like to thank my supervisor Prof. Dr. med. Markus Krane for providing the opportunity to do my training as a Chinese doctoral student at the German Heart Center Munich at the Technical University of Munich. As the head of the Division of Experimental Surgery at the Department of Cardiovascular Surgery Prof. Dr. Krane used his limited time to give me great support for my research during my stay in Munich. He is one of the most intelligent and diligent cardiac surgeons I know. Despite the heavy workload in his clinical duties, Prof. Dr. Krane is keeping up with innovative basic research in the field of cardiovascular disease. His is a paragon for me of how to pursue and organize my career as a good cardiac surgeon.

I am grateful for the help from PD Dr. rer. nat. Harald Lahm and Dr. rer. nat. Martina Dreßen. PD Dr. Lahm is my research tutor. He is a positive and optimistic teacher and constantly encourages me when I am lost. Dr. Dreßen is an intelligent woman with a lot of nice ideas for my experiments. Both taught me a lot during my research such as immunochemical staining, FACS analysis and other techniques of basic research. Due to their support my abstract was accepted as an oral presentation for the ESC congress. I am also extremely thankful for their help with my dissertation.

I am also indebted to Klaudia Adamczyk-Wolf. She was my first cell culture teacher in Germany. She taught me the stem cell culture, directed and spontaneous differentiation assays. Apart from the experimental work we also became good friends. Since my first days in Germany, she helped me a lot and gave many advices to handle my daily life. I

also want to express my thanks to the rest of the human iPS cell group mates, especially Irina Neb and Benjamin Beyersdorf, who supported my lab work. With their help, my experimental life was always full of laugh and joy.

To my collaborators in Hamburg, Prof. Dr. med. Thomas Eschenhagen, Prof. Dr. med. Arne Hansen and Dr. rer. nat. Bärbel Maria Ulmer, I also want to express my thanks for their help in the EHT experiments. They showed me the experimental EHT process without reservation and also gave me a lot of advice on stem cell culture and cardiac differentiation. The one week stay in in their laboratory in Hamburg left me with a deep and beautiful impression.

Last but not least, I want to thank my family for their constant support during my study abroad. Thanks to my wife, Xiangmeng Wang, for her patience and support. I owe a lot to her. We studied and lived in different countries, but she consistently supported and encouraged me throughout the whole period.